Aus der

Universitätsklinik für Radioonkologie mit Poliklinik Sektion für Strahlenbiologie und Molekulare Umweltforschung

Role of PI3K/Akt pathway in cancer stem cell mediated radioresistance

Thesis submitted as requirement to fulfill the degree "Doctor of Philosophy" (Ph.D.)

at the
Faculty of Medicine
Eberhard Karls University
Tübingen

Submitted by
Dehghan Harati, Mozhgan

2019

Dean:	Professor Dr. I. B. Autenrieth
1. Reviewer:	Professor Dr. H. P. Rodemann
2. Reviewer:	Professor Dr. S. Huber
3. Reviewer:	Professor Dr. N. Cordes
Date of oral examination:	18.11.2019

Table of contents

List of abbreviations

AML	Acute myeloid leukaemia
ALDH1	Aldehyde Dehydrogenase 1
ATR	Ataxia telangiectasia and Rad3-related
ATM	Ataxia telangiectasia mutated
ABCB1	ATP-binding cassette sub-family B member 1
ATRA	All-trans retinoic acid
BER	Base excision repair
BAD	Bcl-2-associated death promoter
CSCM	Cancer stem cell markers
CSCs	Cancer stem cells
DEAB	N,N-diethylaminobenzaldehyde
DNA-PKcs	DNA dependent protein kinase
DNA-DSB	DNA double strand breaks
DSB	Double strand breaks
EGFR	Epidermal growth factor receptor
EMT	Epithelial to mesenchymal transition
FOXO	Forkhead box O transcription factor
GCPs	Granule cell precursors
G418	Gentamicin
GSK3ß	Glycogen synthase kinase 3 beta
GPCRs	G-protein coupled receptors
H&N	Head and Neck
HR	Homologous recombination
HA	Hyaluronan
ITH	Intra-tumor heterogeneity
IR	Ionizing radiation
Kap1	KRAB-associated protein 1
MCL	Mantel cell lymphoma
mTORC2	Mechanistic target of rapamycin complex2
MDM2	Mouse double minute 2 homolog

MDR1	Multidrug transporter
NHEJ	Non-homologous end-joining
NICD	Notch intercellular domain
NER	Nucleotide excision repair
PCAF	P300/CBP-associated factor
pen/strep	Penicillin/streptomycin
PTEN	Phosphatase and tensin homolog
PIP3	Phosphatidylinositol 3,4,5-trsphosphate
γH2AX	Phosphorylated H2AX
PgR	Progesterone receptor
RT	Radiotherapy
RA	Retinoic acid
RAR	Retinoic acid receptor
RXR	Retinoid X receptor
RAM	RPBJ-associated molecule
S473	Serine residue 473
SSB	Single strand breaks
SIRT2	Sirtuin 2
S1P	Sphingosine-1-phosphate
TCF	T-cell factor
TME	Tumor microenvironment
WHO	World Health Organization

1 Introduction

1.1 Cancer and breast cancer

Normal cells can transform into cancer cells due to various cellular deregulations, which lead to uncontrolled proliferative growth. The cellular deregulation occurs at various levels including genetic, epigenetic, intracellular signaling and microenvironment or extracellular interactions [1]. The constant and unpredictable changes in tumor cell behavior, especially under treatment stress, increases the complexity of treatment and can cause therapy resistance, relapse of tumor, and intra-tumor heterogeneity (ITH). Accumulation of different types of gene mutations, translocations and altered gene copy numbers lead to deregulation of functional proteins and intracellular signaling cascades. In addition, epigenetic alterations such as histone and methylation modifications can also company the genetic instability of tumor cells [1, 2]. Compared to normal cells in which DNA repair systems will repair DNA damages, deregulation of DNA repair mechanisms in cancer cells increases genome instability [1]. Intracellular signaling is the network of protein-protein interactions and modifications, which transfer environmental stimuli or information into the cells and thus activates or inhibits specific cell responses for instance proliferation, differentiation, survival, and apoptosis [1, 3]. Compared to normal cells in which cellular signaling is controlled by precise crosstalk and feedback systems, in cancer cells the homeostasis of signaling networks is disrupted. In this regard, many cancer cells are characterized by over-activation and overexpression of some pathways, resulting in uncontrolled responses [1, 4]. Over decades, the role of tumor microenvironment (TME) has been highlighted. TME is a highly interactive tissue area in which components of the extracellular matrix as well as various cell types including tumor cells, fibroblasts, endothelial and immune cells are interacting. The bidirectional interaction between tumor cells and microenvironment can, thus, promote tumor growth by different ways, for instance releasing cytokines and growth factors in TME [1, 5].

Breast, lung and colon cancer are the three most common cancers worldwide, and breast cancer is the most common type in women. Although breast cancer incidents are increasing according to the World Health Organization (WHO), mortality from this type

of cancer in the European Union (EU) and North America is decreasing [6, 7]. The increase in survival is mainly due to early diagnosis and detection of the tumor. In this regard, 8% decrease in breast cancer mortality in EU has been reported in 2016 [6]. However, breast cancer is still one of the leading life threatening diseases in less developed countries. Based on the classification of Perou and coworkers [8], breast cancer is divided to four different subtypes including Luminal A, Luminal B, HER2-enriched and basal like. The differences between these four subtypes can be determined based on proliferation marker (Ki67), various receptors such as estrogen receptor (ER), HER2 and Progesterone receptor (PgR) [6]. Thus, dependent on the subtype of breast cancer, systemic therapy can be guided specifically. The proper therapy plan has to be defined based on the stage and subtype of the tumor by a multidisciplinary team. Primary surgery is usually the first step in early stage of breast cancer treatment, which is followed by either chemo- or radiotherapy. Recently, less invasive radiotherapy approaches including partial breast irradiation and hypo-fractionated irradiation has been developed [6].

1.2 Radiotherapy

Radiation can be divided into ionizing and non-ionizing radiations. Ionizing radiation (IR) refers to high-frequency radiations, which can remove an outer electron from the last shell of atom. In this regard, X-rays and gamma rays are counted as ionizing radiation [9]. Nonionizing radiation carries lower-frequency energy and only can move electrons to a higher energy level without removing them. The nonionizing radiations are used routinely such as visible light, radio waves, and microwaves [9]. The radiation energy that is deposited in the exposed material (i.e. skin, tumor or organs) is called absorbed dose. The absorbed dose, which is measured as gray (Gy) is depend on tissue density and depth [9]. One of the most applied features of IR in oncology is the ability to damage DNA preferentially in tumor cells. Due to the high proliferation rate of tumor cells compared with normal cells, radiation induces more DNA damage in tumor cells, which results in stronger sensitivity of these cells to the radiation than in normal cells [10]. In this regard, besides surgery radiotherapy (RT) is the most important therapeutic option for local tumor treatment. Moreover, compared to other types of cancer therapy,

RT has lower costs and currently is used as a common treatment worldwide in which approximately 50% of cancer patients undergo RT during their treatment period [10].

1.2.1 Radiotherapy for breast cancer

RT is applied usually as a primary treatment for various type of cancers especially breast cancer, which need to be treated before or after chemo-therapy or surgery [10]. RT usually applied after removing breast tumor tissue in order to ensure killing of remaining tumor cells in the tumor border site to avoid tumor relapse [11]. For several years, RT was limited to a fixed conventional protocol in which over 5 weeks the whole breast receives fractionated RT with 1.8/2 Gy per fraction. However, nowadays, based on new technologies and increased knowledge in the field of radiation biology, new protocols and modalities are applied. Hypo-fractionated RT, simultaneous integrated boost, intensity modulated RT, volumetric modulated RT, deep-inspiration breath-hold are some of the new modalities of RT [11].

1.2.2 DNA double strand break and repair mechanisms

One of the main features of ionizing radiation (IR) is high frequency induction of DNA damage. DNA damage occurs due to production of free electrons, which are generated by ionizing particles [12]. The accumulation of various ionizations clusters after irradiation and additional free radical products from irradiated water molecules surrounding DNA leads to structural damage and break in the DNA molecule [12]. DNA damage consists of various types of breaks such as single strand breaks (SSB), double strand breaks (DSB), base and sugar damages [12]. At the chemical level of a DNA strand break, it has been demonstrated that hydrogen abstraction in sugar leads to the reaction of neighboring phosphate groups with water and/or oxidation of guanine residue which consequently results in a break of the DNA strand [12]. Depending on the energy deposit, this leads to either DNA single or double strand breaks.

Repair of single strand breaks is performed via at least three main mechanisms including base excision repair (BER), nucleotide excision repair (NER) and mismatch

repair. In BER system, DNA glycosylases provide apurinic or apyrimidinic gaps (AP sites) in the sites of single strand damage and then DNA polymerases with AP endonucleases synthetize a new DNA single strand based on the non-damaged template strand [13]. In addition, NER system usually repairs the massive single strand DNA damages via removing 12-24 nucleotides up and down stream of damage site and resynthesizes the new DNA strand [13]. The mismatch repair system is directed to the mismatched bases after a nick in non-pattern strand. However, the precise mechanism of mismatch repair has not been completely understood in mammalian cells [14]. In this regard, several models have been proposed such as the stationary, translocation and molecular switch models [14].

DNA double strand breaks (DNA-DSB) are the most lethal DNA-lesions, which if not repaired ultimately lead to cell death [15]. Two main different DNA-DSB repair pathways are known, i.e. non-homologous end-joining (NHEJ) and homologous recombination (HR) [15]. In comparison to HR, NHEJ is able to perform repair without the homologous non-damaged template. Thus, NHEJ-repaired can be performed by the cells independent of the cell cycle phase, whereas HR is only possible in late S and G2 phase of the cell cycle when the repair system has access to the non-damaged sister chromatid as homologous template [15].

The first step of NHEJ repair is the recognition of DSB and binding of Ku heterodimer (Ku70 and Ku80) to the site of break [15, 16]. The high affinity of Ku heterodimers for DNA ends is one of the reasons that this heterodimer can recognize DNA-DSB [15]. Binding of Ku heterodimer together with MRE11-Rad50-NBS1 (MRN) complex provides a suitable scaffold for recruiting other proteins involving in NHEJ including DNA dependent protein kinase (DNA-PKcs), ataxia telangiectasia mutated (ATM) and ataxia telangiectasia and Rad3-related (ATR) [15]. The connection of Ku heterodimer and DNA-PKcs leads to the activation of the DNA-PKcs kinase activity. Activation and auto-phosphorylation of DNA-PKcs provide the energy and structural shift for DNA end processing such as polymerization and ligation [12, 15]. In the last step, the XRCC4/Ligase IV complex is recruited to mediate ligation of the DSB [12, 15]. The role of chromatin structure during DNA-DSB has been investigated over decades. In this regard, Rogakou and coworkers [17] have discovered phosphorylation of a variant of histone H2A (H2AX) at serine 139 after ionizing radiation. This study has

demonstrated that phosphorylated H2AX (γH2AX) accumulates in foci formed after irradiation, which are countable and can, thus, be quantified [17, 18]. Moreover, it has been shown that a multi-domain scaffolding protein called MDC1 binds to γH2AX and also recruits MRN complex to the site of DNA damage in which it has a crucial role in the early step of DNA repair [17, 18].

1.3 Cancer Stem Cells

Genomic diversity of tumors within patients presenting the same type of cancer has been known as intra-tumor heterogeneity (ITH) [19]. The degree of genomic diversity can range between zero and over eight thousand coding mutations across individual tumors [19]. ITH occurs as a result of micro-environmental selection processes and mutations, which arise during tumor expansion. Accordingly, ITH reflects cancer cell evolution in order to enhance the tumor progression and metastasis [20]. It is also evident that ITH is not restricted to genetic abnormalities as it includes as well cell surface markers, growth rate and therapeutic response patterns [21, 22]. Tumor heterogeneity can change during cancer development as well as in response to the treatment regime [22]. Predominantly, phenotype variations in the tumor reflect existence of cancer stem cells, which are a result of tumor evolution [21].

The concept of stemness has been addressed in several studies in the late 1990th by Till and McCulloch who identified the self-renewal potential of hematopoietic cells with a clonal in vivo repopulation assay [23-25]. Self-renewal is an asymmetric division process in which one of daughter cells keep the capacity of stemness and can ensure the maintenance of stem cell populations [21]. Although for several decades, the definition of stem cells has been only known for normal tissues, in the 1990th Dick and coworkers have experimentally developed the concept of tumor-initiating cells [26]. This group proved that human acute myeloid leukemia (AML) cells with CD34+ CD38- surface marker expression are able to engraft SCID mice and this specific population defines the leukemia-initiating cells [26]. Based on this study, the concept of tumor-initiating cells or cancer stem cells (CSCs) has been developed for various types solid tumors, including breast, brain and colon cancers [21, 22]. By definition, the stemness feature

of CSCs refers to self-renewal ability and a variety of cellular functions that enable these cells to survive conventional antitumor treatments [21]. As indicated in Table 1.3 for each type of tumor CSCs are now characterized with specific surface markers.

Tumor type	**CSCs specific marker [27]**
Breast	CD24, CD44, ALDH enzyme activity
Head and Neck	CD44, CD271, ALDH enzyme activity
Colon	CD44, CD133, CD166, ALDH enzyme activity
Lung	CD44, CD133, ALDH enzyme activity
Brain	CD133, Nestin
Liver	CD44, CD90, CD133, ALDH enzyme activity

Table 1.3: cancer stem cells surface marker [27]

1.3.1 $CD44^{+}/CD24^{-}$ as CSC markers for Breast cancer

CD44 is a 80- to 95-kDa transmembrane protein, which has a role in cell-cell and cell-matrix adhesion [28]. One of the major ligand of CD44 is hyaluronan (HA), which specially supports stemness of hematopoietic cells. The ubiquitinated form of HA can be found in the extracellular matrix in which it supports cell proliferation and migration [29]. CD44 can be involved in the intracellular signaling via cytoplasmic tail. In this regard, the interaction between CD44 and HA induces of matrix metalloproteinase 9 (MMP9) activity, which support the metastasis via their accumulation on cell membrane [30, 31]. In addition, HA-dependent interaction of CD44 and epidermal growth factor receptor (EGFR) is crucial for the cell migration via inducing Akt and Rac1 activity [32]. CD44 has not only a functional role but is one of the most prominent markers of CSCs. The specific role of CD44 on the expression of putative stem cells markers such as Nanog, Oct4 and Sox2 has been shown for several tumor types [33-35]. HA-CD44 interaction leads to the nuclear translocation of Nanog, Sox2 and Oct4 complex, which induce microRNA-302 expression with the final goal of self-renewal and cell survival [34]. Activation of PKC via HA-CD44 interaction leads to the phosphorylation of

Nanog, which induces microRNA-21 production [33]. Moreover, microRNA-21 inhibits the tumor suppressor proteins such as PDCD4 and stimulates chemotherapy resistance of breast cancer cells [33]. These studies highlight the importance of CD44 in stemness, therapy resistance and survival of tumor cells.

1.3.2 Aldehyde Dehydrogenase 1 (ALDH1) as CSC markers for Breast cancer

Nineteen different variants of ALDH have been described to date [36]. ALDH isoforms are expressed in a variety of tissues and especially in tumor cells [37]. ALDH is an enzyme that catalyzes aldehydes to the carboxylic acids. Early studies revealed that bone marrow cells with high ALDH activity are prompted stronger to hematopoietic progenitor lineage cells and enriched in self-renewal potential [38, 39]. In this line, it has been shown that tumor cells with higher ALDH activity are enriched in stem like characteristics [37]. In this regard, high ALDH activity level has been demonstrated as a potential CSC marker in many types of tumors including breast, lung, colon, prostate, brain, and ovary [40]. Various studies on different tumor entities provide evidence that, ALDH-positive subpopulations cells are more tumorigenic than the ALDH negative cells [41-44]. Moreover, clinically high ALDH activity is correlated with poor prognosis [45-47]. The development of a specific flow cytometric assay (ALDEFLUOR), which identifies the activity of ALDH based on fluorescence of the substrate (BODIPY-aminoacetaldehyde). In general this specific assay system has moved stem cell research forward [48].

1.3.2.1 ALDH and retinoic acid biosynthesis

The isoforms ALDH1A1 and ALDH1A3 are able to convert retinaldehyde to the retinoic acid (RA), which regulates the retinoic acid pathway in CSCs [40, 49]. The produced RA then binds to the retinoic acid receptor (RAR) and retinoid X receptor (RXR), which as heterodimer complex can translocate to the nucleus and regulate the expression of more than 500 genes [50]. Based on a negative feedback mechanism this heterodimer complex can regulate ALDH expression [51]. As a consequence when the

concentration of RA is low, the complex binds to the C/EBPß transcription factor in the CCAAT box of the ALDH1 promoter and induces the transcription of ALDH1 gene. Conversely, when the concentration of RA is high, C/EBPß make a complex with GADD153 in order to block the CCAAT box and to reduce transcription of the ALDH1 gene [51]. In general, the retinoic pathway is involved in several functional roles in tumor cells such as epigenetic modifications, tumor growth and apoptosis [50].

1.3.2.2 Role of ALDH in radio- and chemoresistance

Detoxification is one of the functions of ALDH that can protect cells against harmful aldehydes [37]. Analyses of various metabolic syndromes and diseases in which different ALDH enzymes are deficient have demonstrated the role of ALDH for the detoxification role of ALDH [37]. Moreover, the detoxification aspect of ALDH can protect cells to cytotoxic drugs. In this regard, it was first shown that hematopoietic cells with high ALDH activity are resistant to the anticancer agents such as mafosfamide and oxazaphosphorine [52, 53]. Based on these observations, several consecutive studies demonstrated high ALDH activity in various CSCs, which confers their resistance to anticancer agents. For example, ALDH-positive populations of mantel cell lymphoma (MCL) are resistant to a variety of chemotherapeutic drugs [54]. On the contrary, inhibition of ALDH activity improves therapy response of high-grade ovarian cancer [55]. Moreover, data from over 100 breast cancer patients indicated, that ALDH-positivity of tumor cells was related to paclitaxel and epirubicin resistance of the corresponding patients [41]. Likewise, it has also been shown that ALDH activity is one of the predictors for paclitaxel and epirubicin response in breast cancer patients [56]. Regarding the role of ALDH in resistance to radiotherapy, it has been demonstrated that subpopulations of $HER2^{+}CD44^{+}CD24$ tumor cells presenting high ALDH activity are radioresistant [57]. Moreover, post-treatment of irradiated breast cancer cells with disulfiram, which inhibits ALDH activity, leads to the suppression of stemness gene expression and stem like features [58].

1.3.2.3 Regulation of ALDH1 activity and gene expression

The responsible molecular mechanisms, which regulate ALDH activity and gene expression, are not completely discovered so far. Based on functional characterization of ALDH1 promotor, the CCAAT box as the main mediator of ALDH promotor activity has been identified in Hep3B cells [59]. It has been shown that the oncogenic subunit of mucin 1 (MUC1-C) via ERK signaling can bind to the C/EBPß transcription factor, subsequently this complex can bind to the CCAAT box of ALDH1A1 promoter as shown for breast cancer cells [60]. Regarding to these findings, a pathway of MUC1-C/ERK/ C/EBPß regulates ALDH1A1 gene expression in breast cancer cells. Moreover, the role of C/EBPß transcription factor has been identified not only on ALDH1A1 gene regulation but also on ALDH1A3. It has been shown that C/EBPß in a complex with DDIT3 cannot bind to CCAAT box, which leads to a reduction of ALDH1A3 gene expression [61]. In this context, it has been demonstrated that inhibition of STAT3-NFkB activity results in the formation of DDIT- C/EBPß mediates sensitivity of ALDH1A3-positive cells to pemetrexed and cisplatin [61]. These findings support the prominent role of STAT3-NFkB pathway on ALDH1A3 regulation. Similarly, a complex of ß-catenin and T-cell factor (TCF) transcription factors can induce radioresistance of prostate cancer cells via direct gene regulation of ALDH1A1 [62]. In this study, cells transfected with ß-catenin siRNA were sensitized to ionizing radiation [62]. It also has been shown that transforming growth factor ß (TGF-ß) negatively regulates transcription of ALDH1A1 gene [63]. The complex of Smad4 and Smad2/3, the main mediator of TGF-ß action, can bind to the regulatory region of ALDH1A1 gene, resulting in reduced proportion of ALDH-positive cells of pancreatic tumor cell populations [63]. Moreover, epigenetic regulation of ALDH1A1 by BRD4 proteins, a member of BET protein family, which recruits the transcriptional machinery, has been recently identified [64, 65]. Importantly, clinical application of a small molecule inhibitor of BRD4 successfully suppressed the ALDH1A1 gene expression in ovarian cancer cells [65]. In this context it has been shown that treatment with a BRD-4 inhibitor abrogated the chromatin loop formation between promoter and enhancer of the ALDH1A1. This result confirms the importance of BRD4 as a regulatory factor for gene expression of ALDH1A1 [65]. In this study, Yokayama and coworkers [65] also

provided evidence for the translational potential of BRD4 antagonists as the combination of BRD4 inhibitor and cisplatin efficiently improved survival rate of tumor bearing mice and suppressed the regrowth of cisplatin-treated tumors in vivo and in vitro.

One of the regulatory mechanisms of ALDH1 expression is posttranslational modification. In this regard, the lysine 353 (K353) acetylation site has a regulatory role in ALDH1 enzyme activity [66]. Breast cancer cells with reduced levels of ALDH1A1 acetylation show increased ALDH1 activity, which leads to a improved self-renewal capacity [66]. It has been shown that P300/CBP-associated factor (PCAF) as an acetyltransferase is responsible for K353 acetylation of ALDH1A1. In contrast, sirtuin 2 (SIRT2), which as downstream protein of the Notch1 pathway modulates deacetylation at K353 of ALDH1A [66]. This result implies that Notch promotes stemness feature of breast cancer cells via a SIRT2-dependent deacetylation of ALDH1A1 (Fig.1.5). Similarly, the binding of sphingosine-1-phosphate (S1P) to the related receptor (S1PR3) induces ALDH-positive populations and thus cancer stem cells (CSCs) in MCF-7 cells via ligand-independent Notch1 induction [67].

1.3.3 Nanog as putative stem cell marker

Nanog is one of the transcription factors, which has a crucial role in self-renewal capacity of stem cells. In 2003 Nanog has been discovered by Ian Chambers and Kaoru Mitsui and coworkers in mouse embryonic cells [68, 69]. Based on their studies, Nanog has the potential to maintenance the self-renewal capacity of embryonic cells independent of the LIF/Stat3 proteins [69]. The human Nanog gene is located on chromosome 12 at 12p13.31 known as Nanog1 [70]. In addition, there are several pseudogenes of Nanog, which contain premature stop codons inhibiting transcription and translation to the functional protein [71]. There is only one pseudogenes of Nanog, NanogP8, which encodes the functional protein with differences in 3 amino acids [72]. The 305 amino acids length protein of human Nanog consists of three domains including the N-terminus (94 amino acids), homeodomain (60 amino acids) and C-terminus (151 amino acids) [72, 73]. It has been shown that the C-terminal domain of

Nanog contains a tryptophan-rich region, which has a role in homodimerization and nuclear export of Nanog protein. The C-terminal subdomain also plays a role in transactivation of Oct4 promotor and transcriptional activity of Nanog [73]. In contrast, the N-terminal domain has a gene interference role in the transcriptional function of Nanog [73]. Moreover, homeodomain of Nanog consists of a region with six amino acids (^{136} YKQVKT ^{141}), which exerts a specific role in nuclear translocation of Nanog [73]. It has been demonstrated that Nanog in a complex with other transcription factors including Oct4, Sox2 and Lin28 provide the self-renewal capacity of stem cells or can reprogram differentiated somatic cells to the stem like state [74]. It has been reported that serin 315 phosphorylated P53 can bind to the promoter of Nanog and downregulate the gene expression in embryonic cells. In this regard, P53 can suppress the self-renewal capacity in order to decrease the genomic instability of cells under DNA damage stress [75]. Similarly, the regulatory role of P53 on Nanog has been shown in brain CSCs as well [76]. Based on this study, Nanog can promote the stemness feature in P53 deficient mouse astrocytes [76]. It has been reported that Gli and GLI family zinc finger 2, as downstream component of the Hedgehog pathway can activate the transcription of Nanog gene and as a consequence can induce self-renewal of neural stem cells [77]. The direct interaction between Nanog and Stat3 has been shown [78, 79]. Based on these findings, this complex can translocate to the nucleus and activate production of microRNA-21, which results in downregulation of tumor suppressor proteins including PDCD4 in head and neck (H&N) squamous carcinoma cells [78]. Moreover, the phosphorylated form of Stat3 can bind to the Nanog enhancer region in order to induce the expression of Nanog in mouse embryonic cells [79].

Yet, Nanog does have a role not only in embryonic cells but also in tumor cells. Several studies have identified the role of Nanog in CSCs of different types of tumors [80-83]. In this regard, it has been shown that NanogP8 similar/comparable to other stem cell factors including Oct4 and Sox2 has a direct function in stemness of colorectal cancer cells [80]. Moreover, isolated hepatocellular carcinoma cells positive for Nanog, exert a stronger ability for self renewal, tumorigenesis as well as resistance to chemotherapeutic agents sorafenib and cisplatin [81]. It has also been demonstrated that high expression of Nanog together with Oct4 leads to an epithelial-mesenchymal transition, which is related to the stemness and tumorigenic potential of lung adenocarcinoma [83]. Based

on these studies, Nanog is not only a CSCs marker, which regulates stemness but is also involved in various regulatory functions mediating metastasis, proliferation and apoptosis [84-86]. In addition, overexpression of Nanog leads to upregulation of ATP-binding cassette sub-family B member 1 (ABCB1), which is one of the resistance strategies of lung adenocarcinoma cells in order to tolerate the chemotherapy including cisplatin treatment [83]. Likewise, complex formation of Nanog and Stat3 in breast and ovarian cancer cells can activate the expression of multidrug transporter (MDR1) gene, which mediates chemoresistance [35].

1.3.4 Functional assays for cancer stem cells

Several methodologies have been developed over the last years in order to overcome the challenges regarding identification, isolation and characterization of CSCs subpopulation within a tumor population. Tumorigenicity of CSCs in immune-deficient mice is one of the gold standard functional assay for characterization of CSCs [87]. Tumor cells that not only have the capacity to initiate a new growing tumor population in vivo but are also serially transplantable resemble CSCs. It has been shown that the ratio of CSCs in a tumor is less than one into 2500 cells [88]. However, several limitations of the in vivo model have been observed including the short life span of mice and reversibility of CSCs phenotype in the mouse microenvironment when compared to the human situation [87, 88]. The ability of CSCs to form a sphere under defined culture conditions is one of the routine in vitro methods to assess the self-renewal potential [87]. This method has been developed from the neurosphere culture, which has been used for maintenance of brain stem cells [87]. For the first time in 2004 Galli and coworkers could demonstrate self-renewal capacity of glioblastoma cells under sphere forming conditions [89]. Various conditions of sphere formation as standard methods for CSCs studies have been developed including culture technics in low adherent dishes with a covalent hydrogel surface to allow cells grow in sphere not in an adherent form. Likewise other culture technologies involve growth factors such as epidermal, fibroblast (EGF, FGF) and B27 supplemented medium or culture technics in matrigel, which consists of extracellular matrix proteins resembling tumor matrix conditions [90]. However, none of these methods do represent so far the in vivo tumor

microenvironment, which in several studies has been reported as one of the drawbacks of the sphere formation assay [90].

1.4 Radio- and chemoresistance of cancer stem cells

Based on various studies [91-93], therapy resistance of CSCs seems to be related to cell biological features including low proliferation capacity, adaptation to hypoxic conditions, activation of drug efflux systems (i.e. ABC transporters), improved DNA repair capacity, epithelial to mesenchymal transition (EMT), and upregulation of several survival pathways. As reviewed by Nunes and co workers [91] various signaling pathways, which are activated in CSCs of various tumor types like PI3K/Akt and NOTCH as well as WNT/β-catenin, Hedgehog and JAK/STAT seem to be involved in the regulation of radio- and/or chemoresistance of CSCs.

1.4.1 PI3K/Akt pathway

PI3K/Akt pathway can be activated by a variety of growth factors and cytokines including EGFR, VEGFR, PDGFR or Ras and G-protein coupled receptors (GPCRs) [94]. PI3K belongs to the family of lipid kinases and phosphorylates the inositol ring of phospholipids [94]. The PI3K family has been categorized into four different classes named I, II, III, IV [94, 95]. Among these different PI3K classes, it has been demonstrated that primarily class I PI3K is involved in growth factor related proliferation signaling and tumor growth [94, 95]. PI3K is a heterodimeric protein, which consist of regulatory and catalytic subunits named p85 and p110 respectively [94, 95]. Class I PI3K has been divided to 2 further subclasses including Ia and Ib. Subclass Ia is mainly involved in signaling pathway related to the tyrosine kinases and RAS, while Ib is involved through GPCRs activation [94, 95]. The regulatory subunit is responsible for the connection of the PI3K to the upstream mediators, while the catalytic subunit generates the lipid messenger phosphatidylinositol 3,4,5-trsphosphate (PIP3) [94, 95]. In this regard, PIP3 plays a role in activation of various proteins that have a phenylalanine-tyrosine-valine-glutamate (FYVE) domain, including PDK1 and Protein Kinase B (PKB/Akt) [94].

Akt, as one of the downstream regulators of the PI3K pathway, consists of three isoforms Akt1, Akt2, Akt3. Akt isoforms share 80% similarity in a conserved amino acid sequences that include the N-terminal, central kinase and C-terminal domains [96]. The three isoforms play different roles in cellular functions. Akt1 is mainly involved in cellular growth, while Akt2 has a role in glucose metabolism [96]. The Akt molecule contains a specific catalytic domain that can regulate downstream pathways. Several phosphorylation sites have been identified on Akt1 including T308 (located in kinase domain), S473 (located in C-terminal domain) [97-99]. Moreover, phosphorylation also can occur in other Akt isoforms such as in Akt2 (T309 and S474) and Akt3 (T305 and S472) [97-99]. PDK1 is the responsible protein for the phosphorylation at T308 site, while the mechanistic target of rapamycin complex2 (mTORC2) phosphorylates Akt1 at S473 site [97, 100, 101]. Once phosphorylated Akt regulates various downstream proteins such as glycogen synthase kinase 3 beta (GSK3ß), forkhead box O transcription factor (FOXO), mouse double minute 2 homolog (MDM2), p21, p27 and Bcl-2-associated death promoter (BAD) [95]. Akt via regulating the activation of downstream proteins plays an important role in cell growth, proliferation and survival [95]. It has been reported that Akt via phosphorylation of GSK-3 at serin 21 and serine 9, which leads to the inactivation of GSK3, plays an important role in cell cycle progression and growth in cancer cells.

More recent studies addressed the role of Akt in DNA-DSB repair pathways such as non-homologous end joining and homologous recombination has been demonstrated in several studies [96, 102]. In irradiated cells, the C-terminal domain of Akt directly interacts with DNA-PKcs, the major enzyme in NHEJ repair, [103-105]. This complex stimulates kinase activity of DNA-PKc at the site of DNA damage, which initiates the DNA repair processes [96]. Moreover, Akt induces the accumulation of DNA-PKcs after irradiation in the nucleus and especially at the DNA-DSB [96]. It also has been shown that Akt indirectly via ATM regulates DNA-PKcs [96]. In this regard, Akt1 and Akt3 mediate ATM-dependent DNA-PKcs phosphorylation in lung cancer cells and glioma cells [96, 102, 106]. Based on these results, activation of upstream proteins of Akt such as erbB receptors, PTEN, Ras and PI3K lead to induction of NHEJ DNA repair capacity in Akt-dependent manner [96]. In addition, it has been demonstrated that activation of Akt leads to MRE11 upregulation and induction of DNA repair [96, 107].

MRE11 compared to DNA-PKcs is involved in the slow component of DNA repair [96]. Thus, Akt plays role in both fast and slow component of DNA repair. The role of Akt in HR DNA repair pathway has been addressed in several studies presenting contradictive results. As demonstrated by Mueck and coworkers, downregulation of Akt1 leads to a reduction of Rad51 protein level and foci formation after irradiation [108]. However, it has also been shown that Akt does impair the nuclear translocation of Chk1 and complex formation of Chk1-Rad51 in Brca1-deficient tumor cells [109]. In addition, high activation of Akt by phosphorylation at serine 473 site is related to BRCA1 deficiency [110].

1.4.2 Notch Pathway

Notch receptor as a single-pass transmembrane protein consists of an extracellular and intracellular region. The extracellular region of Notch contains a negative regulatory domain and a heterodimerization domain. The intracellular region is composed of a protein-binding site named RPBJ-associated molecule (RAM) and a transcriptional activation domain [111]. In mammals different coding genes give raise to four different types of Notch receptors (Notch1-4) [111] and among them, Notch1 and Notch2 are the most common Notch receptors, which are expressed in a wide range of tissues. Notch3 and Notch4 receptors are primarily expressed in vascular smooth muscle and endothelium only [111]. Ligand binding to the Notch receptor induces protease activity of γ-secretase, which cleavages the receptor and releases Notch intercellular domain (NICD), which results in activation of Notch [112]. NICD can translocate to the nucleus, which binds to DNA via the RAM domain in order to regulate the transcriptional activity of downstream target genes including p21, cyclin D1, c-Myc, NF-kB2, ErbB2 and apoptosis regulator genes [111-117]. Upregulation and ligand activation of Notch seems to be associated with progression of various tumors via overexpression of cyclin D1 [118]. Furthermore, Notch represses expression of cell cycle inhibitor proteins such as p27 and p57, which induce cyclin D1 [119]. In this line, it has been shown that Notch via direct induction of c-Myc leads to cell proliferation [120]. Moreover several studies indicated that Notch via cross talks with other signaling pathways including PI3K/Akt, Ras and EGFR73 does activate cell survival and

proliferation of tumor cells [121, 122]. In addition, the regulatory function of Notch on tumor expression of suppressor genes has also been investigated with respect to the downregulation of p53 and PTEN activity, which are involved in apoptosis [121, 123]. Moreover, Notch via HIF-1 signaling can lead to VEGF expression, which is a crucial protein for blood vessels development in tumors [124]. Several studies have demonstrated the role of Notch in chemo- and radioresistance of tumor cells. It has been shown that combination therapy with Notch inhibitors increases colon cancer cell sensitivity to treatment with oxaliplatin or taxanes [125]. Additionally, it has been observed a Notch mediates chemoresistance of tumor cells of ovarian cancer and hepatocellular carcinoma to cisplatin and doxorubicin [126, 127]. Likewise, Notch via overexpression of survivin leads to the inhibition of apoptosis in breast cancer cells [128] and the combination of Notch inhibitor and trastuzumab is able to sensitize HER2-positive breast cancer cells [129]. As Notch is one of the major regulators of cancer stemness, inhibition of Notch (e.g. by Notch inhibitors GSI or a Notch4 monoclonal antibody) in combination with gefetinib impairs sphere formation of breast CSCs [93]. This study demonstrates the correlation of EGFR and Notch pathway in CSCs maintenance. In addition and of special interest for the present study, GSI treatment impairs tumor cell radioresistance and Notch knockdown combined with Akt inhibitor induced cell death of glioma CSCs[130, 131].

Figure 1.5 presents a schematic illustration of regulation of ALDH activity and Akt signaling and the impact of these processes on resistances mechanisms of tumor cells. The question marks illustrate the aspects to be investigated in the present thesis, which are defined in the following hypothesis.

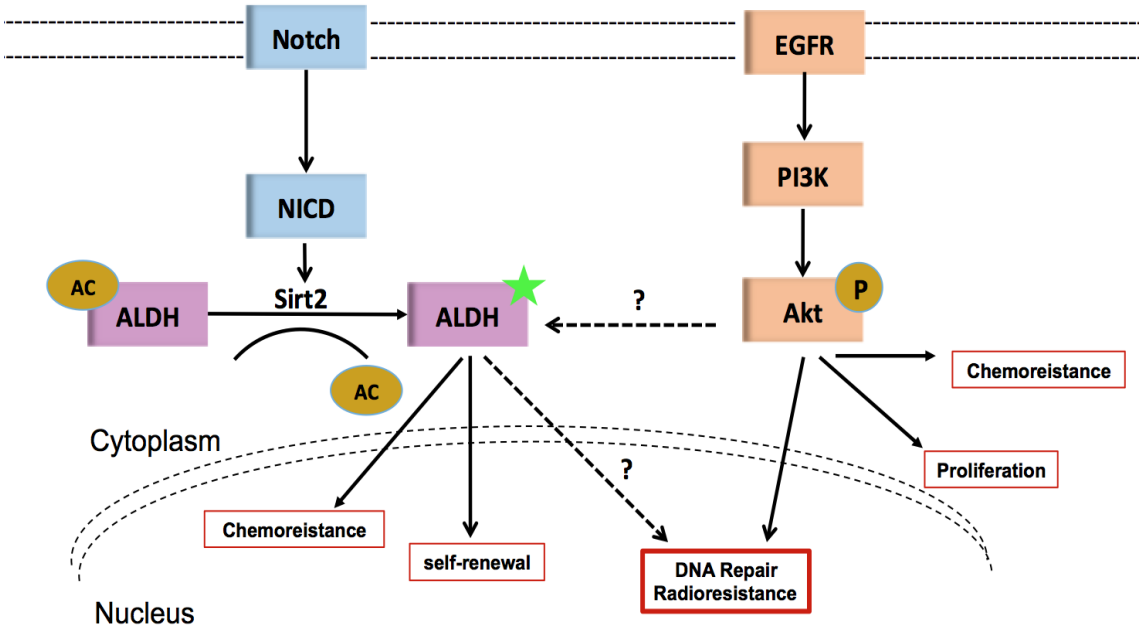

Fig. 1.5: Summary of function of PI3K/Akt and Notch in the regulating ALDH activity and radiation response of CSCs. Notch promotes stemness features via a SIRT2-dependent deacetylation of ALDH1A1. PI3K/Akt mediates the regulation of radio- and/or chemoresistance of CSCs.

1.5 Hypothesis

Hyperactivation of the PI3K/Akt pathway occurs in many tumor entities presenting mutations in epidermal growth factor receptor (EGFR) downstream signaling i.e. as phosphatase and tensin homolog (PTEN), PIK3CA and Ras [96]. PI3K/Akt pathway activity is involved in majority of hallmarks of cancer including cell proliferation, survival and metabolism. In the context of tumorigenesis these functions are well described nevertheless, the importance of PI3K/Akt signaling in radioresistance through stimulating DNA-DSB repair predominantly through the NHEJ-mechanism has been highlighted [96]. Furthermore, evidence from experimental and clinical studies indicates that cancer-initiating cells, or cancer stem cells (CSC), are resistant to radiotherapy [91]. Among various CSC markers, the role of ALDH activity has been highlighted in the last decades. As reported in different studies [56-58], stimulated/increased ALDH activity leads to radioresistance of CSCs in various tumor

entities. Likewise, Sirt2-dependent deacetylation of ALDH promotes its enzyme activity and stimulates stemness feature of breast cancer cells [66]. Moreover, the enhanced CSC phenotype is also described to be associated with the activation of the PI3K/Akt/mTOR pathway in radioresistant prostate cancer cells (Fig. 1.5) [92]. Specifically, it has been demonstrated that the expression of Akt1 and Akt2 increases after irradiation of MCF-7 breast cancer [132]. Thus, it seems that Akt isoforms and ALDH activity, through an as of yet unknown mechanism, are involved in radioresistance of CSCs. It is assumed that CSCs with high ALDH activity (ALDH-positive cells) are more radioresistant than tumor bulk cells and that they present hyperactivated PI3K/Akt pathway. In this regard, a previous study from our laboratory has indicated that a selected radioresistant subpopulation of NSCLC-A549 cells and of the breast cancer cell line SKBr3 presenting high level of ALDH1 can be radiosensitized by the PI3K inhibitor LY294002 [133]. Furthermore, it has been reported that targeting EGFR as the major regulator of PI3K/Akt pathway blocks repair of DNA DSB and enhances the radiation response of tumor cells [134]. Thus, based on the role of ALDH-positive cells in cancer stemness and the role of Akt isoforms in radioresistance, the major focus of this project was the investigation of the function of PI3K/Akt signaling in radioresistant ALDH-positive breast cancer cells. Therefore, the aim of the thesis was to answerd the following questions:

I. What is the role of Akt isoforms and ALDH activity in DNA repair and radioresistance?

II. Do Akt isoforms regulate ALDH activity and the expression of CSC markers?

III. What is the function PI3K/Akt pathway and other CSC markers on ALDH activity?

IV. Are Akt and/or other CSC markers critical for radioresistance of ALDH positive tumour cells?

2 Materials and Methods

2.1 Materials

2.1.1 Equipments

The following instruments were used in this study

Equipment	Company
Analytical balance	Kern & Sohn
Binocular	Carl Zeiss
Cell counting chamber	Fuchs-Rosenthal - Witeg Labortechnik
Detection machine – western blot	LI-COR
Drying Incubator	Heraeus
ELISA-Reader	Anthos Labtec Instruments
Electrophoresis	Hoefer
Flow cytometer	BD Bioscience
Incubator	Binder, Heraeus
Light microscope	Leitz
pH-Meter	WTW
Semi-Dry-Blot-System	Hoefer
Tissue Grinder Comp	Thomas Scientific
Vortexer	UniEquip
X-Ray irradiation device	Gulmay

2.1.2 Chemicals

Chemicals	Company
Acetic acid	Merk
Acrylamide	Roth
Agarose	Sigma-Aldrich
APS	Aldrich

β-Mercaptoethanol	Sigma-Aldrich
Bromphenol blue	Pharmacia Biotech
BSA	Roth
DMSO	Sigma-Aldrich
DTT	Sigma-Aldrich
EDTA	Sigma-Aldrich
Ethanol	Merk
Formaldhyde	Merk
HCL	Roth
NP-40	Sigma-Aldrich
Ponceau S	Sigma-Aldrich
Sodium dodecylsulfate (SDS)	Serva
Sodium chloride	Merk
TEMED	Sigma-Aldrich
Triton X-100	Sigma-Aldrich
Tris-base	Sigma-Aldrich
Tris-HCL	Sigma-Aldrich
Tween 20	Roth

2.1.3 Other materials: biochemical and kits

Biochemical and kits	Company
ALDEFLUOR assay	Cell signaling
DC protein assay reagents (A, B)	BioRad
ECL detection kit	Amersham Pharmacia Biotech
Nitrocellulose membrane	Roth
Phosphatase inhibitor cocktail 2,3	Sigma-Aldrich
Protein standard (ladder)	BioRad
Protease inhibitor	Roche
Propidium iodide	Roth
Vectashield Mounting Medium (DAPI)	Vector Laboratories
Watmann paper	Schleicher & Schüll

2.1.4 siRNA, Plasmids and Inhibitors

siRNA, Plasmid, Inhibitors	Company	Catalog Number
ALDH1 siRNA	Dharmacon	L-008722-00-0005
Akt1 siRNA	Dharmacon	M-003000-03-0005
Akt2 siRNA	Dharmacon	M-003001-02-0005
Akt3 siRNA	Dharmacon	M-003002-02-0005
DEAB	Sigma-Aldrich	D86256
LY-29004	Calbiochem	440202-5MG
MK-2206	Selleckchem	S1078
Nanog siRNA	Dharmacon	M-014489-02-0005
Notch1 siRNA	Dharmacon	M-007771-02-0005
Nanog Plasmid	Addgene	#28221
Non-targeting siRNA	Dharmacon	D-001206-13-05

2.1.5 Cell culture materials and cell lines

Cell culture materials:

Cell culture materials	Company
1, 2, 5, 10 and 25 mL sterile pipets	Costar
6 wells plates	Falcon
60 and 150 mm tissue culture plates	Falcon
DMEM/RPMI meduim	Gibco
FBS	PAN-Biotech / Lot No: P170102
Four chambers polystyrene culture slide	Falcon
LipofectamineTM 2000	Invitrogen
Matrigel	Corning BD
Optimem Meduim	Gibco
Penicilin-Streptomycin	Gibco

T-25 and T-75 tissue culture flasks	Falcon
Trypsin	Serva

Cell lines:

Cell line	Tumor Type	AACR Number/Company
A549	Lung	CCL-185
DU145	Prostate	A gift from Prof. Yasufumi
DU145 Nanog1-/-	Prostate	Kaneda and Prof. Keisuke Nimura
HBL-100	Breast	HTB-124
HCT116 parental	Colon	Horizon Discovery/ HDPAR-007
HCT116 Akt1-/-	Colon	Horizon Discovery/ HDRO-004
HCT116 Akt2-/-	Colon	Horizon Discovery/ HDRO-005
MDA-MB-231 Akt1,2,3 KD	Breast	A gift from Prof. Manfred Jücker
MCF-7	Breast	HTB-22
NM2C5	Melanoma	CRL-2918
SKBR3	Breast	HTB-30

2.1.6 Antibodies

Antibodies	Company	Catalog Number
Actin	Sigma-Aldrich	A2066
ALDH1	Cell signaling	36671
Akt1	Cell signaling	2967
Akt2	Cell signaling	2964
Akt3	Cell signaling	8018
Alexa Fluor 488 goat antimouse	Life technologies	A11001
Bmi-1	Cell signaling	5856
GAPDH	Cell signaling	2118
HRP-linked sheep anti mouse	GE Healthcare	NA931
HRP-linked sheep anti Rabbit	GE Healthcare	NA934

Lamin A/C	Abcam	40567
Nanog	Cell signaling	3580
Notch1	Cell signaling	3608
Oct-4	Cell signaling	75463
P-Akt (S473)	Cell signaling	4060
P-H2AX (S139)	Millipore	05-636
Sirt-2	Cell signaling	12672
Sox2	Cell signaling	4900

2.1.7 Buffers and solutions

Anode buffer	3.10 g boric acid 4 ml 10% SDS 200 ml methanol 1 l ddH2O pH 9.0
Cathode buffer	3.10 g boric acid 4 ml 10% SDS 50 ml methanol 1 l ddH2O pH 9.0
DMEM medium	12.04 g DMEM 3.30 g NaHCO3 900 ml ddH2O pH 7.2
RPMI meduim	9.38 g RPMI-1640 1.80 g NaHCO3 900 ml ddH2O pH 7.2

Lysis buffer	3.94 g Tris-HCl 5.40 g ß-glycerol phosphate 4.38 g NaCl 0.09 g Na3VO4 50 ml glycerol 5 ml Tween-20 0.02 g NaF 500 ml ddH2O / pH 7.5
Lysis buffer Cytoplasmic/Nuclear extraction (Buffer A)	300 µl Hepes (1M) 150 µl KCL (1M) 30 µl MgCl2 (1M) 75 µl NP40 (10%) 14450 ml ddH2O
Lysis buffer Cytoplasmic/Nuclear extraction (Buffer B)	100 µl Tris-HCl (1M) 150 µl NaCl (5M) 50 µl EDTA (100 mM) 25 µl NP40 (10%) 4650 ml ddH2O
PBS	13.7 mM NaCl 2.7 mM KCl 80.9 mM Na2HPO4 1.5 mM KH2PO4 pH 7.4
Protein loading buffer	20 ml glycerin 20 ml 10% SDS 2.50 mg bromophenol blue 25 ml stacking gel buffer (4x) 95 ml ddH2O

	56.2 µl β-mercaptoethanol per 1000 µl
SDS running buffer (5x)	144.10 g glycin 30.30 g Tris-base 10.00 g SDS 2 liter ddH2O pH 8.6
Separation gel buffer (4x)	90.85 g Tris-base 20 ml 10% SDS 500 ml ddH2O pH 8.8
Stacking gel buffer (4x)	30.30 g Tris-base 20 ml 10% SDS 500 ml ddH2O pH 6.8
Staining solution	0.50 g crystal violet 27 ml formaldehyde 1 liter PBS
Stripping buffer	4.50 g glycin 3 ml 10% SDS 3 ml Tween-20 300 ml ddH2O pH 2.2
TBST	3.15 g Tris-HCl 11.70 g NaCl 2 ml Tween-20 2 liter ddH2O

	pH 7.5

2.2 Methods:

2.2.1 Cell culture

Cell lines:

In the current thesis, several human breast, colon (HCT116), prostate (DU145) and lung (A549) cancer cell lines as well as melanoma (NM2C5) were used. SKBR3, MCF-7, MDA-MB-231 and HBL-100 cells are breast cancer cell lines derived from metastatic site of mammary gland.

Culture media:

Cells were cultured in RPMI (MCF-7, HBL-100, SKBR3, HCT-116) or DMEM (A549, MDA-MB-231) supplemented with 10 % fetal bovine serum (FBS, PAN Biotech) and 1 % penicillin/streptomycin (pen/strep). The cells were incubated in 37 ^{0}C / 5% CO2 and passaged weekly when the cells reached 80-100 % confluency.

2.2.2 Colony formation assay

In order to determine the post irradiation cell survival in vitro, the ability of single cells to form a clone after ionizing radiation were evaluated under 2D culture. In order to perform pre-plated colony forming assay, cells were seeded in a very low concentration (250-500 cells per 6 well plates) in supplemented medium with 20 % FBS in 6 well plates to form single colon. Twenty-four hour after seeding, cells were irradiated (0-4 Gy). Then the cells were incubated for 10-20 days, depending to the type of cells. In the experiments that cells were treated with inhibitors (DEAB or MK-2206), the treatments were done 24 hours after seeding cells as single cells and next day of treatment (for DEAB treatment) or 2 hours later (for MK-2206 treatment), cells were irradiated. When cells formed colonies in the size of 50 cells or bigger in control group (0 Gy), cells were washed with PBS and fixed with staining solution containing formaldehyde and crystal

violet color. The staining solution was incubated for half an hour on the cells and then the color washed out by drowning plates in water. After drying the plates, colonies, bigger than 50 cells, were counted per well. Plating efficiency (PE) is calculated based on counted colonies divided to the number of seeded cells. The surviving fraction curves were obtained by Sigmaplot software.

2.2.3 3D sphere formation assay

In order to assess the stemness feature of cells, the sphere formation ability of cells under 3D-culture were applied. 96 well plates were coated with 1 % agarose (50 µl) and were cooled down. Suspended cells in a defined concentration were mixed with medium and 10% matrigel (5mg/ml) in a total volume of 100 µl per well and splitted on the coated wells. Four hours after seeding cell suspensions with matrigel, 100 µl meduin were added in order to overlay the 3D-culture. In order to avoid drying of upper medium layer, the outer wells were filled with 200 µl PBS.

In order to find the proper concentration of cells which allows the formation of individual spheres without merging with neighboring spheres, different cell numbers (500, 1000, 2000, 3000 and 4000 cells per well) were seeded and after 8-20 days the concentration with the best platting efficiency has been chosen. Irradiation (0-6 Gy) 24 hours after seeding the mentioned concentration of cells has been applied. Based on this setting, following cell concentrations have been used for further experiments:

Cell line	Number per well	Incubation days
MCF-7	4000	12
MDA-MB-231	2000	9
SKBR3	4000	20

In order to receive single cell suspensions from spheres formed in matrigel for further experiments (i.e. flow cytometery), spheres were incubated in 5mM EDTA/PBS solution for 20 min on ice. Solution was then centrifuged (5 min, 200g, 4^0C) and the

pellet was resuspended in 2 ml trypsin/EDTA for 10 min at 37^0C on the shaker. In next step, the resuspended solution was centrifuged (5 min, 200g, 4^0C), the supernatant was removed and cells were further processed for flow cytometery or western blotting.

2.2.4 ALDEFLUOR Assay

Aldefluor assay is a flow-cytometry-based assay to measure the activity of ALDH enzyme. Based on this assay, ALDH enzyme is able to catalyze an artificial ALDH substrate called BODIPY-aminoacetaldehyde (BAAA) to its fluorescent product (BODIPY-aminoacetate (BAA)), which can be measured by flow cytometry. In advance, the mixture of activated Aldefluor reagent and assay buffer in the concentration of 0.625 µl/125 µl were prepared and kept on ice. After preparation of cell suspensions in concentration of 250000 per FACS tube, cells were washed with PBS (one time). The ready mixed buffer of Aldefluor reagent and assay buffer were added on the cells (125 µl per FACS tube). Cells were incubated for 40 minutes in 37^0C incubator. After incubation, cells were washed 2 times with assay buffer and then mixture of assay buffer and 1 µg/mL propidium iodide (PI) color were added on the cells (100 µl per tube). FACS tubes were kept on ice in dark condition. Thereafter, fluorescence signal was measured by flow cytometery.

The negative sample/tube is treated with 40 µM DEAB. In this regard, first DEAB was added in an empty tube and the mixture of cells with activated Aldefluor reagent was then added to the DEAB. The negative sample was incubated under the same condition as the test samples.

Tube	Cell number	Activated Aldefluor reagent	Assay buffer	DEAB
Negative	250000	0.625 µl	125 µl	40 µM
Test	250000	0.625 µl	125 µl	---

2.2.5 Flow cytometery / cell sorting

In order to measure fluorescence signal, side and forward scatters (SSC, FSC) of unstained cells, based on the size of cells, were adjusted and the first population (P1) was gated. The next population, based on negative signal of PI color (less than 10^3), was gated as living cells (P2) after P1. Thereafter, single cells were gated based on the ratio of height to area/(width) as P3. In the last step, cells with low FITC signal were gated as ALDH negative population and cells with high FITC signal were gated as ALDH positive population. In order to identify the low FITC signal parameter, DEAB treated cell sample was measured.

The same strategy of gating was applied for sorting the cells. Since, cells pump out the fluorescence signal very fast over 2-3 hours of sorting, cells had to be aliquoted in FACS tubes (1 million cells /100 µl) and kept on ice. By this strategy, cells are longer on ice and the activity of ABC transporters is reduced. In the next step, in order to avoid the influence of loosing fluorescence signal with respect to the purity of sorting, a distance between the gating of negative and positive populations was implicated. The collection tubes contained sterile RPMI medium supplemented with 10 % FBS and 1 % pen/strep. After sorting cells were washed with fresh medium and then seeded for the aimed experiments.

2.2.6 Irradiation of cells

Irradiation was performed by Gulmay RS225 X-ray machine using a 0.5-mm copper filter with additional settings of 200 kVp, 15 mA. X-ray irradiation has been performed based on following settings:

Gy	Time	Distance to the source
1 Gy	1.06 min	50 cm
2 Gy	2.12 min	50 cm
3 Gy	3.18 min	50 cm
4 Gy	4.24 min	50 cm

5 Gy	5.30 min	50 cm
6 Gy	6.36 min	50 cm

2.2.7 siRNA/plasmid transfection

In order to assess the role proteins of interest, the expression of specific proteins was either downregulated or upregulated by siRNA/plasmid transfection. Stock concentration (20 µM) of siRNA was prepared by adding 250 µl of 1X siRNA buffer to 5nM siRNA powder. Then the mixture was aliquoted in 20 µl per tube and kept in -20^0C freezer. In all experiments, the end concentration of siRNA in which cells were treated was 50 nM. Cells were seeded in 6 well plates or 6 cm dishes in a concentration that the confluency of cells is around 60-70 % on the following day. For transfection of siRNA and plasmids the following mixtures were prepared.

Mix A	6 well plates (µl)	6 cm dishes (µl)
Optimem	48	120
Lipofectamin	2	5
Total Volume	50	125

Mix B1	6 well plates (µl)	6 cm dishes (µl)
Optimem	47.5	113.75
Target siRNA Nanog/ALDH1/Notch1	2.5	6.25
Total Volume	50	125

Mix B2	6 well plates (µl)	6 cm dishes (µl)
Optimem	47.5	113.75
Non-target siRNA (Ctrl)	2.5	6.25
Total Volume	50	125

Lipofectamin was incubated for 5 min with optimum (Mix A), the solution was added to target and control siRNA mixture (Mix B1 and B2). Then the tubes were incubated for 20 minutes in room temperature. During the 20 minutes incubation, the previous culture medium was changed with fresh medium (without pen/strep). After the incubation the mixture of siRNA and lipofectamin was added drop by drop to the cells. The following table indicates the required volume of medium and siRNA:

	6 well plates	6 cm dishes
Volume of final transfection mixture	100 µl	250 µl
Volume of fresh medium	900 µl	2250µl

Twenty-four hours after transfection, medium was changed and forty-eight hours after transfection cells were used for the aimed experiment, such as colony forming assay, Aldefluor assay, residual γH2AX and western blotting. Nanog plasmid (450 ng/µl) transfection were performed with the same protocol as for siRNA transfection.

Cotransfection of Nanog plasmid and Akt/Notch1 siRNA:

Twenty-four hours after seeding cells, Nanog plasmid was transfected. Twenty-four hours after Nanog transfection, Akt/Notch1 siRNA were transfected and next day the protein were isolated or cells were used for FACS and colony formation assay.

2.2.8 Residual γH2AX assay

In order to determine the efficiency of DNA-DSB repair after irradiation, the formation of residual γH2AX at the site of break in the nucleus were imaged by immunofluorescence staining. Cells were seeded in 4 chamber slides in concentration of 80000-150000 cells per well depending to the type of cell line. 24 hrs later cells were irradiated with 0 and 4 Gy and 24 hours after irradiation cells were fixed with 70 % ethanol. For the experiments with Nanog transfected cells, cells were irradiated 24 h after transfection and 48 h after irradiation cells were fixed with ethanol.

Staining fixed cells for residual H2AX:

Fixed cells were washed two times with cold PBS and then cells were permeabilized for 10 minutes with 500 µl cold solution of 0.1% Triton/PBS. After permeabilization, cells

were washed with cold PBS and blocked with 3% BSA/PBS solution for 30 minutes. After blocking, cells were incubated for one hour with the primary antibody of phospho-ser139 H2AX in 1:500 concentration with solution of 1% BSA/PBS. After primary antibody incubation, cells were washed three times with cold PBS and then incubated for 45 minutes with fluorescence conjugated secondary antibody (anti-mouse) in concentration of 1:500 in a dark place. After incubation with secondary antibody, cells were washed two times with cold PBS and then a drop of DAPI containing solution (Vectashield) was added to the cells. In the last step, cells were covered with a glass and kept in dark box under cold temperature (+4^{o} C). Cells were imaged by fluorescence microscope in two different colors including Alexa flour 488 (H2AX) and DAPI (nucleus).

2.2.9 SDS-PAGE and Western blotting

SDS-PAGE is a conventional technique for the separation of proteins according to their molecular weight. Western blotting is a method to define the expression of different proteins under various treatment conditions in the cells by specific antibodies. In this regard, the differences in the expression of interest proteins were determined after applying the treatment such as siRNA or plasmid transfection as well as irradiation. Before protein extraction, 5 ml lysis buffer were mixed with 50 µl phosphatase inhibitor II, 50 µl of phosphatase inhibitor III, half tablet of protease inhibitors and 5 µl DDT. Western blot were done in different steps as described bellow:

Protein isolation:

The cells were washed 2 times with cold PBS. The rest of PBS was sucked out completely with vacuum. Then the prepared lysis buffer was added on the cells (200µl per 6 cm dishes for 70-80% confluent cells, and 350 µl per 6 cm dishes for 90-100% confluent cells). Cells were scratched with cell lifter and collected in tubes on ice. In next step, cells were sonicated 20 times at low power and centrifuged 15 min, 14000 rpm, 4°C. Supernatants which has protein extraction were collected.

Protein concentration measurement:

ELISA 96 wells were filled with 5 µl BSA standards (0, 1, 2, 4, 6 and 8 µg) and 5µl of extracted proteins (all have to be triplicate) and then 25 µl of buffer A and 200 µl of buffer B from protein reagent assay kit were added. After 7 min of incubation, the optical density (OD) was measured by ELISA reader. The protein concentration was calculated based on standard curve and obtained OD. After finding the concentration of proteins, 100 µg protein were mixed with the equal volume of loading buffer and the solutions was boiled for 5 minutes at 100^0C. After boiling samples were shortly centrifuged and loaded on the SDS gel.

Running and semi dry transferring:

Samples were run on SDS gels with 72 mA for 2.5 h (for two gels) or with lower mA (3-6 mA) overnight. After running SDS gel were covered by nitrocellulose membrane and 3layers of whatman paper on each side and anode and cathode buffers were applied. Protein transfer was done at 270 mA for 2.5 h. After transferring the membrane was stained with ponceau color and then blocked for one hour with 3% milk or BSA solution. After blocking the membrane was cut based on the size/molecular weight (MW) of the proteins of interest and incubated with the primary antibody overnight. On the next day, after three times washing the membrane with TBST, the membrane was incubated with horseradish peroxidase (HRP)-secondary antibody for one hour. After three times washing with tris-buffered saline (TBST), proteins were detected with ECL kit for 10 min.

2.2.10 Subcellular fractionation - Separation of nuclear and cytoplasmic proteins

In order to determine the expression of different proteins in the nucleus compared to cytoplasmic fraction of cells, subcellular fractions were used. Cells were cultured in 15 cm dishes. After 7 days, when confluency of cells reached 80-100 %, cells were irradiated (4 Gy). Protein isolation was done at different time points after irradiation (30 min, 1 h, 16 h and 24 h). In specific experiments cells were irradiated 2 h after treatment with LY29004, and proteins were isolated 24 h after irradiation. The protein extraction and nuclear/cytoplasmic separation has been done based on following description:

Cells were washed 2 times with cold PBS. The rest of PBS was sucked out completely with vacuum. 1 ml cold PBS was added to the cells and then cells were scratched with cell lifter and collected on ice in tubes. Thereafter, cells were centrifuged for 10 min, 1100 rpm, 4°C. Supernatants were carefully removed in order to get a proper pellet. The pellets were resuspended in 700 µl lysis buffer A and were incubated 10 min on ice. After incubation, cell lysates were completely smashed with glass tissue grinder (20 times). Then, cell lysates were centrifuged for 10 min, 2330 rpm, 4°C. After centrifugation, the upper supernatants were collected as cytoplasmic fraction. The pellets were washed 3 times with 500 µl lysis buffer A (5min, 2330 rpm, 4°C). After the last washing, the supernatants were completely removed in order to have dry pellets. The pellets, representing the nuclear fraction, were resuspended in 80-120 µl lysis buffer B. Sonication was done only for nuclear fraction as described in the western blot section. Thereafter, the nuclear and cytoplasmic fractions were centrifuged and supernatants were collected. Protein content was quantified and samples were run on the SDS-gels as described in SDS-PAGE and western blot section.

2.2.11 Statistical analysis

Results obtained from colony formation assays, residual γH2AX-foci and ALDH activity were tested for statistical significant differences by applying the Student T-Test based on the SigmaPlot software version 2001.

3 Results

3.1 Expression profile of stem cell markers in breast cancer cell lines and role of Akt isoforms on the expression of these marker proteins

3.1.1 CSC marker (CSCM) expression in different breast cancer cell lines

It is known that the expression of some transcription factors, also called putative stem cell markers, is important during the maintenance of a cancer stem cell population. To identify potential stem cell levels of different breast cancer cell lines, the protein expression of putative stem cell markers including Nanog, Oct4, Sox2, Bmi-1 and ALDH1 was evaluated. In this regard, four breast cancer cell lines namely MDA-MB-231, SKBR3, HBL-100, MCF-7 and in addition the melanoma cell line NM2C5 have been investigated. The expression of Oct-4 and Sox2 was more pronounced in SKBR-3, compared with the other cell lines (Fig. 3.1). Nanog and ALDH1 were strongly expressed in MCF-7. Furthermore, Bmi-1 was strongly expressed in MCF-7 and NM2C5. Based on these data, each breast cancer cell line shows a different pattern of putative stem cell marker expression indicating the importance of each marker for a specific cell line. To determine whether a correlation exists between CSCM expression and Akt activity, the phosphorylation level of Akt at serine residue (S473) has been analyzed. As it is shown in Fig. 3.1, the ratio of the band intensities of P-Akt to total Akt did was strongly elevated in SKBR3 and HBL-100 as compared with MCF-7 and NM2C5, whereas for MDA-MB-231 only a faint Akt phosphorylation was to be observed. Based on these data, there exists no direct correlation of the expression of cancer stem cell markers (CSCM) and Akt expression and its phosphorylation level, which is an indicator of its activity.

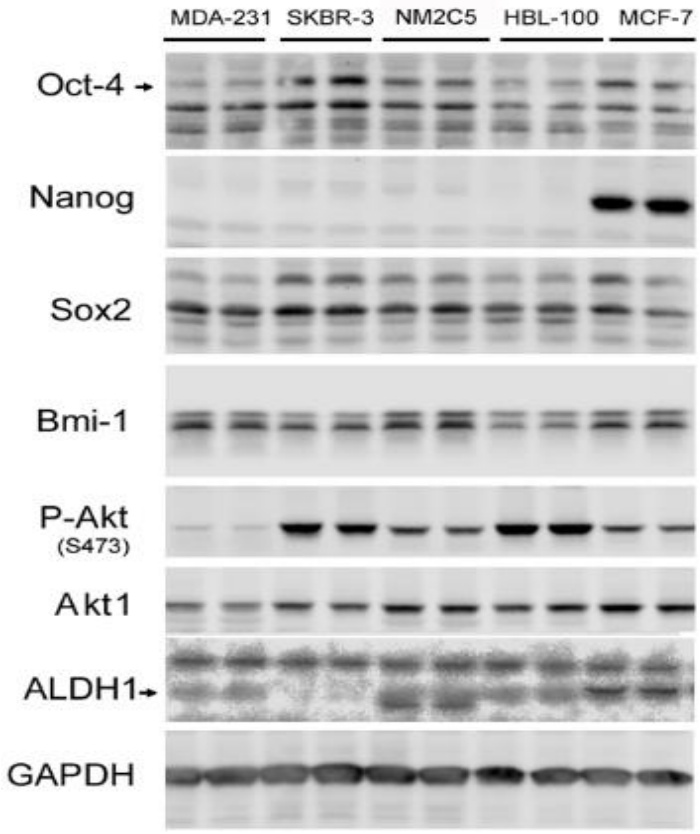

Figure 3.1. CSC marker (CSCM) protein expression level in five different breast cancer cell lines. Protein samples from all cell lines were isolated at the same time and conditions (confluency state of 80-100%). The expression level of the indicated proteins was analyzed using Western blotting. In order to detect proteins with similar molecular weights, after each detection the blots were stripped and then incubated with next antibody. The figure illustrates one experiment with duplicate cultures.

3.1.2 Effect of Akt isoforms on the expression of CSCM in breast cancer cells

The protein Akt is expressed in three different isoforms with different functions. In order to identify which isoform plays the main role in stemness and CSCM expression, protein analyses of MDA-MB-231 cells with stable knockdown of individual Akt isoforms were applied. In order to keep the knockdown level stable, cells were constantly cultured under 1.5 µg/ml puromycin treatment. As shown in Fig. 3.2, selective knock down of Akt1 resulted in a strong downregulation of the CSCM protein

expression such as Nanog and Bmi-1. This data shows that Akt1 expression is necessary for the expression of stem cell markers in breast cancer cells.

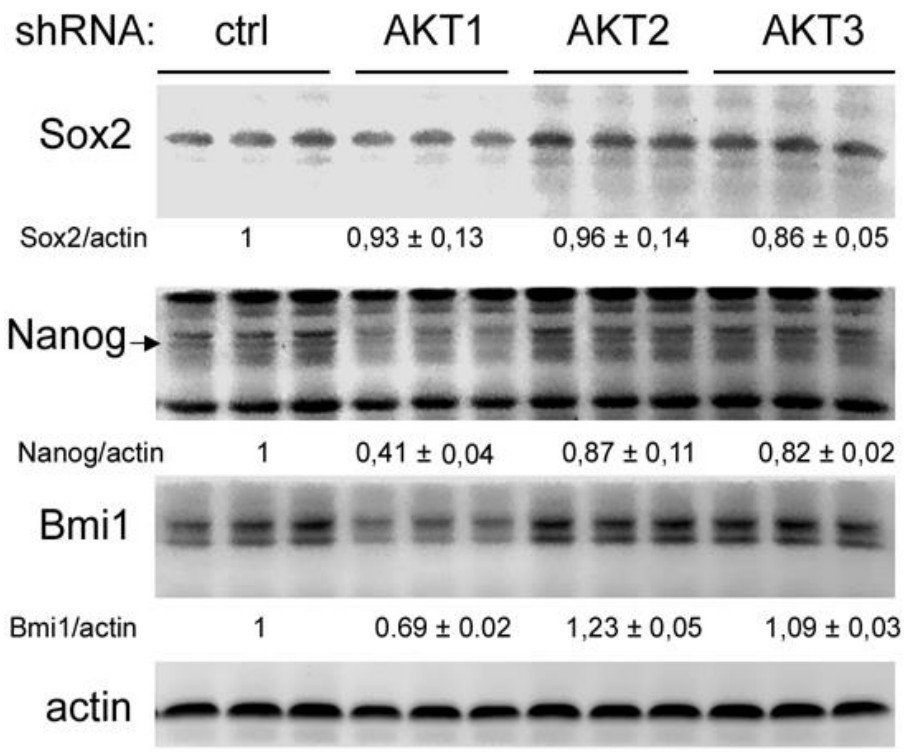

Figure 3.2. Effect of Akt isoforms on the expression of CSCM in breast cancer cell line MDA-MB-231. Protein samples from parental (control) and Akt1, 2 and 3 shRNA knockdown cells were isolated. The expression level of the indicated proteins was analyzed using Western blotting. In order to detect the proteins with similar molecular weight, after each detection the blots were stripped and then incubated with next antibody. Densitometry values ± SD, represent the ratio of the specific protein band intensities to actin. The figure illustrates one experiment with triplicate cultures.

3.2 ALDH as a mediator of post irradiation cell survival in breast cancer cell lines

3.2.1 Effect of ALDH inhibition by DEAB on post-irradiation cell survival

ALDH activity has been described to maintain stemness of tumor cells as well as to mediate chemo- and radioresistance. Thus, in order to investigate the role of ALDH activity on post-irradiation cell survival, different concentrations of DEAB (N,N-diethylaminobenzaldehyde), a general inhibitor of ALDH activity, were used. To this aim, 24 h after seeding different breast cancer cell lines, i.e. MDA-MB-231, SKBR3, HBL-100, MCF-7 as well as the lung cancer cell line A549 and the melanoma cell line NM2C5 were treated with 0, 20, 40, 60, 80, 100 or 200 µM DEAB for 24 hours. Thereafter, cells were either mock irradiated (0 Gy) or irradiated with a single dose of 3 Gy. After irradiation and depending on the cell line, the used cells were incubated for 10 to 14 days to allow colony formation. Fig. 3.3 shows the results with respect to the surviving fraction of the individual cell lines with and without radiation exposure as well as with and without DEAE treatment. According to the cellular radiation response profile, the applied cell lines can be classified into the categories radiosentization, radioprotection, and no effect. When compared to DEAB-non treated conditions, irradiated MDA-MB-231 and SKBR3 cells showed radio-protection after inhibition of ALDH (in different concentrations). In contrast ALDH inhibition led to radio-sensitization of the cell lines HBL-100 and A549. Finally, post-irradiation survival of MCF-7 and NM2C5 treated with DEAB was not affected (no effect). Thus, based on these results, breast cancer cell lines can be separated into the presented three groups showing different radiation responses when ALDH activity is inhibited by DEAB.

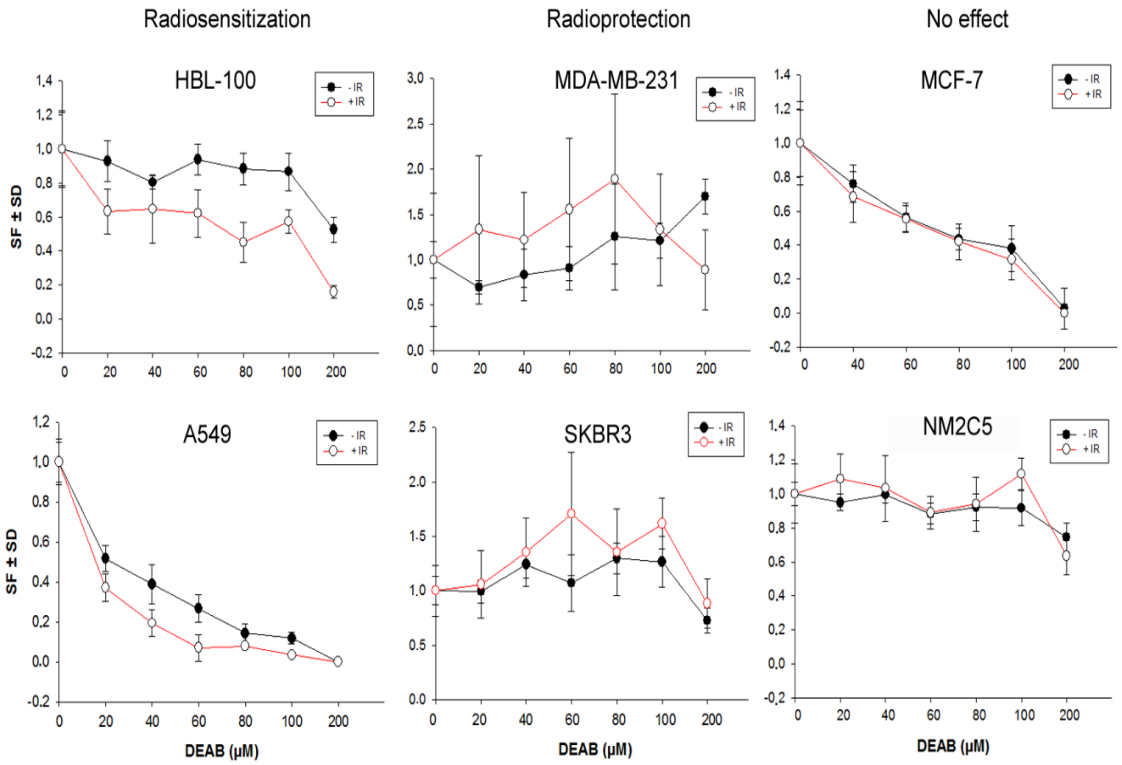

Figure 3.3. Effect of ALDH inhibition by DEAB on post-irradiation cell survival. Cells (confluency state of 80-100%) were seeded in 6 well plates for colony formation assay as described in materials and methods. Twenty-four hours after seeding, cells were treated with DEAB (0-200 µM) for 24 h followed by irradiation with doses of 0 and 3 Gy. The incubation time for different cell lines differed between 10 to 14 days. Survival curves (SF ± SD) were calculated based on one experiment with six parallel samples.

High ALDH activity level has been demonstrated as a potential CSC marker in many types of cancers. In order to determine the activity of this enzyme, the Aldefluor assay has been used. In this regard, to determine the actual activity of ALDH enzyme, cells treated with the ALDH-inhibitor DEAB were used as negative control. To define the minimum concentration of DEAB that is able to inhibit ALDH activity completely, different concentrations of ALDH (0, 15, 20, 40, 60, 80, and 100 µM) were tested in two different cell lines originally established from lung (A549) and colon (HCT116) carcinoma. Data shown in Fig. 3.4 indicate that 40 µM DEAB is able to completely inhibit ALDH activity in two mentioned cell lines. Based on this data for further experiments 40 µM of DEAB was constantly used to inhibit ALDH activity of the cell lines to be tested.

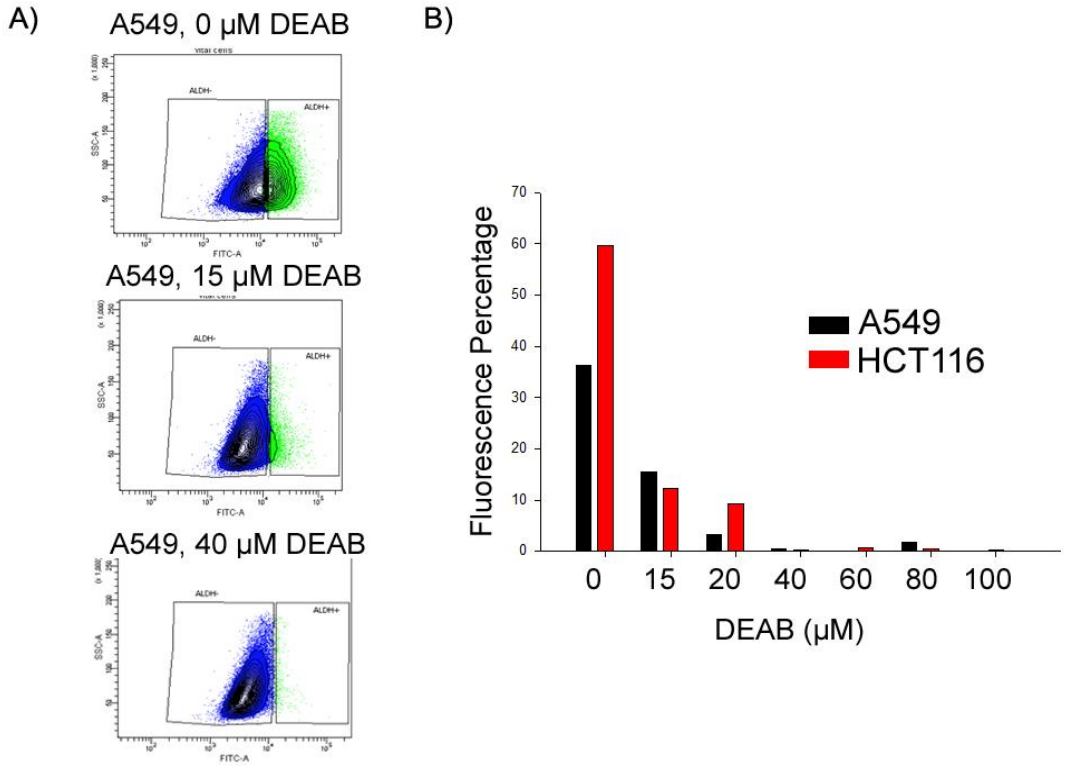

Figure 3.4. Determination of the minimum concentration of DEAB to blocks ALDH1 activity. For this analysis, A549 and HCT116 cells were used. Cells were treated with ALDH substrate BAAA according to the Aldefluor assay protocol (see materials and methods) and were incubated for 40 min incubation at 37 degree. **A)** A fluorescence signal obtained after treatment with 0, 15 and 40 µM DEAB in A549 cell line. **B)** Quantitative presentation of ALDH activity in two cell lines analyzed after different concentration of DEAB. Bars represent the mean value of ALDH percentage from two independent experiments with duplicate cultures.

3.2.2 Dependency of radiation response to the proportion of ALDH positive cells

Based on the results shown in Fig. 3.3 we investigated whether the differential post-irradiation results of the different breast cancer cell lines are due to off-target effects of DEAB. To test this, ALDH expression was downregulated by a specific siRNA approach directed against the isoform ALDH1. ALDH1 downregulation was confirmed for MCF-7 and HBL-100 using western blot analysis (Fig. 3.5A). However, due to the already very low basal expression of ALDH1 in MDA-MB-231 cells, no further knockdown effect could be detected in this cell line. In order to test colony formation

ability under ALDH-siRNA knockdown, cells were seeded 48 h after ALDH1 siRNA transfection for colony formation and irradiated 24 h after seeding with doses of 0, 1, 2, 3, and 4 Gy. Colony formation data shown in Fig. 3.5B are in line with the previous data depicted in Fig. 3.3 based on DEAB treatment. MDA-MB-231 cells presented a slight radio-protection effect after ALDH1 knockdown at doses of 3 and 4 Gy, whereas HBL-100 showed a slight radio-sensitization at doses of 3 and 4 Gy. MCF-7 cells were not affected by this treatment approach. Furthermore, in order to investigate the differential post-irradiation response pattern of breast cancer cell lines after ALDH inhibition, the cell type specific level of ALDH activity in the three cell lines was evaluated. To this aim, the activity level of ALDH was evaluated by the Aldefluor assay. The results shown in Fig. 3.5C indicate that for MDA-MB-231 cells no ALDH activity could be detected, whereas in the cell line HBL-100 approximately 30 % and in cell line MCF-7 less than 10% of the cells presented high ALDH-activity. Based on this data, it can be concluded that the ratio of ALDH activity in the cells determines the post-radiation behavior of the cells to the inhibition of the enzyme. In other words, cells with high ALDH activity (i.e. HBL-100) show stronger radio-sensitization effect to ALDH-inhibnition than cells with low ALDH activity (i.e. MCF-7 and MDA-MB-231).

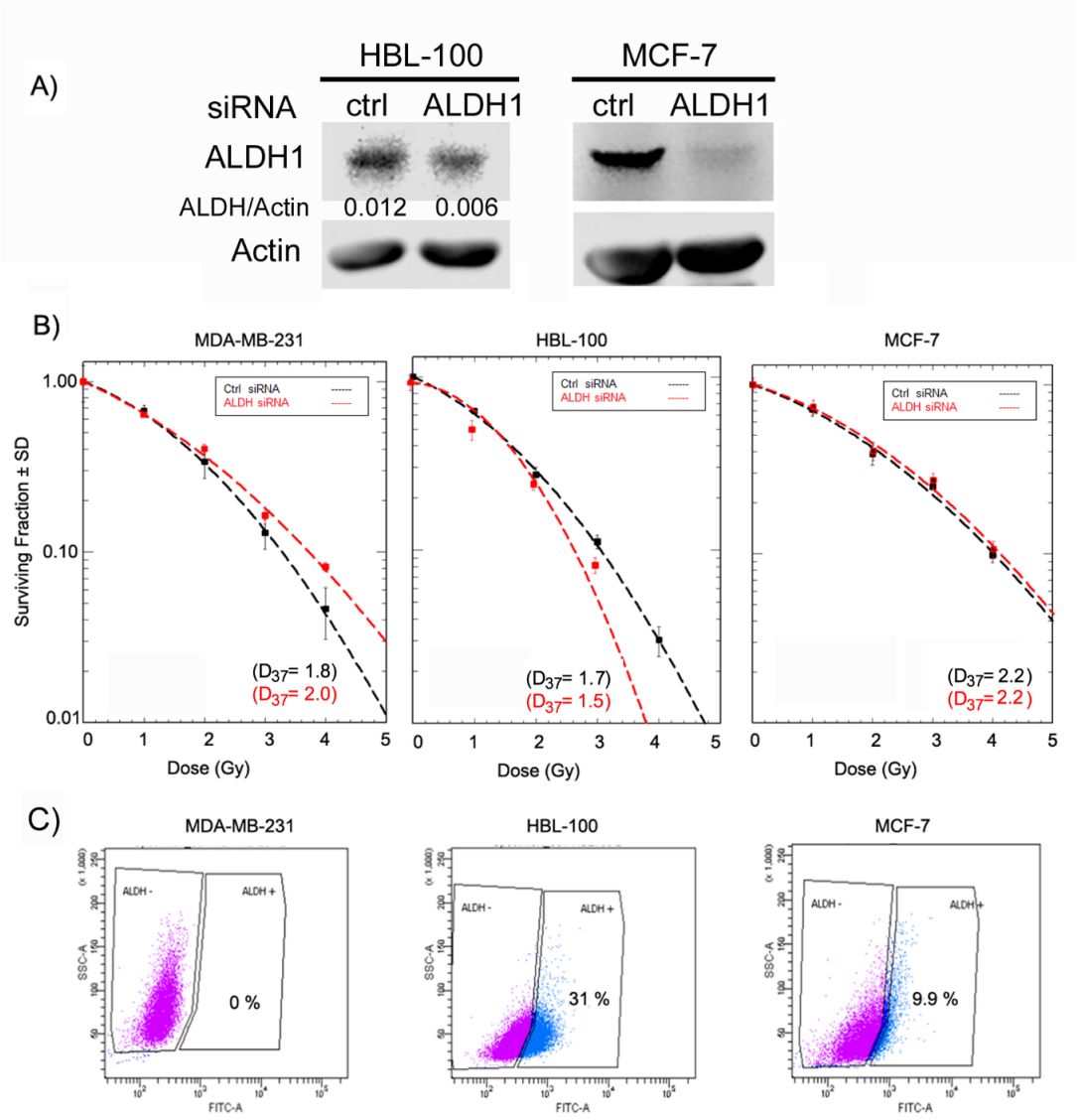

Figure 3.5. Relation of ALDH activity level and post irradiation cell survival with and without ALDH siRNA knockdown in breast cancer cell lines. A) Western blots data of ALDH1 protein expression with and without siRNA knockdown in HBL-100 and MCF-7 cells. **B)** Survival curves of the three irradiated breast cancer cell lines with and without ALDH1 siRNA knockdown. The incubation time for different cell lines differed between 10-14 days. Data points and survival curves (SF ± SD) were calculated based on one experiment with 6 parallel cultures. **C)** Cells were incubated with Aldefluor reagent as described in materials and methods and ALDH activity was measured by flow cytometry. Gating of the fluorescence signal was set after treatment of the cells with 40 µM DEAB as negative control.

3.3 Role of Akt isoforms on ALDH activity and post irradiation cell survival

3.3.1 Role of different Akt isoforms on ALDH activity

According to the western-blot data presented in Fig. 3.2, the expression of the CSC marker proteins Nanog and Bmi-1 seems to be dependent on the Akt1-isoform. Thus, the question was addressed whether the additional isoforms Akt2 and Akt3 exert similar effects on ALDH activity. To test this, ALDH activity of parental as well as Akt1 and Akt2 knockout-HCT116 cells were analyzed with the Aldefluor assay. In order to keep the knockout-status stable, cells were cultured in the presence of 0.3 mg/ml gentamicin (G418) (Fig. 3.6A). As shown in Fig. 3.6B, knockout of Akt1 and Akt2 resulted in a strong reduction of ALDH activity when compared with the parental cells. To confirm these results Akt1, Akt 2 and Akt 3 isoforms were downregulated by transfection of HCT116 parental cells with Akt-isoform specific siRNAs (Fig. 3.6C). Aldefluor assay analyses indicated a significant reduction of ALDH activity in Akt1 and Akt3 downregulated HCT116 cells (Fig. 3.6D). In order to investigate the role of Akt on ALDH activity further the breast cancer cell lines HBL-100 and MCF7 were additionally analyzed by the described knockdown approach (Fig. 3.6E, G). Knockdown of Akt1 and 2 in HBL-100 cells, exerted also a significant effect on ALDH activity (Fig. 3.6F). However, knockdown of Akt1, Akt2 and Akt3 in MCF-7 cells did not affect the level of ALDH activity (Fig. 3.6H). Thus, at least for HBL-100 and HCT116 cells, these data indicate a distinct role of Akt on ALDH. Moreover, these results indicate that ALDH activity in MCF-7 cells is not dependent on Akt expression.

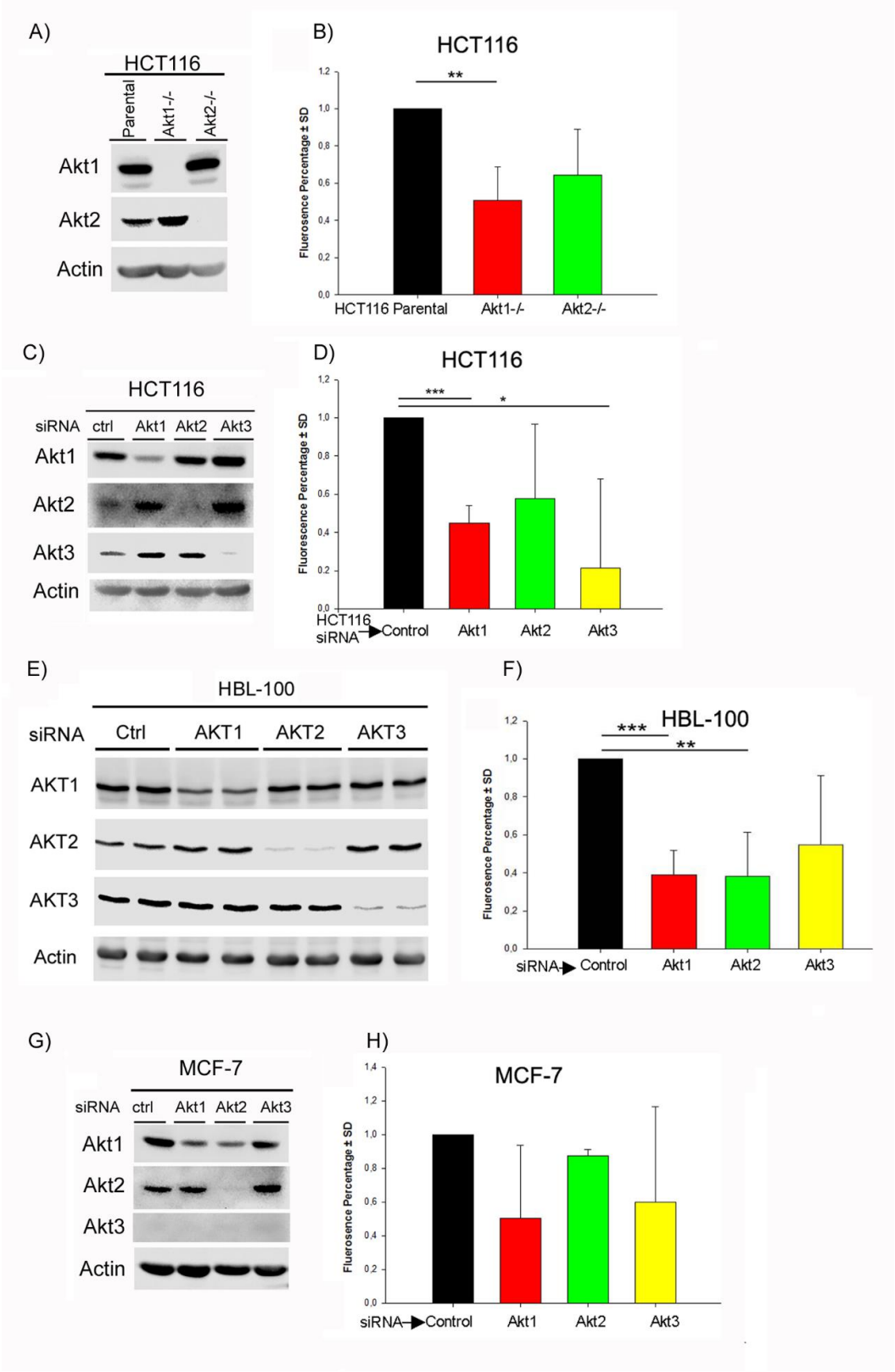
A)
HCT116
Parental
Akt1-/-
Akt2-/-
Akt1
Akt2
Actin
B)
HCT116
**
Fluorescence Percentage ± SD
HCT116 Parental
Akt1-/-
Akt2-/-
C)
HCT116
siRNA
ctrl
Akt1
Akt2
Akt3
Akt1
Akt2
Akt3
Actin
D)
HCT116
***
*
Fluorescence Percentage ± SD
HCT116 siRNA
Control
Akt1
Akt2
Akt3
E)
HBL-100
siRNA
Ctrl
AKT1
AKT2
AKT3
AKT1
AKT2
AKT3
Actin
F)
HBL-100
***
**
Fluorescence Percentage ± SD
siRNA
Control
Akt1
Akt2
Akt3
G)
MCF-7
siRNA
ctrl
Akt1
Akt2
Akt3
Akt1
Akt2
Akt3
Actin
H)
MCF-7
Fluorescence Percentage ± SD
siRNA
Control
Akt1
Akt2
Akt3

Figure 3.6

Figure 3.6. Role of different Akt isoforms on ALDH activity. A, C, E, G) Expression level of the Akt isoforms in HCT116 Akt1 and 2 knockout cells as well as in cells after siRNA knockdown of Akt1, Akt2 and Akt3 in HCT116, HBL-100 and MCF-7 cells were analyzed using Western blotting. **B, D, F, H)** Cells (confluency state of 80-100%) were seeded for transfection in 6 well plates as described in materials and methods. Forty-eight hours after siRNA transfection, cells were analyzed by Aldefluor assay. Gating of the fluorescence signal was set after treatment of the cells with 40 µM DEAB as negative control. Each bare represent the mean value of the percentage of ALDH activity ± standard deviations (SD) from three independent experiments with three parallel cultures. (* $p < 0.05$, ** $p < 0.01$, and *** $p < 0.001$, Student's t-test). These data has been already published in Harati MD, et al. IJMS 2019 [135].

3.3.2 The role of different Akt isoforms on post-irradiation cell survival

3.3.2.1 HBL-100

In several studies, it has been demonstrated that CSCs are chemo- and radioresistance. Thus, the determination of the underlying regulatory pathways in CSCs is important. To this aim, the role of Akt isoforms and ALDH on post-irradiation cell survival of breast cancer cells was investigated. Therefore, colony formation after knockdown of the three different Akt isoforms (1, 2 and 3) in HBL-100 cells was analyzed. As shown in Fig. 3.7A, downregulation of all Akt isoforms led to a significant radiosensitization in HBL-100 cells; the strongest effect was apparent when Akt3 was knocked down (Fig. 3.7A and 3.7C). Moreover, in order to investigate the correlation of Akt and ALDH on post-irradiation cell survival, siRNA based knock down of Akt1, 2 and 3 was combined with a subsequent DEAB (40µM) treatment. Yet, as shown in Fig. 3.7B, DEAB inhibition of ALDH and knockdown of the three Akt isoforms did not result in a further radiosensitization of HBL-100 cells. So far, these results indicate that Akt in the context of radiation sensitivity seems to act upstream of ALDH. Thus, when Akt is downregulated inhibition of ALDH does not show any additional effect on post-irradiation cell survival.

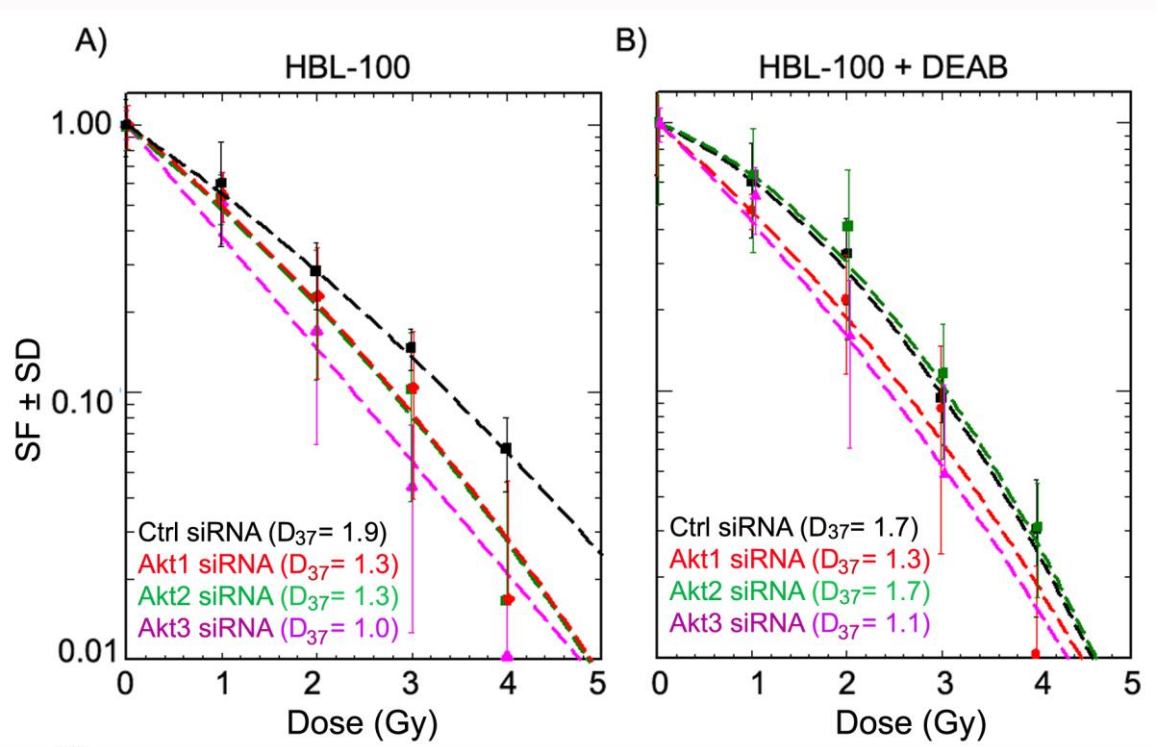

C)

IR	Akt1 siRNA P-Value	Akt2 siRNA P-Value	Akt3 siRNA P-Value
2 Gy	0,1991387780	0,1991387780	0,0063747060
3 Gy	0,0472704879	0,0472704879	0,0000000114
4 Gy	0,0002509425	0,0002509425	0,0000006990

Figure 3.7. Role of different Akt isoforms in combination with DEAB treatment on post-irradiation cell survival of HBL-100 cells. A) Cells (confluency state of 80-100%) were seeded for transfection in 6 well plates as described in materials and methods. Forty-eight hours after siRNA directed against Akt isforms (1, 2 and 3), cells were seeded and then 24 h later cells were irradiated and incubated for colony formation as described in materials and methods. **B)** siRNA transfected cells were treated with 40 µM DEAB after seeding for colony formation and irradiated 24 h later. Survival curves (SF ± SD) were analyzed based on two independent experiments with 12 parallel samples. **C)** Numbers shown indicate the P-values for cell survival shown in figure A for specific irradiation and Akt 1, 2 and 3 siRNA curves compared to controle siRNA.

3.3.2.2 MCF-7 and MDA-MB-231

In order to evaluate the role of Akt isoforms and ALDH on post-irradiation cell survival of the other breast cancer cell lines, i.e. MCF-7 and MDA-MB-231, the same experimental strategy as addressed before (se Fig. 3.7A and B) has been applied. Thus, colony formation ability after knockdown of three different Akt isoforms (1, 2 and 3) was analysed. Yet, the results shown in Fig. 3.8A and 3.8C indicate that downregulation of all Akt isoforms did not affect the radiation response of MCF-7 as well as MDA-MB-231 cells. To investigate the potential correlation of Akt and ALDH on post-irradiation cell survival further, a combination of Akt siRNA transfection with DEAB (40µM) treatment was applied. As shown in Fig. 3.8B, ALDH inhibition in combination with knockdown of Akt isoforms did not change the radiation response of MCF-7 cells. However, Akt3-knockdown in MDA-MB-231 cells resulted in radio-sensitization (Fig. 3.8D) indicating the importance of the Akt3 isoform in in the radiation response of this cell line. Together, these data show that the role of Akt and ALDH on post-irradiation cell survival is dependent on the cell lines and each isoform of Akt has different role in the different breast cancer cells.

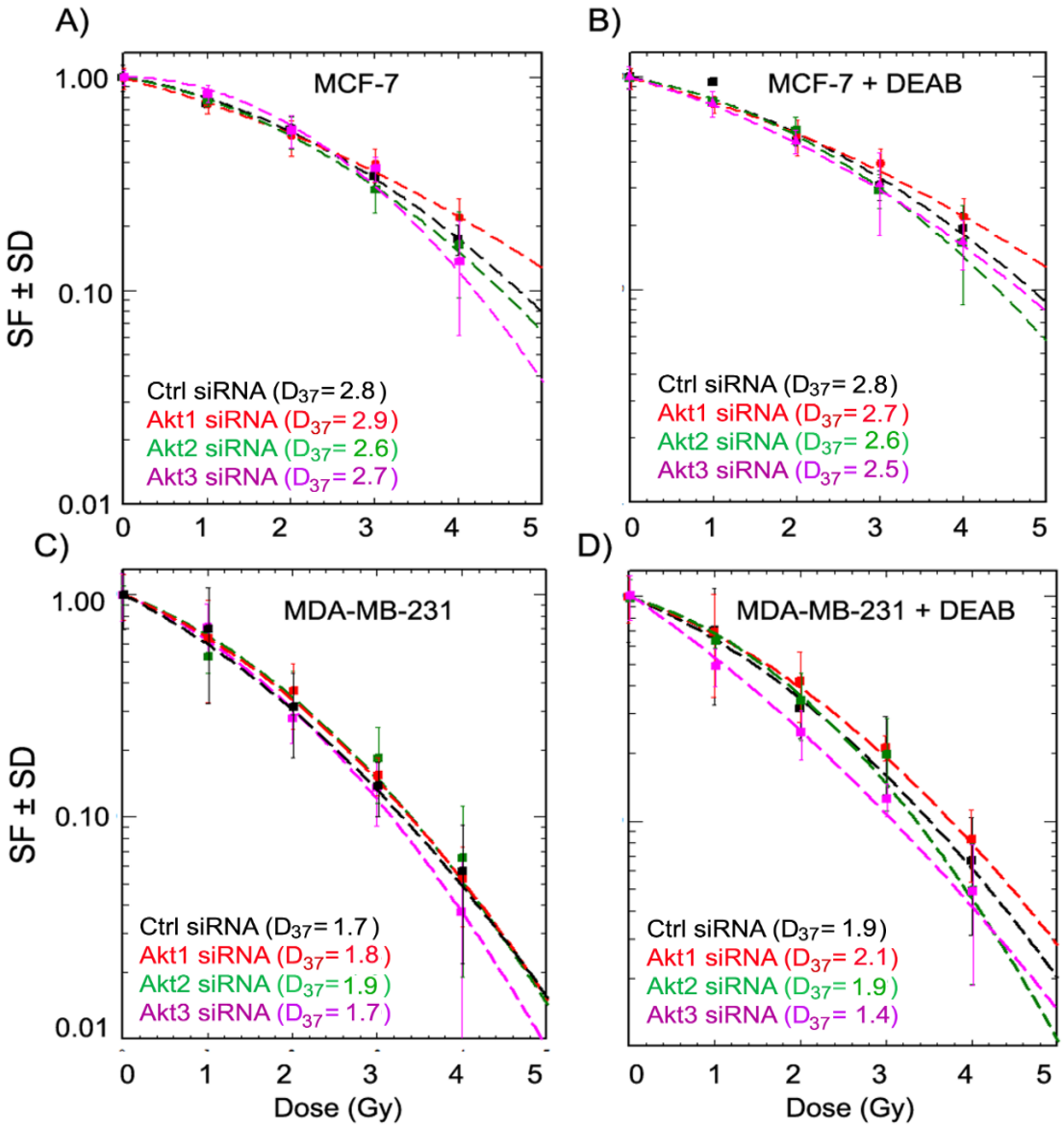

Figure 3.8. Role of different Akt isoforms in combination with DEAB treatment on post-irradiation cell survival of MCF-7 and MDA-MB-231 cells. A, C) Cells (confluency state of 80-100%) were seeded for transfection in 6 well plates as described in materials and methods. Forty-eight hours after siRNA directed against Akt isoforms (1, 2 and 3), cells were seeded and then 24 h later cells were irradiated and incubated for colony formation as described in materials and methods. **B, D)** siRNA transfected cells were treated with 40 µM DEAB after seeding for colony formation and irradiated 24 h later. Survival curves (SF ± SD) were analyzed based on two independent experiments with 12 parallel samples.

3.4 ALDH activity and radiation response in 3D-culture

3.4.1 Different pattern of sphere formation under 3D-culture condition

One characteristic of cancer stem cells is their ability to form spheres. To analyze this ability, the breast cancer cell lines used in this study were cultured under 3D condition with and without radiation exposure. To this aim, the five different breast cancer cell lines were cultured at different cell number concentrations (500 to 4000 cells per well in 96 well plates) in matrigel as described in the Materials and Methods section. Sphere formation of the individual cell lines occurred differentially between day 9 and 20 after seeding in matrigel, i.e. 9 days for MDA-MB-231, 12 days for MCF-7 and 20 days for SKBR3. Likewise, the morphology of spheres is also dependent on the type of cell line used. As shown in the Fig. 3.9A, MCF-7 presented a round morphology, SKBR3 a grape shape and MDA-MB-231 stellate morphology. When compared with non-irradiated cells, the number and size of the spheres of irradiated cells was markedly reduced with increasing radiation dose (2, 4 and 6 Gy) (Fig. 3.9B-D).

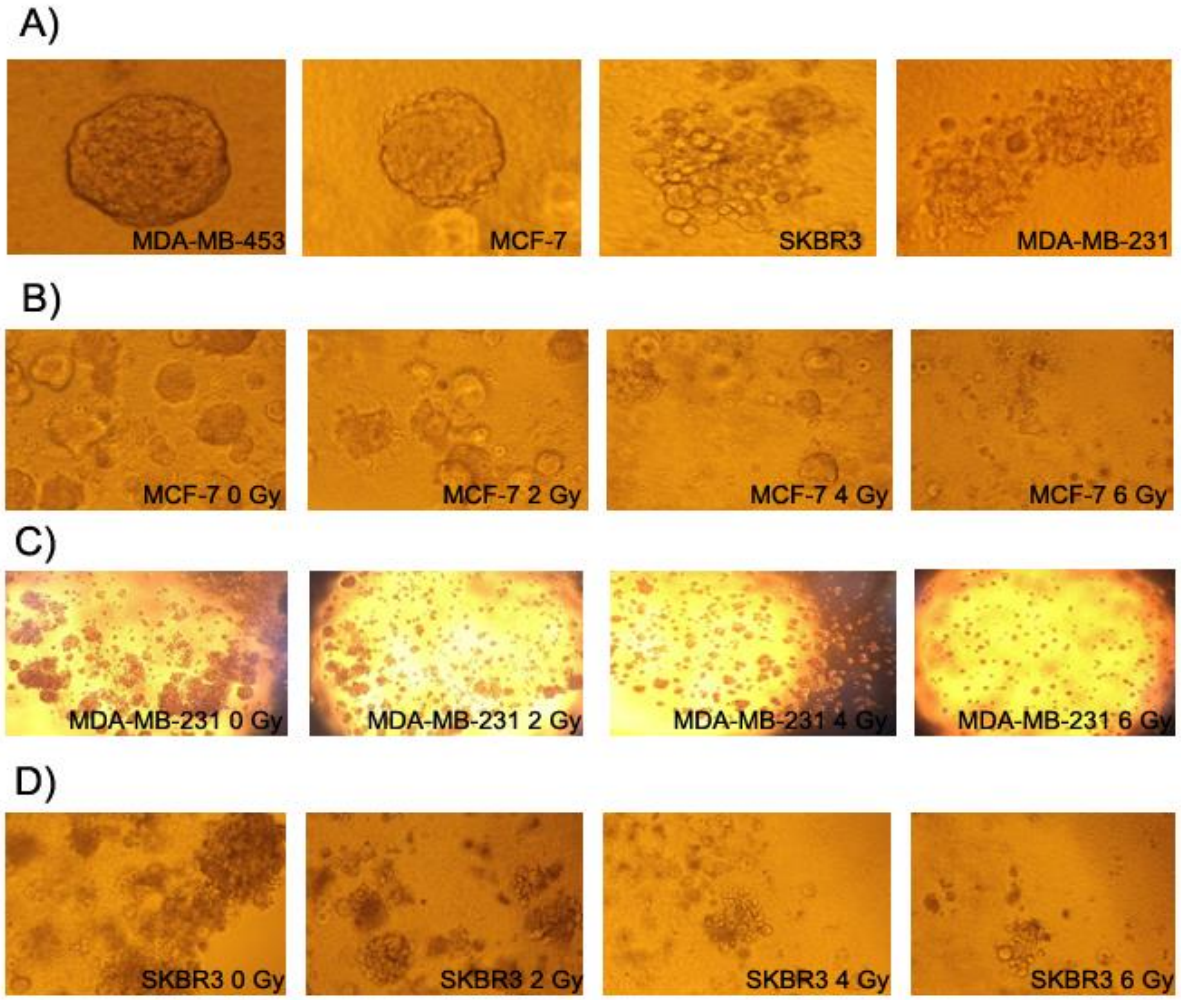

Figure 3.9. Pattern of sphere formation under 3D-culture condition in breast cancer cell lines. Cells density of (4000 for MCF-7, SKBR3 and 2000 for MDA-MB-231 per 96 well plates) were seeded in to three dimensional culture system using matrigel (0.5 mg/ml) and RPMI (for MCF-7 and SKBR3) or DMEM (for MDA-MB-231) with total volume of 200 µl per 96 well. After 4 h incubation of cells and matrigel in 37 degree, the extra medium (100 µl) has been added to each well. **A)** Morphology of spheres for different cell lines. **B-D)** Sphere formation after irradiation exposure (0, 2, 4 and 6 Gy) of each breast cancer cells was determined after 7 to 20 days. The data shown are based on one experiment with four parallel cultures for each cell line.

3.4.2 Determination of plating efficacy under 3D-culture

In order to determine the optimal cell number for colony formation under 3D-culture condition, the platting efficacy (PE) of the three breast cancer cell lines was analyzed by applying different starting cell numbers (500-4000 cells per well). For non-irradiated

controls the PE under 3D is about 4% for MCF-7 as well as MDA-MB-231 (Fig. 3.10A,B) and about 2.5% for SKBR3 (Fig. 3.10C). The optimized seeding density for the individual cell lines was determined based on the best PE obtained for each cell line under 3D-culture (Fig. 3.10D). Based on these data, it can be concluded that a low frequency of CSCs in the total tumor cell population does lead to a lower PE under 3D-culture condition.

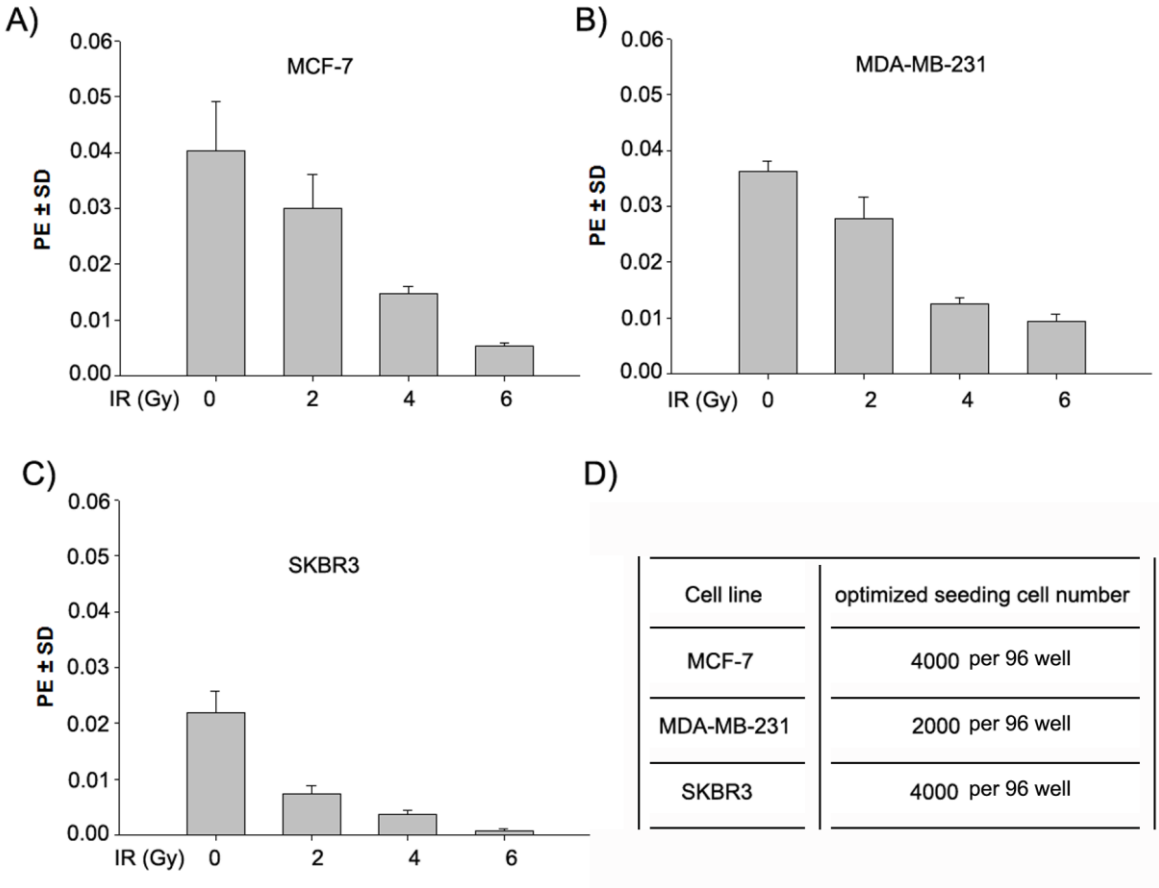

Figure 3.10. Plating efficacy under 3D-culture condition (i.e. sphere formation) of breast cancer cell lines. A-C) Plating efficacy under 3D-culture. Spheres bigger than 50 cells were counted after 7 to 20 days incubation. Plating efficacy was calculated as described in materials and methods. **D)** The table represents the optimized cell number to be seeded for determination of sphere formation under 3D-culture condition. Each bare represent the mean value of plating efficacy ± standard deviations (SD) from one experiment with four parallel cultures for each radiation dose.

3.4.3 ALDH activity and CSCM expression under 3D-culture

In order to investigate the expression of CSCM and ALDH activity in formed spheres of MCF-7 and MDA-MB-231 cells, Aldefluor assay to determine ALDH activity and the protein expression profile of Nanog and ALDH1 was evaluated. Therefore, single cell suspension of formed spheres, 12 days after starting the 3D-culture, were prepared and analyzed. As shown in Fig. 3.11A and B, cells under 3D-culture condition present express a significantly inducted of ALDH activity (83% in MCF-7 and 72% in MDA-MB-231) when compared with the ALDH activity of cells under 2D-culture condition (see Fig. 3.5B). Moreover, as shown in the Fig. 3.11 C, the protein expressions of Nanog as well as of the expression of ALDH1 was upregulated under 3D-culture condition in 6 Gy irradiated MDA-MB-231 cells when compared to non-irradiated control cells. Thus, it can be concluded that the expression of the stem cell markers Nanog and ALDH1 is stimulated under/after irradiation.

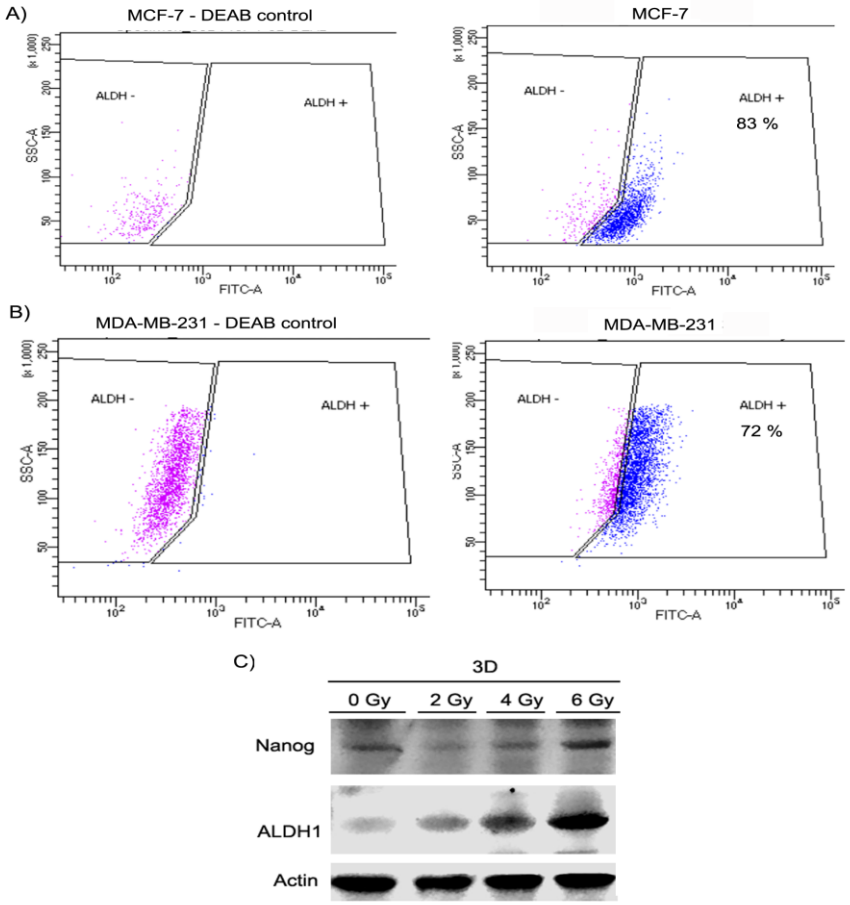

Fig .3.11.

Figure 3.11. ALDH activity and CSCM expression of the irradiated breast cancer cell lines MDA-MB-231 and MCF-7 under 3D-culture. A, B) MCF-7 and MDA-MB-231 cells were seeded in matrigel (0.5 mg/ml) and medium with total volume of 200 µl per 96 well. After 12 days, the spheres formed were brought to the single cell suspensions as described in materials and methods. Cells were incubated with Aldefluor reagent as described above and ALDH activity has been measured by flow cytometry. Data shown are based on one experiment. **C)** Protein samples were isolated after washing out the matrigel from MDA-MB-231 cells. The expression level of the indicated proteins (Nanog and ALDH1) was analyzed using Western blotting. Data represent one experiment.

3.5 Radiation response and DNA repair capacity of ALDH-positive and negative cells

3.5.1 Profile of protein expression of ALDH positive and negative breast cancer cells

In order to investigate the role of ALDH activity in radioresistance further, SKBR3 and HBL-100 cells have been sorted for subpopulations presenting high and low ALDH activity profiles via FACS applying the Aldefluor assay. Thus, in order to define the accurate border of low ALDH activity, DEAB treated (40 µM) SKBR3 and HBL-100 cells have been recorded as negative control. Moreover, to avoid possible mixture of two subpopulations during sorting, a secure gating distance between ALDH-positive and -negative populations was applied (Fig. 3.12 A). In order to investigate the expression profile of stem cell markers, protein samples were analyzed by SDS-PAGE and western blotting as indicated in Fig. 3.12 B. Among the different putative stem cell markers analyzed only Nanog and Bmi-1 were markedly overexpressed in ALDH-positive cells when compared with ALDH-negative cells. Likewise, phosphorylated Akt (S473) was upregulated in ALDH-positive cells, indicating an activation of Akt in these cells. Moreover, as the Notch pathway plays an important role in CSCs, the expression of Notch (NICD) has been specifically investigated in ALDH-positive and ALDH-negative cell populations. As demonstrated in Fig. 3.12 B, expression of Notch but not of Sirt2 was upregulated in ALDH-positive cells when compared with ALDH-negative cells. Furthermore, in order to determine the ALDH isoform responsible for the measured ALDH activity, the protein expression profile of ALDH1 and ALDH1A3 was determined in ALDH-positive and ALDH-negative cells. As shown in Fig. 3.12 B and

C, the expression level of ALDH1A3 but not ALDH1 was upregulated in ALDH-positive cells when compared to ALDH-negative ones. Based on these data, it can be assumed that the interaction of several proteins including Akt1, Notch1, Nanog and Bmi-1 plays an important role in the stimulation/induction of ALDH activity in CSCs.

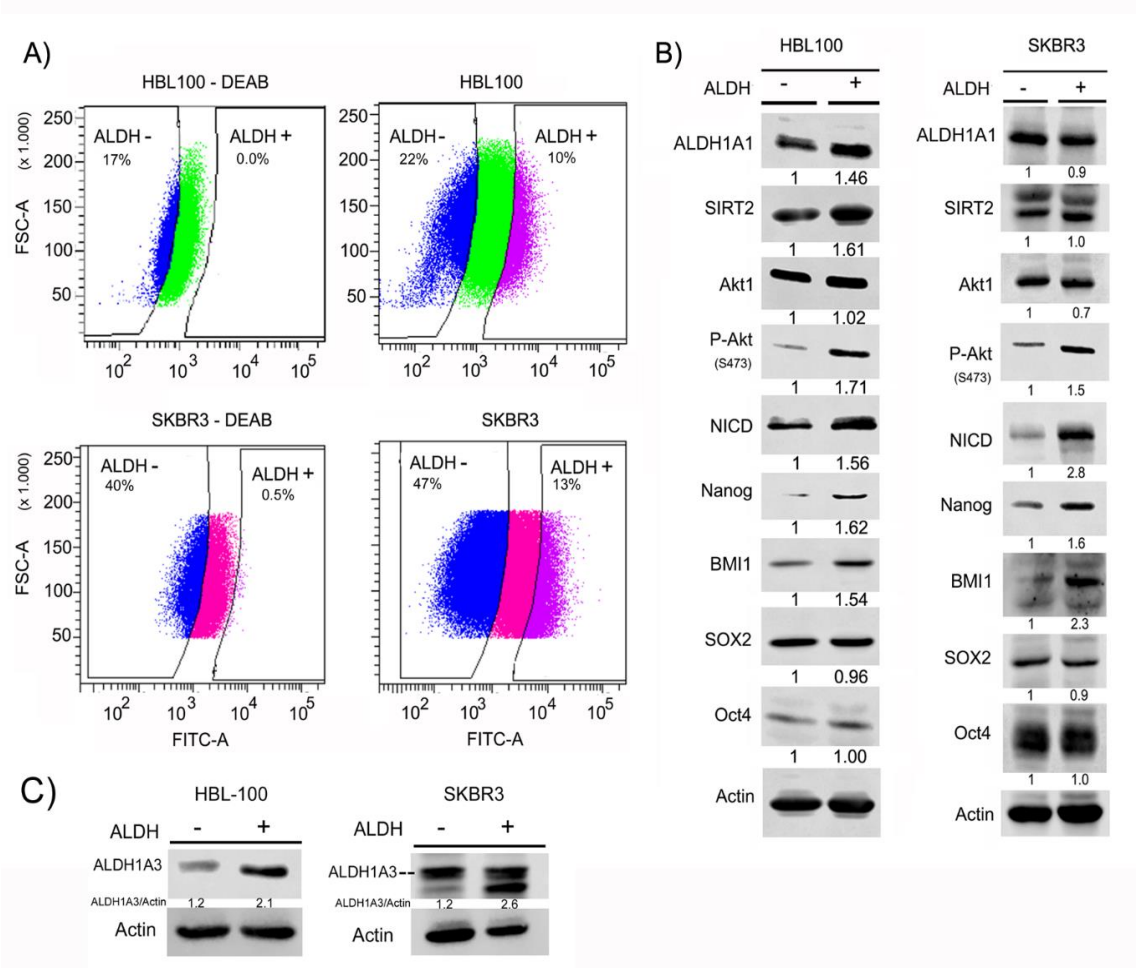

Figure 3.12. Protein expression profile of ALDH positive and negative cells. A) Strategy of separating ALDH-positive and -negative cell populations in FACS. **B, C)** Expression profile of indicated proteins in HBL-100 and SKBR3 cells were analyzed using Western blotting. In order to detect the proteins with similar molecular weight, after each detection the blots were stripped and then incubated with next antibody. Densitometry values represent the ratio of the specific protein band intensity to actin. Data presented are based on two independent experiments for each cell line. These data has been already published in Harati MD, et al. IJMS 2019 [135].

3.5.2 Comparison of DNA repair capacity of ALDH-positive cells and negative cells

It is known that CSCs are characterized by resistance to chemo- and radiotherapy. In order to investigate the role of ALDH activity on post-irradiation cell survival, the colony formation assays applying for SKBR3 and HBL-100 were performed. Therefore, directly after sorting ALDH-positive and ALDH-negative subpopulations, cells were seeded into 6 wells plates for colony formation for testing post-radiation cell survival by the colony formation ability. Data obtained and presented in Fig. 3.13 indicate a significant improved survival of ALDH-positive cells after irradiation when compared with ALDH-negative cells. Further, to analyze whether the strong post irradiation survival of ALDH-positive cells is related to an improved DNA-DSB repair capacity, the analysis of the number of residual-γH2AX foci 24 h post irradiation has been performed. As indicated in Fig. 3.13 B, ALDH-positive cells presented a significantly lower number of residual γH2AX foci when compared to ALDH-negative cells. These data clearly indicate a significantly improved DNA-DSB repair efficacy in ALDH-positive cells.

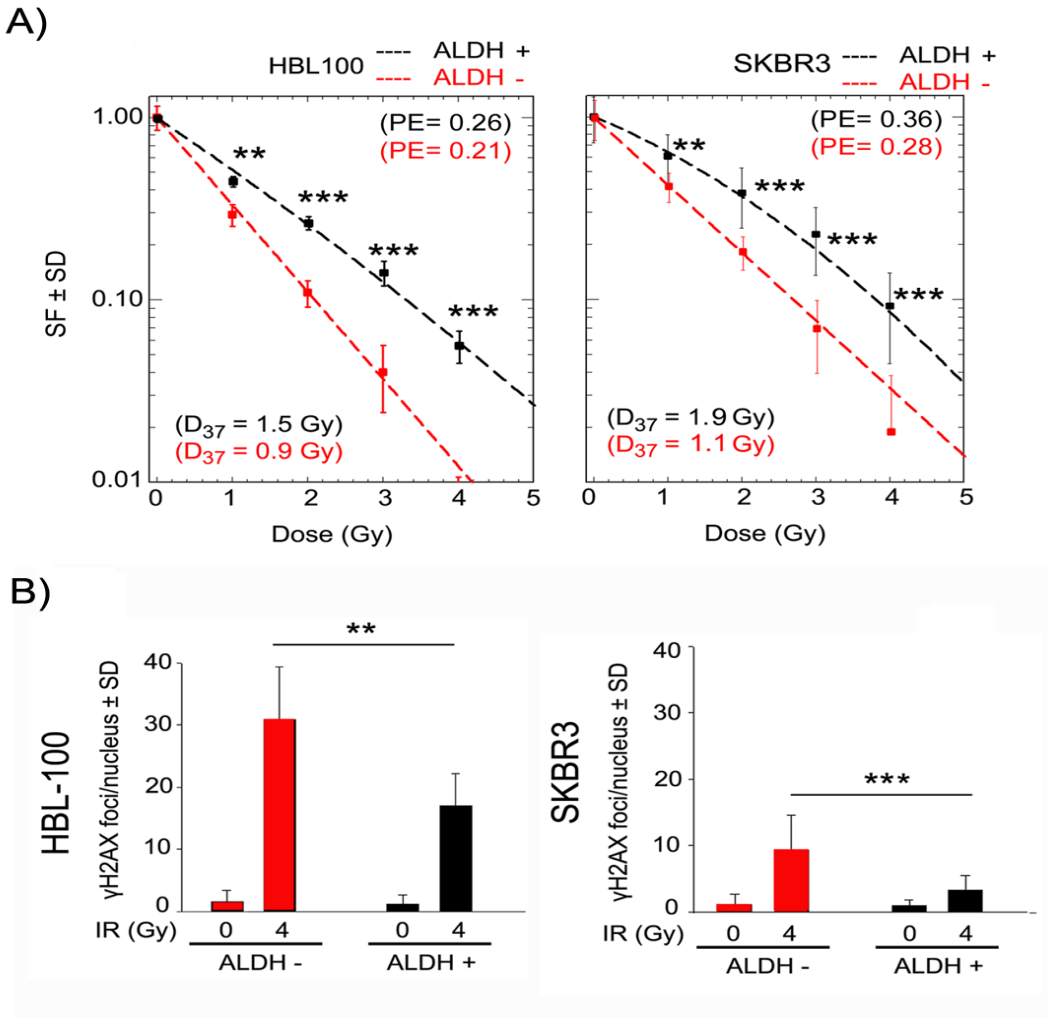

Figure 3.13. ALDH activity promotes clonogenic cell survival through improved DNA-DSB repair. A) Colony forming assay of ALDH-positive and –negative SKBR3 and HBL-100 cells. Sorted cells were seeded for transfection in 6 well plates and then 24 h later cells were irradiated and incubated for colony formation as described in materials and methods. The incubation time for different cell lines differed between 10 to 14 days. Data points of the survival curves represent the mean value of dose dependent of survival fractions ± standard deviations (SD) from three independent experiments with 18 parallel samples. **B)** Residual-γH2AX foci of ALDH-positive and negative sorted cells. Cells were cultured in chamber slides for 2 to 3 days in order to reach the confluency of 60-70%. Twenty-four hours after 4 Gy irradiation cells were fixed and later stained for H2AX phosphorylation as described in materials and methods. Bars represent the mean value of Residual-γH2AX foci per nucleus ± standard deviations (SD) from two independent experiments with at least 100 nuclei per condition. (* $p < 0.05$, **$p < 0.01$, and ***$p < 0.001$, Student's t-test). These data has been already published in Harati MD, et al. IJMS 2019 [135].

3.5.3 Role of Nanog in radiation response and ALDH activity

Based on the Nanog protein expression data obtained so far for ALDH-positive and ALDH-negative cells (see Fig. 3.12B) as well as for Nanog overexpression in irradiated 3D-cultured cells (see Fig. 3.11C), the potential role of Nanog in the regulation of ALDH activity and radioresistance was investigated. Therefore, Nanog protein was either overexpressed or downregulated in HBL-100 and MCF-7 cells (Fig. 3.14A). Fourty-eight hours after Nanog- plasmid or Nanog-siRNA transfection, ALDH activity was determined based on the described protocol. Compared to control cells Nanog-overexpressing cells presented a significantly elevated ALDH activity (Fig. 3.14B) whereas Nanog-knockdown resulted in significant reduction of ALDH (Fig. 3.14B). These data clearly confirm an important role of Nanog in regulating ALDH activity. Furthermore, colony formation ability after up and downregulation of Nanog was tested for these cells. As shown in Fig. 3.14 C, overexpression of Nanog resulted in a significant radioprotective effect and Nanog downregulation by siRNA in a significant radiosensitization of HBL-100 and MCF-7 cells. Thus, these data clearly demonstrate the role of Nanog on ALDH activity regulation and on post-irradiation cell survival of the tested breast cancer cell lines.

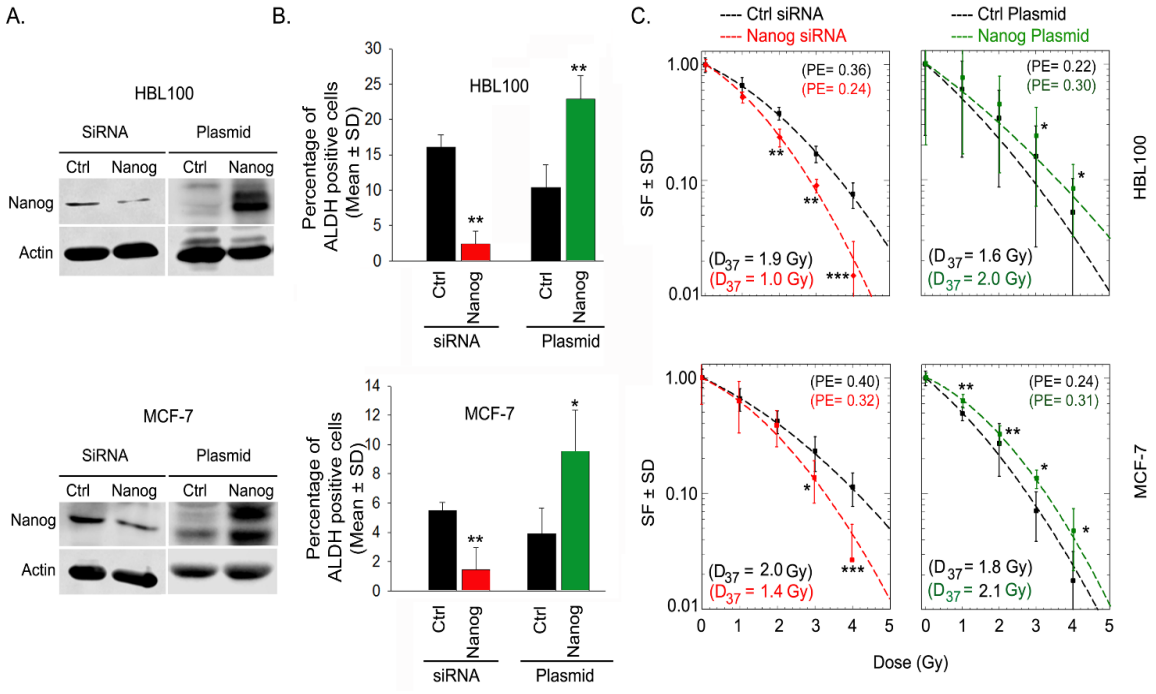

Figure 3.14. Nanog stimulates ALDH activity and clonogenic cell survival of irradiated cells. A) Expression level of Nanog after siRNA mediated knockdown or plasmid overexpression in HBL-100 and MCF-7 cells. **B)** Cells under equal culture condition and confluency (80-100%) were seeded for the siRNA and plasmid transfection in 6 wells plates as described in materials and methods. Forty-eight hours after Nanog siRNA and plasmid transfection, cells were prepared for Aldefluor assay as described before. Bars represent the mean value of percentage of ALDH ± standard deviations (SD) from three independent experiments with 6 parallel samples. **C)** Forty-eight hours after Nanog siRNA and plasmid based overexpression transfection, cells were seeded for colony formation assay and then 24 h later cells were irradiated and incubated for colony formation as described in materials and methods. The incubation time for different cell lines differed between 10 to 14 days. Data points of the survival curves represent the mean value of dose dependent of survival fractions ± standard deviations (SD) from three independent experiments with 12 parallel samples. (* $p < 0.05$, ** $p < 0.01$, and *** $p < 0.001$, Student's t-test). These data has been already published in Harati MD, et al. IJMS 2019 [135].

3.5.4 Role of Nanog in DNA repair capacity of ALDH-positive cells

In order to investigate specifically the role of Nanog on ALDH mediated radioresistance, colony formation ability, i.e. clonogenic activity and the number of residual-γH2AX was determined in ALDH-positive cells of the cell lines HBL-100 and SKBR3. To this aim, Nanog expression was downregulated by siRNA transfection in ALDH-positive HBL-100 and SKBR3 cells (Fig. 3.15A). After irradiation with 4 Gy, residual-γH2AX foci were quantified. As demonstrated in Fig. 3.15B, a significant increase in residual-γH2AX was apparent after downregulation of Nanog in ALDH positive cells when compared with SKBR3 and HBL-100 cells expressing basal level of Nanog. Moreover, as shown in the Fig. 3.15B, siRNA mediated downregulation of Nanog resulted in a significant radiosensitization of ALDH-positive cells. Downregulation of Nanog protein expression in the applied cells was confirmed by western-blotting (Fig. 3.5C). For additional control, the effect of Nanog expression on DNA-DSB repair of parental non ALDH-sorted HBL-100 and SKBR3 cells was determined. As indicated in Fig. 3.15D, in these cells knockdown of Nanog resulted only in a slight but non-significant increase of residual-γH2AX foci in non-ALDH-sorted HBL-100 and SKBR3 cells (Fig. 3.15D). Thus, the results obtained by these experiments confirm a specific role of Nanog on DNA-DSB repair capacity of ALDH-positive cells and cellular radioresistance of the analyzed breast cancer cell lines.

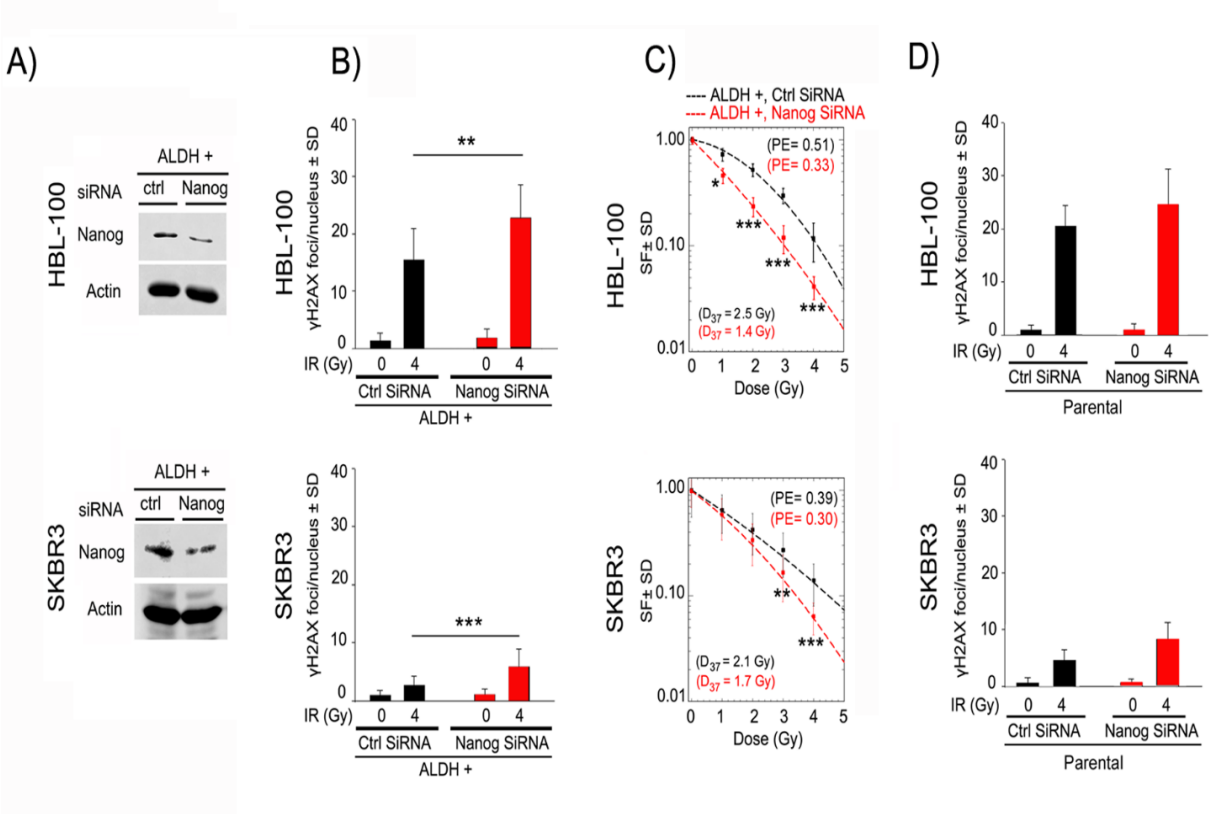

Figure 3.15. Role of Nanog in the radiation response of ALDH-positive cells. A) Expression level of Nanog protein after siRNA mediated knockdown in ALDH-positive HBL-100 and SKBR3 cells was analyzed using Western blotting. **B)** Residual-γH2AX foci assay ALDH-positive cells after Nanog downregulation by specific siRNA. Forty-eight hours after Nanog siRNA transfection, cells were irradiated with 4 Gy dose. Twenty-four hours after irradiation cells were fixed and later stained for H2AX phosphorylation as described in materials and methods. Bars represent the mean value of Residual-γH2AX foci per nucleus ± standard deviations (SD) from two independent experiments with at least 100 nuclei per condition. **C)** Post irradiation cell survival of ALDH-positive cells with and without Nanog siRNA transfection. Forty-eight hours after Nanog siRNA and plasmid based overexpression transfection, cells were seeded for colony formation assay and then 24 h later cells were irradiated and incubated for colony formation as described in materials and methods. The incubation time for different cell lines differed between 10 to 14 days. Data points of the survival curves represent the mean value of dose dependent of survival fractions ± standard deviations (SD) from three independent experiments with 12 parallel samples. **D)** Residual-γH2AX foci in non-sorted cells after Nanog downregulation. Bars represent the mean value of γH2AX foci per nucleus ± standard deviations (SD) from one experiment with at least 50 nuclei per condition. (* $p < 0.05$, ** $p < 0.01$, and *** $p < 0.001$, Student's t-test). These data has been already published in Harati MD, et al. IJMS 2019 [135].

3.6 Subcellular localization of Nanog after irradiation

It is known that Nanog as transcription factor needs to be translocated into the nucleus in order to affect gene expressions by binding to the regulatory components of genes involved in self-renewal. To analyze this in the context of present study, translocation of Nanog to the nucleus was analyzed in the context of exposure of radiation exposure of the cells used for this analysis. Therefore, subcellular fractions of mock-irradiated and irradiated (4Gy) MCF-7 cells were performed. The nuclear and cytoplasmic proteins at different time intervals after radiation exposure (30 min, 60 min, 16 h, 24 h) were analyzed by SDS-PAGE and western blotting. As demonstrated in Fig. 3.16, starting at 30 min post irradiation, a time dependent decrease of Nanog in the cytoplasmic fraction was to be observed. Likewise, a time dependent increase of Nanog in the nucleus fraction was apparent after irradiation, starting at about 1 hr post irradiation. Thus, these results indicate an irradiation induced nuclear translocation of Nanog, which is a prerequisite for its function as a transcription factor.

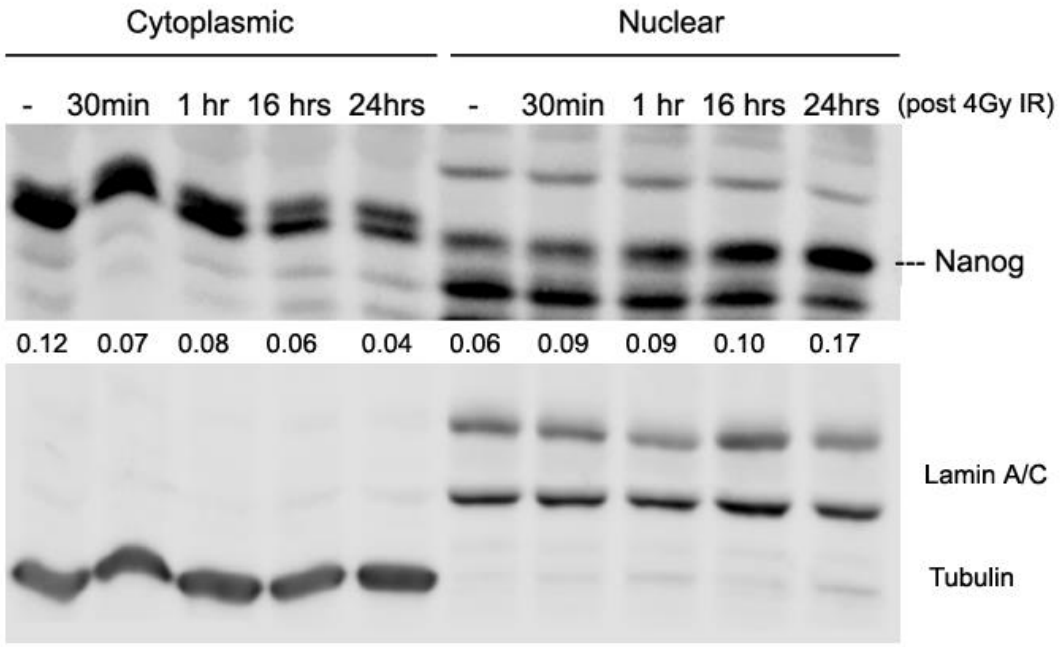

Figure 3.16. Effect of irradiation on nuclear translocation of Nanog. Expression profile of cytoplasmic and nuclear Nanog after radiation exposure. Lamin A/C as a nuclear marker and Tubulin as cytoplasmic marker was used to proof the purity of subcellular fractionation. Densitometry values represent the ratio of specific protein bands intensity to related Lamin A/C and Tubulin. Data are based on two independent experiments.

As it is known that EGFR signaling stimulates cell survival and DNA repair capacity in tumor cells and in order to confirm the data demonstrated in Fig. 3.16, nuclear translocation of Nanog under EGF treatment was additionally investigated. Therefor, MCF-7 cells were treated with EGF (100 ng/ml) and subcellular fractionation was performed at different time points after EGF-treatment (30 min, 60 min, 16 h, 24 h). As shown in the Fig. 3.17, the level of cytoplasmic Nanog protein decreased and nuclear Nanog protein level strongly increased in a time dependent manner after EFG treatment

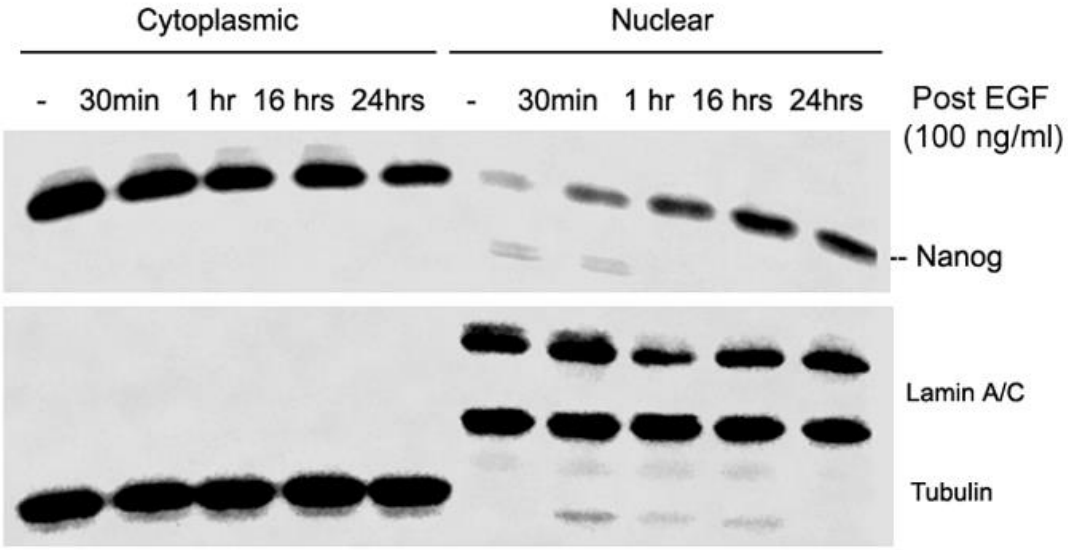

Figure 3.17. Nanog translocates to the nucleus under EGF treatment. Expression profile of cytoplasmic and nuclear Nanog after EGF treatment. Lamin A/C as a nuclear marker and Tubulin as cytoplasmic marker was used to proof the purity of subcellular fractionation. Densitometry values represent the ratio of specific protein bands intensity to related Lamin A/C and Tubulin. Data represent one experiment.

These nuclear translocation data of Nanog after irradiation and EGF indicate an important role of Nanog on gene regulation in the context of post-irradiation cell survival. Therefore, it can be proposed that targeting or inhibiting Nanog´s nuclear translocation may sensitize tumor cells to ionizing radiation. Thus, it was tested whether targeting/inhibiting PI3K/Akt signaling can modify nuclear translocation of Nanog in MCF-7 cells. To this aim, cells were treated with the PI3K inhibitor LY294002 for two

hours and subsequently mock irradiated or irradiated with 4 Gy. Twenty-four hours later subcellular fractionation was performed to separate nucleus and cytoplasmic fractions. As demonstrated in Fig. 3.18 in control cells treated with the solvent DMSO the level of cytoplasmic Nanog was markedly decreased and the level of nuclear Nanog was markedly increased 24 hrs after radiation exposure. Yet, post irradiation nuclear translocation of Nanog was markedly reduced when cells were treated with LY294002, which also inhibited radiation-induced phosphorylation of Akt at serine 473. This data clearly indicate that nuclear translocation Nanog in irradiated cells is abrogated by inhibition of PI3K/Akt pathway.

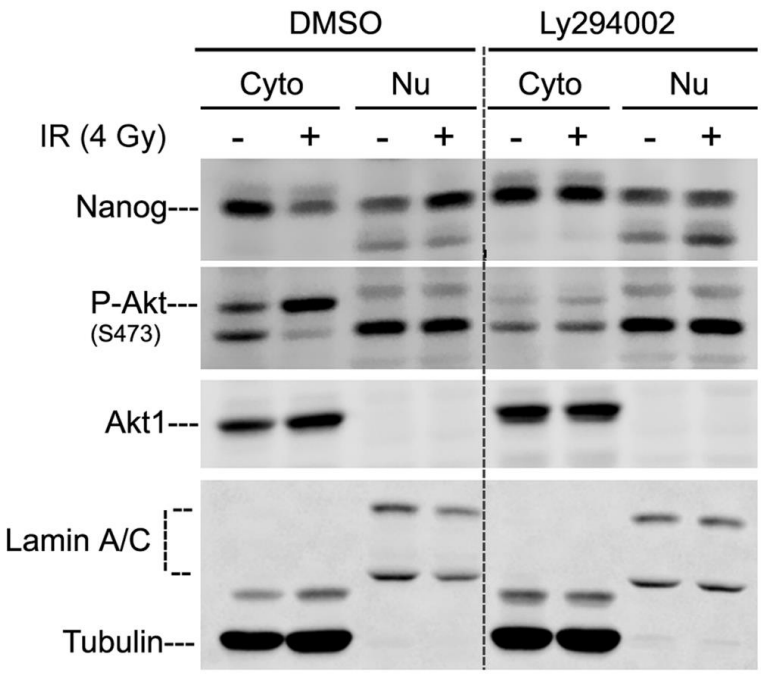

Figure 3.18. Nuclear translocation of Nanog after irradiation is regulated by PI3K/Akt pathway. Protein samples were isolated 24 h after irradiation and 26 h after LY294002 treatment (5 µM). Protein expression was analyzed by Western blotting. Lamin A/C as a nuclear marker and Tubulin as cytoplasmic marker was used to proof the purity of subcellular fractionation. Densitometry values represent the ratio of specific protein bands intensity to related Lamin A/C and Tubulin. Data are based on two independent experiments.

3.7 Functional effect of Nanog via Akt/Notch proteins

3.7.1 Correlation of Nanog expression on expression profile of Akt and Notch protein

Based on the data demonstrated so far and indicating stimulated Nanog, P-Akt and Notch1 expression levels in ALDH-positive versus to ALDH-negative cells (see again Fig. 3.12B), the potential correlation and or interaction of these signaling proteins has been investigated. Therefore, protein expression of Akt1 and Notch1 after overexpression or downregulation of Nanog has been evaluated in SKBR3, HBL-100 and MCF-7 cells. In all three cell lines plasmid mediated overexpression of Nanog did result in an upregulation of Notch1 protein expression and stimulated phosphorylation of Akt at serine 473, but it did not upregulate protein expression of Akt1 and Sirt2 (Fig. 3.19A). Furthermore, siRNA mediated downregulation of Nanog resulted in a decreased Notch1protein expression and reduced phosphorylation of Akt at serine 473 but again Sirt2 and Akt1 protein expression was not affected (Fig. 3.19B). These data imply that Nanog is able to control cellular radiation response patterns via modulating Akt- and Notch-dependent pathways.

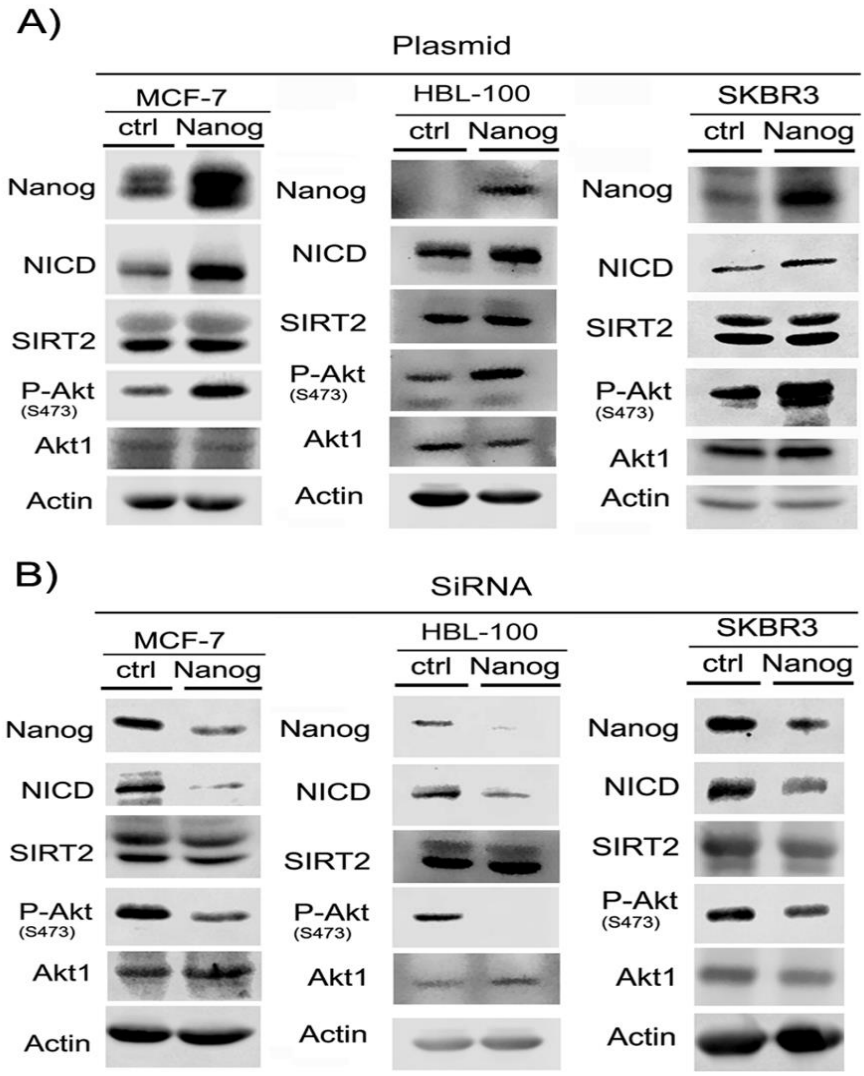

Figure 3.19. Correlation of Nanog with Akt and Notch protein expression. A) Protein expression profile after plasmid based Nanog overexpression in SKBR3, HBL-100 and MCF-7 cell line. **B)** Protein expression profile after Nanog downregulation by specific siRNA. **A, B)** The expression level of the indicated proteins was analyzed using Western blotting. In order to detect the proteins with similar molecular weight, after each detection the blots were stripped and then incubated with next antibody. The data represent one experiment (MCF-7, SKBR3 and HBL-100). These data has been already published in Harati MD, et al. IJMS 2019 [135].

3.7.2 ALDH activity regulated by Nanog depends on expression of Notch and Akt activity

As it has been demonstrated above, Nanog can regulate the activation/phosphorylation of Akt1 and stimulate the protein expression of Notch1 (see Fig. 3.19), Thus, it has been

questioned further, whether Nanog is able to regulate ALDH activity via Akt and Notch1 signaling. To answer this question, Nanog was overexpressed in HBL-100 and MCF-7 cells and subsequently cells were transfected with Notch1 siRNA to downregulate Notch1 expression. Thereafter, ALDH activity was measured while Nanog is overexpressed and Notch1 is downregulated. Under this condition, Nanog was not able to stimulate ALDH activity (Fig. 3.20A). Furthermore, after Nanog overexpression cells were treated with the Akt inhibitor MK2206. As a consequence the stimulatory effect of Nanog overexpression on ALDH activity was blocked when Akt-kinase activity was blocked by MK2206 (Fig. 3.20B). These results indicate that Nanog cannot induce ALDH activity when Akt activity is blocked. Consequently it can be concluded that Nanog is able to regulate ALDH activity only in the presence of a functioning signaling activity via Akt and Notch.

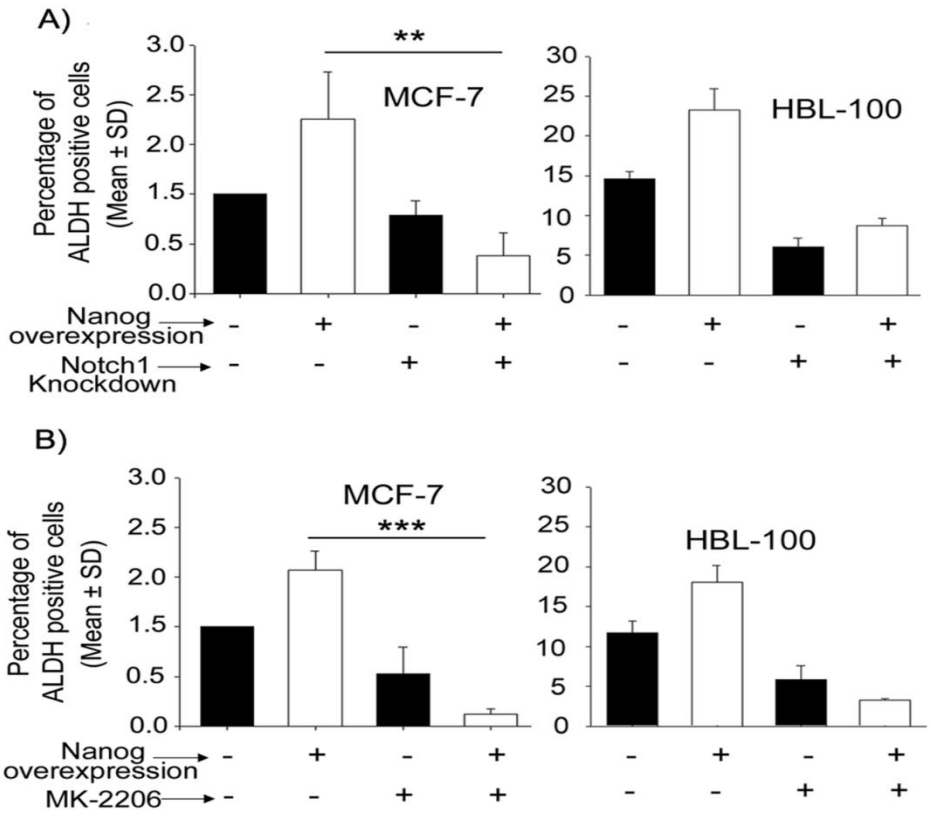

Figure 3.20. Stimulation of ALDH activity by Nanog depends on Notch1 and Akt protein. A) ALDH activity has been measured 48 h after Nanog overexpression and 24 h after Notch1 downregulation. **B)** ALDH activity has been measured 48 h after Nanog overexpression and 2 h after MK2206 treatment (250 nM and 1 µM respectively for MCF-7 and HBL-100). **A, B)** Cells

were incubated with Aldefluor reagent as described in materials and methods. Bars represent the mean values of ALDH percentage ± standard deviations (SD) from three independent experiments for MCF-7 with 2 parallel samples each and one experiment for HBL-100 with 3 parallel samples. (* $p < 0.05$, ** $p < 0.01$, and *** $p < 0.001$, Student's t-test). These data has been already published in Harati MD, et al. IJMS 2019 [135].

3.7.3 Radiaoprotective effect of Nanog depends on expression of Notch and Akt1 activity

Based on the results described above, it was further investigated whether the suggested correlation/interaction of Nanog, Akt1 and Notch1 is active in modifying the radiation response of tumor cells. To test this, Nanog was overexpressed in HBL-100 and MCF-7 cells and subsequently cells were transfected with either Notch1 or Akt1 siRNA. Colony formation assays were performed to analyze the response pattern of these cells to radiation exposure. The obtained clonogenic survival data indicated that Nanog overexpression does result in radioprotection. However, this effect was not apparent when Akt1 and Notch1 were downregulated (Fig. 3.21). In MCF-7 control cells, neither Akt1 nor Notch1 knockdown induced radiosensitization (Fig. 3.21). However, siRNA downregulation of Akt1 and Notch1 in Nanog overexpressing cells did result in radiosensitization of MCF-7 as well as HBL-100 cells. These data have further been confirmed by applying Akt inhibition by MK2206 treatment. As demonstrated in the Fig. 3.22, the radioprotective effect of Nanog is significantly abrogated by inhibition of Akt activity. Thus, these data again confirm a role of Nanog via Akt1 and Notch1 signaling in triggering the cellular radiation response.

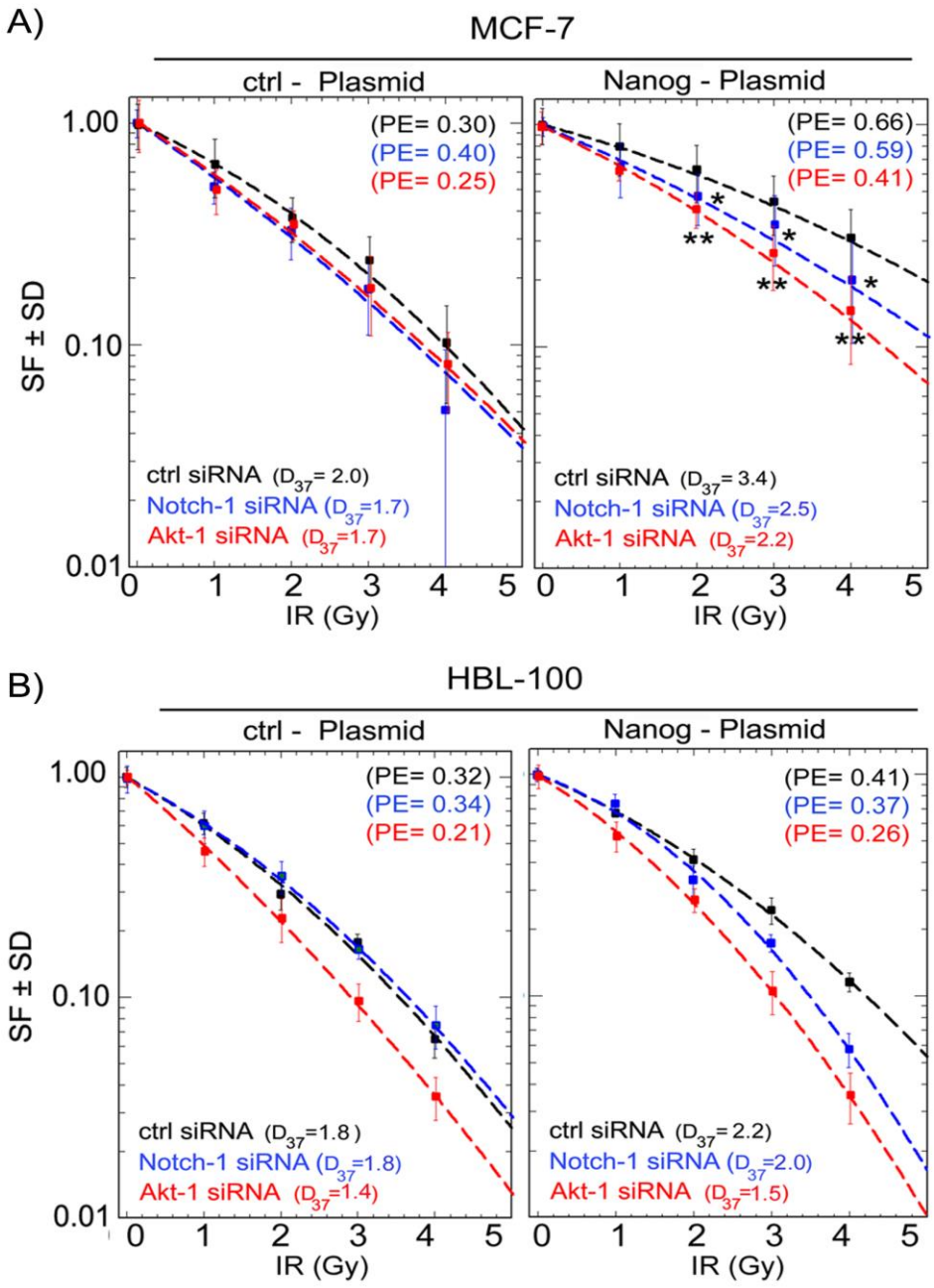

Figure 3.21. Nanog Promotes post-irradiation cell survival via Akt1 and Notch1. The colony formation assay has been done 48 h after control and Nanog plasmid overexpression and 24 h after Notch1 and Akt1 downregulation. MCF-7 **(A)** and HBL-100 **(B)** cells were seeded in 6 wells plates and after 24 h they were irradiated (0-4 Gy). Data points of the survival curves represent the mean value of dose dependent of survival fractions ± standard deviations (SD) from two independent experiments for MCF-7 with 6 parallel samples each and one experiment for HBL-100 with 6 parallel samples per condition. (* $p < 0.05$, **$p < 0.01$, and ***$p < 0.001$, Student's t-test). These data has been already published in Harati MD, et al. IJMS 2019 [135].

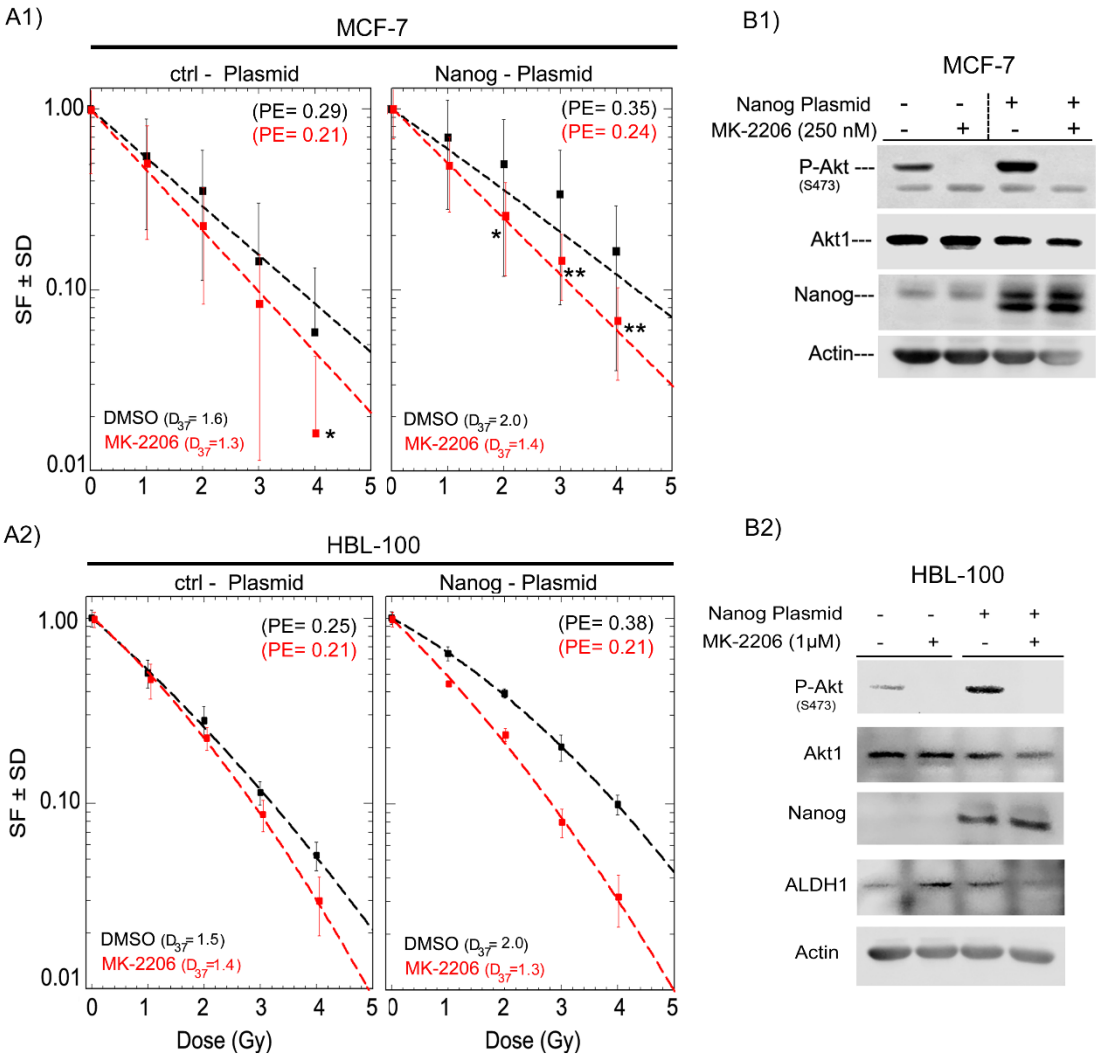

Figure 3.22. Nanog promotes post-irradiation cell survival via Akt1 and Notch1. A1, A2) Cell were seeded for colony formation assay 48 h after Nanog overexpression. Then 22 h after seeding, cells were treated with MK2206 and 2 h later (24 h after seeding) were irradiated (0-4 Gy). Data points of the survival curves represent the mean value of dose dependent of survival fractions ± standard deviations (SD) from two independent experiments for MCF-7 with 6 parallel samples each and one experiment for HBL-100 with 6 parallel samples per condition. **B1, B2)** Protein expression profile after plasmid based Nanog overexpression and MK2206 treatment in HBL-100 and MCF-7 cell line. (* $p < 0.05$, **$p < 0.01$, and ***$p < 0.001$, Student's t-test). These data has been already published in Harati MD, et al. IJMS 2019 [135].

3.7.4 Regulatory effect of Nanog on Notch1 and Akt1

In the next experimental approach using the same design, the actual order of Akt and Notch protein within Nanog regulatory pathway was addressed. As shown for two cell lines MCF-7 and HBL-100 in Fig. 3.23, downregulation of Akt did not affect the expression level of Notch1 in both control and Nanog plasmid overexpressing cells. However, downregulation of Notch1 markedly reduced the expression level of total Akt in control and even stronger in Nanog overexpressing cells (Fig. 3.23). These data confirmed the previous finding that Nanog overexpression can is able to stimulate Notch1expression and Akt activity. This result also supports the assumption that the function of both Nanog and Notch1 is upstream of Akt.

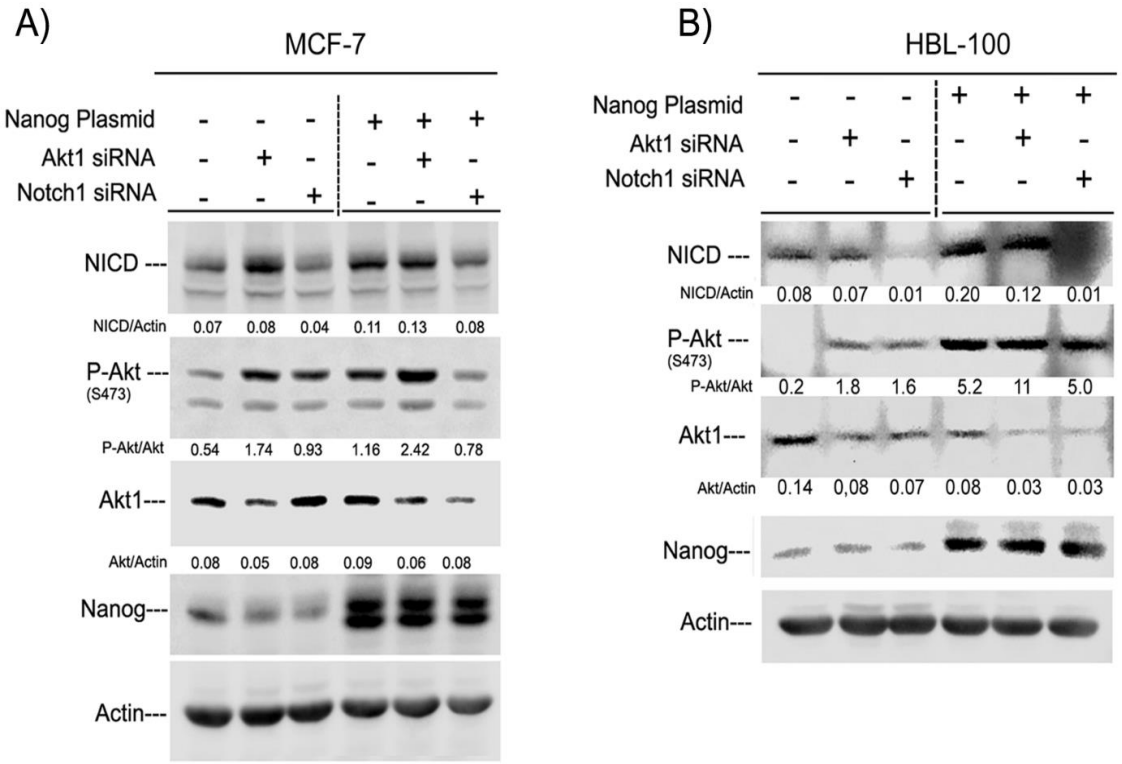

Figure 3.23. Regulatory effect of Nanog on Notch1 and Akt. A, B) Protein samples were isolated 48 h after Nanog overexpression and 24 h after Notch1 and Akt1 downregulation. Protein expression level of the indicated proteins was analyzed using Western blotting. In order to detect the proteins with similar molecular weight, after each detection the blots were stripped and then incubated with next antibody. Densitometry values represent the ratio of the specific protein band intensity to actin. These data has been already published in Harati MD, et al. IJMS 2019 [135].

3.8 Knock-out of Nanog impairs post irradiation cell survival and DNA-DSB repair

In order to confirm the obtained results regarding the role of Nanog in post irradiation response (see Fig. 3.14, 3.15 and 3.19), the prostate cancer cell line DU145 knocked out for Nanog (DU145 Nanog-KO) cell line was used. Colony formation assays under 2D- and 3D-culture conditions were performed to analyze the response pattern of DU145-Nanog knock out and parental DU145 cells to radiation exposure. As demonstrated in Fig. 3.24 A, B Nanog knockout significantly radiosensitized DU145 cells both under 2D- and 3D-culture conditions when compared to parental DU145 controls (Fig. 3.24 A, B). Likewise, a significant increase in residual-γH2AX foci was apparent in Nanog knock out cells (Fig. 3.24 C) indicating a significantly impaired DNA-DSB repair efficacy. Additionally, the role of Nanog on stemness was determined by culturing Nanog knock out and parental cells under 3D-culture condition. As demonstrated in Fig. 3.24 D sphere formation of DU145-Nanog knock out cells was markedly reduced compared with parental control cells (Fig. 3.24 D). Moreover, both in Nanog knock out and in parental cells it was determined whether Nanog-knock out does affect protein expression of Notch1, Bmi1, and Akt1 as well as the phosphorylation status of Akt at serine 473. As demonstrated in Fig. 324E Nanog knock out resulted in decreased protein expression of Notch1 and Bmi1 but neither Akt1 expression nor Akt phosphorylation at serine 473 protein expression was affected. Potentially, this effect might be due to a reactivation of Akt as a compensatory behavior of cells under long-term Nanog knock out condition. Nevertheless, together these results clearly confirmed the importance of Nanog on post-irradiation survival and DNA-DSB repair capacity of the tested tumor cells.

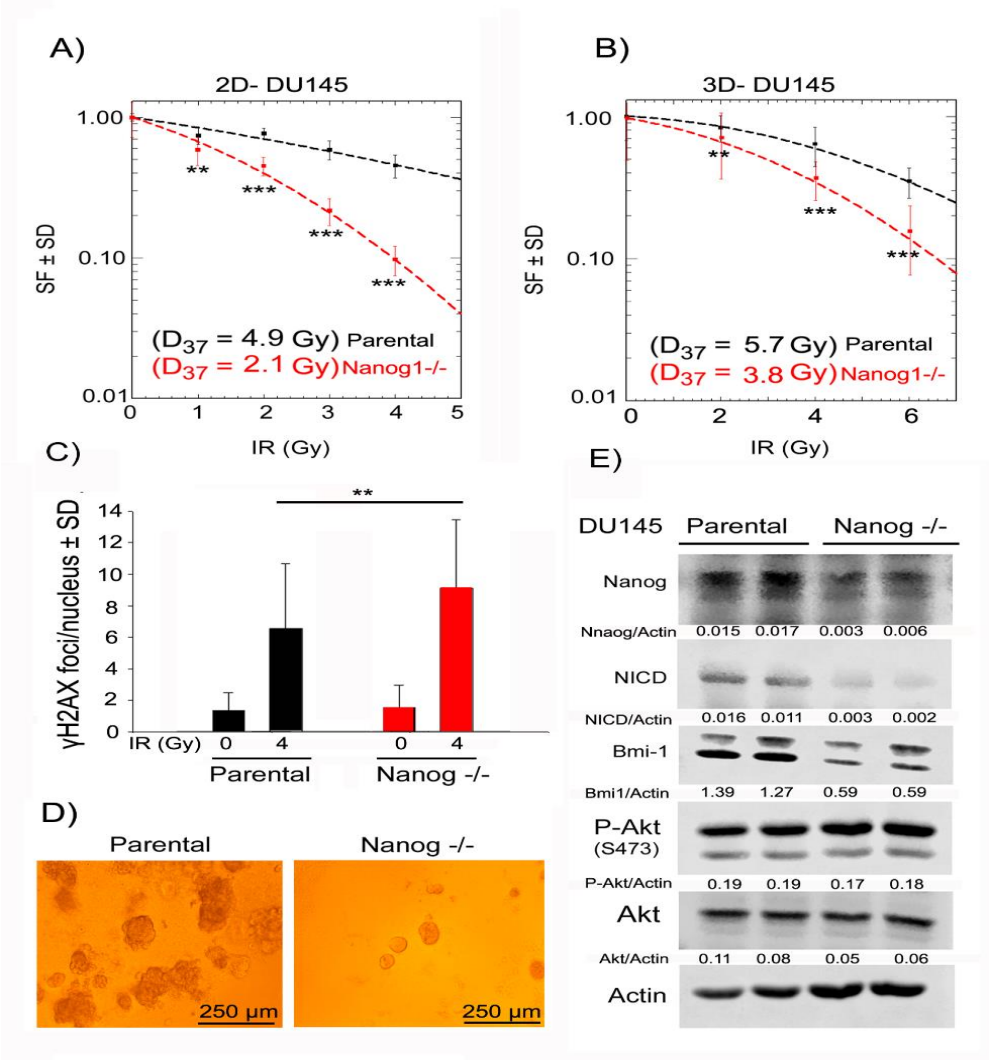

Figure 3.24. Post irradiation cell survival and DNA-DSB repair ability of Nanog knock-out cells. A, B) Colony formation assay of Nanog knock out and parental DU145 cells in 2D- and 3D-culture. Cells were cultured in 6 wells plates (2D-culture) and in matrigel in 96 wells plate (3D-culture) based on mentioned protocol in Materials and Methods section. Twenty-four hours later single cells were irradiated (0-4 Gy) and cells were incubated for 8 days under 3D-culture and 14 days under 2D-culture in order to form colonies/spheres. Data points of the survival curves represent the mean value of dose dependent of survival fractions ± standard deviations (SD) from two independent experiments with 6 parallel samples each. **C)** Residual-γH2AX foci of Nanog knock out and parental cells. Twenty-four hours after 4 Gy irradiation cells were fixed and later stained for H2AX phosphorylation as described in materials and methods. Bars represent the mean value of Residual-γH2AX foci per nucleus ± standard deviations (SD) from two independent experiments with at least 100 nuclei per condition. **D)** Sphere formation under 3D-culture. **E)** Protein expression level of the indicated proteins was analyzed using Western blotting. In order to detect the proteins with similar molecular weight, after each detection the blots were stripped and then incubated with next antibody. Densitometry values represent the ratio of the specific protein band intensity to actin. (**$p < 0.01$, and ***$p < 0.001$, Student's t-test).

4 Discussion

Therapy resistance is still one of the most important issues and problems in cancer treatment. Cancer stem cells (CSCs) represent a small subpopulation within tumor tissues mainly represented by so-called tumor bulk cells [21, 22]. CSCs in contrast to tumor bulk cells can tolerate and survive conventional chemo- as well as radiation therapy protocols [136]. Especially via upregulation of various survival pathways such as PI3K/Akt signaling CSCs can overcome treatment effects [91, 92]. Based on insights that therapy resistance of solid tumors is mainly due to the presence of CSCs many basic as well as translational research activities have been started within the last 5-10 years [137]. Although radiation therapy in combination with surgery is one of the primary treatment options for breast cancer patients, radioresistance of CSCs is still a major issue for treatment success. To further improve treatment outcome, it is desirable to enhance radiotherapy via targeting resistance mechanism of CSCs to radiation. To this aim, and although the basic mechanisms are still not fully understood, targeting strategies directed against molecular pathways in CSCs including ALDH activity and PI3K/Akt pathway may have a strong potential towards improved therapy outcome [137].

4.1 Expression of CSC markers in different breast cancer cell lines in vitro

The differential expression of CSCMs in various types of tumors has been shown in several studies [138-140]. It has been confirmed that putative stem cell markers such as Nanog, Oct4 and Sox2 are not expressed at the same level between different breast cancer cell lines such as MCF-7, MDA-MB-231 and T-47D [138]. Based on this study, Nanog is mainly expressed in MCF-7 but not in the two other cell lines and Sox2 is expressed strongly in T-47D [138]. Data of the present study confirmed the variety of expression of putative stem cell markers in the different breast tumor cell lines used. These data indicated that each CSC marker might play a specific role in the behavior and radiation response of each cancer cell line. It has been described that variations in stem cell marker expression of different tumor cell lines might also be associated with

the specific tumor subtypes [139, 140]. In this regard, Olsson and coauthors [139] have shown that the expression of CD44 isoforms is mainly related to the HER2 status of the tumor and is stronger expressed in basal-like tumor subtypes. In the present thesis, however, it was not the aim to investigate the relation between CSCM expression and tumor subtypes, but to address the cellular consequences of CSCM expression in the context PI3K/Akt signaling and cellular radiation responses.

As demonstrated downregulation of Akt1 exerted a stronger effect on the expression of the CSCM Nanog, Bmi1 and Sox2 as compared to downregulation of the Akt isoforms Akt2 and Akt3. The importance of Akt on CSCM expression is also demonstrated by a report of Gargini and coworkers [141], which indicated a significant reduction of sphere formation of CD44+/CD24- MDA-MB-231 breast cancer cells mainly after knock down of Akt1 when compared to knock down of Akt2.

Likewise, in the present study the activity level of ALDH1 was altered, i.e. significantly reduced after knock out or knock down of Akt 1 and 3 isoforms in HBL-100 and HCT116. However, downregulation of Akt2 resulted only in HBL-100 cells in a significant reduction of ALDH activity, whereas in HCT116 only a marked but not significant reduction of ALDH activity could be demonstrated (Fig. 3.6). In line with these findings, it has been shown that overexpression of total cellular Akt and especially nuclear Akt leads to a stimulated ALDH activity and also increased Nanog as well as Oct-4 expression in SKBR3 and MDA-MB468 cells [142]. In addition, indirect inhibition of Akt using PI3K- or mTOR-inhibitors (B591 and rapamycin respectively) also showed a reduction of ALDH activity in breast cancer and osteosarcoma cells [143, 144]. However, in these studies, the role of different Akt isoforms on ALDH activity was not investigated. Yet, for MCF-7 cells, knock down of the three Akt isoforms did not show a significant reduction of ALDH activity (Fig. 3.6). Likewise in regard to the present result, Vasudevan and coworkers [145] demonstrated that downregulation of three Akt isoforms did not affect tumor cell lines with PIK3CA mutation or with low level of p-AKT such as MCF-7, SW948 and HCT-15 either. Especially for the MCF-7 cells analyzed in the present study, a low level of P-Akt was also to be observed. Thus, this might be the reason why knockdown of Akt isoforms did not regulate ALDH activity in MCF-7 cells. Due to very low amount of ALDH activity in MDA-MB-231

cells (appr. almost 0% ALDH activity), these cells could not be tested for the role of Akt isoforms on ALDH activity.

4.2 Role of Akt and ALDH activity in radiation response of CSC in vitro

Based on the importance of Akt on radiation response of tumor cells described in previous stuedies and reports by our laboratory [102, 104], the role Akt isoforms and ALDH activity was first tested on the clonogenic activity of irradiated breast cancer cell lines. These data study indicated that knockdown of Akt isoforms (Akt1, 2 and 3) leads to radio-sensitization of HBL-100 cells but not of MCF-7 cells. For MDA-MB-231 cells only knockdown of Akt3 resulted in radiosensitization (Fig. 3.8). These findings clearly indicate that Akt isoforms do affect the radiation response in a tumor cell type dependent manner. In this regard, it has previously been shown that Akt1 and Akt3 but not Akt2 via interaction with DNA-PKcs lead to a better DNA-DSB repair capacity and clonogenic activity in KRAS muted cells such as A549 and MDA-MB-231 [146]. Furthermore, Sahlberg and coworkers [147] demonstrated that knockdown of Akt1 and Akt2 results in radiosensitization of the colon cancer cells lines DLD-1 and HCT116. Accordingly, it has been demonstrated that knockout of both isoforms (Akt1 and 2) leads to radio-sensitization of DLD-1 and HCT116 tumor cells [147]; however in this report - due to a low expression level - the role of Akt3 in these cells was not investigated (147). Based on the data presented in this thesis (see Fig. 3.8), after knockdown of all three Akt isoforms the inhibition of ALDH activity with DEAB did not further affect the radiation response of the three tested cell lines HBL-100, MCF-7 and MDA-MB-231. These results provide evidence that Akt functions upstream of ALDH and consequently knockdown depletion of Akt results in inhibition of ALDH. Accordingly, ALDH inhibition by DEAB treatment induces radiosensitization as it was shown herein for HBL-100 cells. This data is in line with findings by Krocer and coworkers [148], who have demonstrated that ALDH inhibition by DEAB or ATRA (all-trans retinoic acid) leads to radio and chemo-sensitization of CD44+/ALDH+ breast cancer cell lines.

The data of the present study demonstrating that inhibition or down regulation of ALDH1 affects differentially the radiation response of breast cancer cell lines are of special interest, since the used cell lines presented quite different radiation responses to DEAB treatment or siRNA mediated downregulation of ALDH1 (Fig. 3.3 and 3.5). Therefore, the percentage of ALDH activity in theses cell lines was analyzed. As it is shown in Fig. 3.5, HBL-100 cells with the highest ALDH activity were markedly stronger radiosensitized after inhibition of ALDH, as compared with the cell lines MDA-MB-231 and MCF-7 which presented the lowest ALDH activity. These findings indicate the importance and necessity of ALDH for the radiation response of these cancer cell lines. This assumption is also supported by data published by Charafe-Jauffret and coworkers [149] and Marcato and coworkers [150] who demonstrated on the basis of 33 breast cancer cell lines presenting very low ALDH activity (0-1%, i.e. MCF-7 and MDA-MB-231) to very high ALDH activity that both, the metastatic potential as well as stem cell features clearly depend on the level of ALDH activity. With respect to the correlation of ALDH activity and cellular radiation response it needs also to be reflected that ALDH activity dependents not only on one isoform of ALDH but also on the isoforms such as ALDH1A1, ALDH1A3 and ALDH3 [151]. This assumption is supported by the report of Marcato and coworkers [150] who demonstrated that knockdown of ALDH1A3 in comparison to knockdown of ALDH1A1 results in a stronger suppression of ALDH activity in the three breast cancer cell lines MDA-MB-231, SKBR3 and MDA-MB-468. Moreover, Zhau and coworkers [152] investigated the role of 19 different ALDH isoforms on ALDH activity determined by the Aldefluor assay. This study indicated that nine out of nineteen ALDH isoforms are contributing to ALDH activity. These isoforms of ALDH were named by Zhau and coworkers as active ALDH isoforms [152]. In this report, based on endogenous mRNA profiles it could also demonstrate that MCF-7 breast cancer cells express primarily the isoform ALDH3A2 but not ALDH1 [152]. This result is in very good agreement with the data of ALDH activity determined in MCF-7 cells presented herein. In the context of the observation reported by Zhou and coworkers [152] it is of further interest, that DEAB does not inhibit the enzyme activity of all active ALDH isoforms (i.e. ALDH3B1 and ALDH5A1). Thus both, the report by Zhou and coworkers [152] as well as the data presented herein clearly indicate that the importance of specific

ALDH isoforms for the ALDH enzyme activity not only needs to be verify but also that more investigations are necessary in order to define a specific inhibitors of each active ALDH isoforms.

4.3 Radiation response under 3D-culture condition

A 3D-culture system is the gold standard method in in vitro stem cell research [153]. Thus, in the present study the sphere formation assay was applied to investigate breast cancer cell lines under 3D-culture condition. For these purposes, the breast cancer cell lines MCF-7, SKBR3 and MDA-MB-231 were applied. A cell line specific time period for the formation of spheres was observed; likewise, the shape of spheres was dependent of the tumor cell line used. MCF-7 presented a round, SKBR3 a grape shape, and MDA-MB-231 a stellate sphere morphology (see Fig. 3.9). The data presented are in good agreement with data reported by Kenny and coworkers [154] who demonstrated a correlation of sphere morphology and gene expression for 25 breast cancer cell lines under 3D-culture condition. Four morphology characteristics, i.e. mass, round, grape-like and satellite shapes were described by Kenny and coworkers (154). Interestingly, they also demonstrated that the cell lines with similar sphere shape morphology showed an equal gene expression pattern [154].

Based on the clonogenic assay data under 3D-culture condition obtained in the present study, it is obvious that the plating efficacy of all breast cancer cell lines tested (in average less than 10 %) is markedly lower than that for the same cell lines under 2D-condition. This effect is most likely to be explained by the fact that 3D-culture conditions provide a specific environment in which only CSCs can grow and form spheres. This is supported by previous reports indicating that depending on the tumor type the proportion of CSCs compared to tumor bulk cells is rather low [133, 155]. Moreover, Bahmad and coworkers [156] reported that the low plating efficiency under 3D-culture is potentially also due to the strong tendency of formed neighboring spheres to merge in matrigel. Bodgi and coworkers [157] provided evidence that although the plating efficacy of the bladder cancer cell lines RT4 and UM-UC-3 is low under 3D-culture condition, nevertheless the survival curves of these cells indicated a stimulated

and increased radioresistance of these cells both under 3D- and 2D-culture conditions. These authors postulated that the applied 3D-matrigel culture condition mediated the ability of these cells to survive even after exposure to high doses of ionizing radiation (8 or 10 Gy) most likely due to the efficacy of matrigel to induce and stimulate cell proliferation after irradiation [157].

Thus, the results on radioresistance of 3D-cultures of breast cancer cells presented herein are in good agreement with the previous literature report. The data of the present study even expand the mechanistic interpretation of the demonstrated cell- and radiobiological effects to the qualitative and quantitative level of CSC marker proteins. As it has been demonstrated in Fig. 11, ALDH activity of MCF-7 and MDA-MB-231 cells is drastically increased under 3D-culture condition. Likewise, protein expression of the CSC markers Nanog and ALDH1 is elevated as well when cells are irradiated with a dose of 6 Gy. These findings together with the 3D-culture analyses indicate that mainly CSCs with high ALDH activity are able to form spheres under 3D-culture condition, whereas cells with low ALDH activity are rather limited in their ability to form spheres. These data also confirm the notion that sphere-culture systems indeed provide a suitable method for enrichment of CSCs populations.

The presented data of this thesis are further in agreement with results reported by Lagadec and coworkers [158]. This group reported that irradiation (i.e. 4 and 8 Gy) stimulates ALDH activity of ALDH1-negative sorted SUM159PT breast cancer cells and additionally increases the percentage of CD24-/CD44+ cells in MCF-7 cultures [158]. Lagadec and coworkers [158] have also demonstrated that induction of CSCM such as Nanog, Oct-4 and Sox2 after irradiation is dependent on the dose of irradiation applied. Stimulated ALDH activity has further been reported by Reynolds and coworkers [159] for MDA-MB-231 under 3D- versus 2D-culture conditions. Likewise, gene expression of ALDH1A3, Sox2, Nanog and Oct4 increased markedly in spheroids when compared to 2D-cultured control cells [159]. In similar studies performed by Ghisolfi and coworkers [160] it was demonstrated that doses of 2 and 4 Gy but not higher doses (i.e. 6 and 8 Gy) of ionizing radiation did induce the expression of CSCM Sox2 and Oct-4 6 hours after radiation exposure and promoted sphere formation in hepatocellular carcinoma cells in vitro. Accordingly, knockdown of Sox2 and Oct4 radiosensitized these cells and abrogated sphere formation [160].

4.4 Molecular radiobiological and differences of ALDH-positive and negative cells

To address potential cell- and radiobiological differences in ALDH-positive and ALDH-negative breast cancer cells, the ALDH-high expressing SKBR3 and HBL-100 cell lines were analyzed after sorting ALDH-positive and ALDH-negative subpopulations of these cell lines. The breast cancer cell lines MCF-7 and MDA-MB231 were excluded from the analyses due to the low levels of ALDH-activity expressed in these cells. To avoid mixture of ALDH-positive and ALDH-negative subpopulations of the cell lines analysed, a specific distance between the gates of ALDH high and low cells has been introduced to ensure the purity of sorting. One reasons that originally strong ALDH-positive cells loose the produced fluorescence signal is due to the increased level and presence of ATP-binding cassette transporters **(**ABC transporters). This was shown by Awad and coauthors [161] who demonstrated that Ewing's sarcoma cells with high ALDH activity have more ABC transporter activity, which enables these cells to efflux chemotherapeutic drugs more efficiently. Accordingly, it has been shown that keeping cells on ice or at least at cool temperature slows down the activity of ABC transporters; thus, this methodology was used in the present study during cell sorting as well [162].

The direct comparison of sorted ALDH-positive and ALDH-negative subpopulations of the applied breast cancer cell lines SKBR3 and HBL-100 cells indicated that only Nanog and Bmi-1 but not Oct4 and Sox2 are overexpressed in ALDH-positive cells (Fig. 12). In line with these data, it has been shown by Wu and coworkers [163] that ALDH-positive sorted cells from the gastric cancer cell lines MKN-45 and SGC-7901could be characterized by an elevated expression of Nanog, Bmi-1 and Oct-4 when compared to ALDH-negative cells. Similar results were described by Awad and coworkers [161] based on q-PCR studies indicating that ALDH-positive but not ALDH-negative Ewing's sarcoma cells (TC-71) show elevated expression of Nanog, Bmi-1 and Oct-4. Likewise, reports by various groups [164-166] provided evidence that Sox2 [164, 166], Bmi-1 [165] and Nanog [166] overexpression is apparent in side-population ALDH positive ovarian cancer cells, ALDH-positive head and neck (H&N) squamous cell carcinoma patient samples and in ALDH-positive melanoma cells. Thus, these literature data clearly indicate that ALDH-positive cells from different types of tumors

overexpress a variety of different stem cell markers. However, the fact that not all stem cell markers are equally overexpressed in different subpopulations of ALDH-positive tumor cell lines, may be indicative of a tumor type specificity.

In this context, it needs to be discussed that also the specific expression of different ALDH-isoforms has importance. As shown herein, ALDH1A1 protein level was slightly overexpressed in ALDH positive HBL-100 cells but not in ALDH-positive SKBR3 cells. This data provided evidence for the assumption that different ALDH isoforms are of relevance for the ALDH-enzyme activity determined by the Aldefluor assay. To address this topic, the expression of ALDH1A3 was investigated in ALDH-positive and ALDH-negative sorted subpopulations of the breast cancer cell lines HBL-100 and SKBR3. The data received indicate an upregulation of ALDH1A3 in ALDH-positive cells of both HBL-100 and SKBR3 cells. Similar data were reported by Kurth and coworkers [167] indicating that ALDH1A3 is the main responsible isoform for ALDH activity in the H&N cancer cell lines FaDu and Cal33. Likewise, it has been reported by Marcato and coworkers [150] that mainly ALDH1A3 but not ALDH1A1 is responsible for ALDH activity in breast cancer cell lines such as MDA-MB-231, SKBR3 and MDA-MB-468. Thus, with respect to the importance of ALDH1A3, the data reported in the present study for breast cancer cell lines is in good agreement with the existing literature.

Another important aspect of ALDH activity and its role and function in the context of the expression of other CSC markers relates to the activity level of the signaling component Akt. Akt has been described by our laboratory and others to be a main mediator of resistance of tumor cells to various forms of cancer treatments including radiation therapy [96]. Moreover, in the context of treatment resistance Mihatsch and coworkers [133] described previously that the radioresistance of ALDH-positive cancer cells in vitro can be antagonized by inhibitors of PI3K/Akt signaling. In the present study, it could be demonstrated that Akt activity as well as Notch protein expression is upregulated in ALDH-positive HBL-100 and SKBR3 cells. Similar data has been presented for ALDH positive murine osteosarcoma cells (K7M2) [168]. In these cells Notch signaling pathway components such as Notch1 and Hes1 are overexpressed and inhibition of Notch by DAPT treatment leads to reduction of ALDH activity [168]. In accordance with this data, it has also been reported [169, 170] that treatment with the

Notch inhibitor Psoralidin reduces ALDH activity of sorted ALDH-positive breast cancer cell lines as well as in ex vivo tumor samples from breast cancer patients. In the context of these data, it is of special importance that Psoralidin has also been identified to inhibit Akt activity in ALDH-positive cells via downregulation of Akt phosphorylation [169, 170].

By applying clonogenic survival assays as well as the determination of residual-γH2AX foci as indicator of DNA-DSB repair efficacy it could be demonstrated in the present study that ALDH-positive breast cancer cells are more resistant to ionizing radiation and present a stimulated DNA-DSB repair capacity (Fig. 3.13). These results are in line with previous reports demonstrating chemo- and radioresistance of ALDH-positive tumor cells in conventional 2D-culture systems [55-57, 133]. Similar results of radioresistance of ALDH-positive cells have been reported by Kurth and coworkers [167] for 3D-cultures of the H&N cancer cell lines FaDu and Cal33. These authors [167] also observed less residual-γH2AX foci 24 and 48 h after irradiation of ALDH-positive cells when compared with ALDH-negative cells indicating a specific role of ALDH in DNA-DSB repair [167]. Radioresistance and stimulated DNA-DSB repair efficacy via upregulation of P-Chk2 (Thr68) has also been shown for ALDH positive prostate cancer cells DU145 and PC53 [62]. Yet, neither in the studies described by Kurth and coworkers [167] nor by Cojoc and coworkers [62], the regulatory role of ALDH activity on different DNA-DSB repair pathways such as NHEJ and HR have investigated.

4.5 Role of Nanog in DNA repair and ALDH activity

For the present study and as already addressed in the context of various CSCM analyzed in strong ALDH positive breast cancer cells the protein Nanog was of special interest in the present study. This interest was based on the result that the expression of Nanog was clearly affected by ALDH activity of the cells tested. This was clearly demonstrated by the use of Nanog overexpression as well as downregulation using either a plasmid-based overexpression or siRNA-based downregulation. The data received clearly indicated that Nanog promotes ALDH activity in MCF-7 and HBL-100 breast cancer cell lines (Fig. 3.14). In line with this finding, Jeter and coworkers [171] have also shown that Nanog overexpression stimulated ALDH activity in MCF-7 cells. This study was based on the use of a lentiviral transduction of the Nanog variants Nanogp8 and

Nanog1. Both variants induced ALDH activity and concomitantly led to upregulation of other CSCM, i.e. CD133 and CD44 [171].

As shown in Fig. 3.15 of the present study downregulation of Nanog significantly impaired DNA-DSB repair and radiosensitized ALDH positive MCF-7 and HBL-100 cells. Tanno and coauthors [172] have demonstrated that Nanog is highly overexpressed after irradiation (1Gy) of medulloblastoma bearing mice. In this study, it has also been shown that radiation-induced overexpression of Nanog promotes the selfrenewal capacity of GCPs (granule cell precursors), which can induce regrowth of medulloblastoma after irradiation [172]. Yet, a direct involvement of Nanog as a regulatory component DNA-DSB repair signaling was not investigated by Tanno and coworkers [172]. In the present study, however, this aspect was addressed in more detail. In this context, it has also been demonstrated by Cojoc and coworkers [62] that fractionated radiation induces the expression of Nanog and P-Akt in the prostate cancer cell line LNCaP. In contrast to the study by Cojoc and coworkers [62] and the study reported in the present thesis, Kim and coworkers [173] reported data indicating that the number of residual-γH2AX foci in Nanog-overexpressing mouse skin cells (K14-Na mouse model) is higher than in normal cells and that overexpression of Nanog in 293-cells upregulates the phosphorylation of ATM and KRAB-associated protein 1 (Kap1). As a consequence these authors conclude that Nanog abrogates the DNA repair progress potentially via disturbance of Kap1 function. However, the contradiction of Kim and coworkers data [173] to the results presented in study herein as well as by Cojoc and coworkers [62] may be reflected in the interpretation of Nanog´s function in DNA-DSB repair. Thus, the different functions of Nanog in DNA repair might be due to potential differences between the cell types used or might be dependent on the time of evaluating residual-γH2AX foci. Yet and unfortunately, in contrast to the present study herein and the study by Cojoc and coworkers [62] the report by Kim and coworkers [173] does not indicate the exact evaluation time of residual-γH2AX foci after irradiation.

To fulfill its regulatory function on various cellular processes Nanog needs to be translocated to the nucleus [70]. Based on the data present in this thesis, Nanog translocates to the nucleus in a time dependent manner both, after irradiation as well as ligand activation of EGFR (Fig. 16, 17). Do and coauthors [174] demonstrated by applying mutations in different domains of Nanog (N-terminal, Homeodomain and C-

terminal) in the kidney fibroblast cell line COS-7 c that the nuclear localization signal (NLS) motif is located in the homeodomain of Nanog and is essential for nuclear translocation. Bourguignon and coworkers [34] reported that CD44 stimulation by hyaluronan treatment promotes nuclear translocation of Nanog in complex with Oct-4 and Sox2 in tumor-derived HSC-3 cells presenting CD44 high/ALDH1 high. As described [34] nuclear translocation of the Oct4/Sox2/Nanog complex leads to upregulation of miR302 expression, which induces selfrenewal and chemoresistance of CD44 high/ALDH high HSC-3 cells. In this context it is of interest that in the present thesis, it could be demonstrated that inhibition of PI3K/Akt signaling abrogates post-irradiation nuclear translocation of Nanog (Fig. 3.18). In line with this data, it has been shown that EGF treatment drastically stimulates nuclear localization of Nanog and nuclear translocation of β-catenin in the lung cancer cell lines A549 and H23 [175]. Furthermore, and in line with the results presented herein, evidence was provided that inhibition of EGFR signaling by the tyrosine kinase inhibitor gefitinib and inhibition of PI3K/Akt pathway by the kinase inhibitor LY294002 results in downregulation of Nanog and nuclear level of β-catenin in nasopharyngeal carcinoma CNE2 cells [176]. So far however, neither the critical level of nuclear Nanog needed for its specific role nor the role of irradiation or EGFR signaling pathway on nuclear translocation of Nanog has been described in the literature. Especially against this background, the correlation of nuclear translocation of Nanog and radiation response needs to be investigated further.

4.6 Functional role of Nanog for expression of Notch1 and Akt activity

In the context of potential signaling interactions of Akt, Notch and Nanog, which may regulate radiation responses of breast cancer cells, specifically the role of Notch and Akt proteins for Nanog expression was analyzed. To this aspect, Noh and coworkers [177] have shown that downregulation of Nanog in the cervical cancer cell line Caski, leads to inhibition of P-Akt whereas overexpression of Nanog strongly induces P-Akt level in these cells. Moreover, inhibition of Akt activity by using API2 treatment abrogated sphere formation and apoptosis of immune selected Nanog overexpressing Caski cells [177]. Thus, in the present study the signaling pathways through which Nanog may

regulate both ALDH activity and radiation response of breast cancer cells were investigated. By various approaches, it could be demonstrated that overexpression as well as downregulation of Nanog can modulate Akt activity and Notch expression (Fig. 3.19). These results indicate that Nanog functions as upstream component of Akt and Notch expression. However, based on data reported by Chang and coauthors [92] showing that dual targeting of Akt and mTOR with BEZ235 downregulates CSCM expression and especially that of Nanog in the prostate cancer cell lines. Chang and coworkers [92] also demonstrated that the combination of BEZ235 with radiation (6 Gy) efficiently reduced colony formation of radioresistant prostate cancer cells. Thus, these results do indicate that Akt can function upstream of Nanog. Additional reports [178, 179] demonstrated that Notch inhibition can lead to downregulation of Nanog and Sox2; these results thus indicate that Notch can regulate Nanog.

Yet, the data shown in Fig. 3.21 of the present thesis indicated that downregulation of Notch and Akt results in radiosensitization of Nanog overexpressing cells. In line with this data, it has been shown that knockout of Notch in glioblastoma cells (i.e. U87MG and U251) mediates an impaired DNA-DSB repair [130]. Similarly, in a further study by Wang and coworkers [127], it has been demonstrated that Notch inhibition by GSI (gamma secretase inhibitor) in combination with radiation exposure results in an impaired clonogenic cell survival and induction of caspase 3/7 activity in CD133+ glioma stem cells, which suggests stimulation of radiation induced apoptosis. Moreover, these data also demonstrate that Notch via regulating Akt activity promotes radioresistance in CD133+ glioblastoma cells [127] (see summary figure).

In the context of upregulated ALDH activity in Nanog overexpressing cells, the potential signaling interactions of Akt, Notch and Nanog were also analyzed in the present thesis. It could be demonstrated that Nanog via Akt and Notch signaling induces ALDH activity (Fig. 20). To this aspect, Zhao and coworkers [66] have shown that Notch via Sirt2 stimulates deacetylation of ALDH1, which leads to the induction of ALDH1 enzyme activity in the MDA-MB-468 breast cancer cell line. In addition, Notch inhibition by DAPT (N-[N-(3,5-difluorophenacetyl)- L-alanyl]-S-phenylglycine t-butyl ester) treatment reduces more than 50% of ALDH activity in MDA-MB-468 [66]. Accordingly, it has been reported [180], that inhibition of the PI3K/Akt pathway by LY29004 treatment reduces ALDH activity in multidrug-resistance derived breast

cancer cell lines MCF-7/A02 and CALDOX. Based on these reports to the topic and the data presented in the thesis it can be concluded as demonstrated in the summary figure below that Nanog via regulating Akt and Notch signaling promotes ALDH activity in tumor cells.

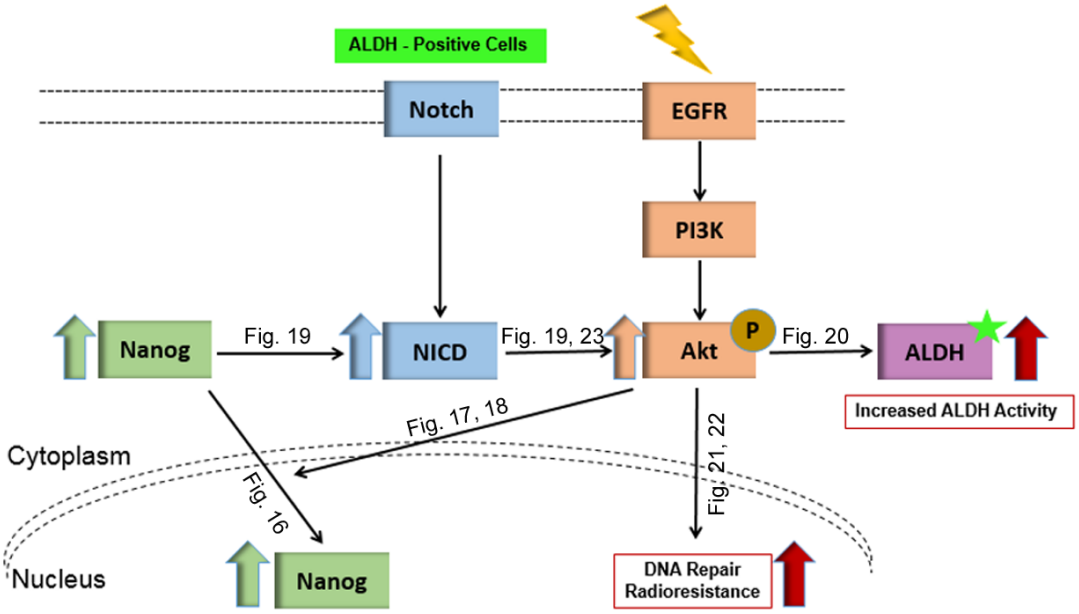

Summary Figure: schematic summary of the potential regulatory mechanisms based on the data presented in the current thesis**.** The written figure numbers on each arrow refers to the related data in the result section 3.

4.7 Conclusion and Outlook

Based on the presented data of this thesis, it can be concluded that ALDH inhibition with specific siRNA or DEAB treatment differentially affects the radiation response of different breast cancer cell lines. This finding might be due to the dependency of cells to ALDH activity and the basal level of ALDH expression and activity in the different cell lines analyzed. Moreover, downregulation of the Akt isoforms Akt1, Akt2 and Akt3 leads to reduction of ALDH activity in HBL-100 and HCT116 cells but not MCF-7 cells. The non-responsiveness of MCF-7 cells is most likely due to the independency of MCF-7 cells to PI3K/Akt signaling based on described PIK3CA mutation. Similarly, knockdown of the Akt isoforms Akt1, Akt2 and Akt3 did not alter the radiation

response of MCF-7 cells. However, downregulation of these Akt isoforms radiosensitized HBL-100 cells and additional inhibition of ALDH by DEAB treatment did not lead to a further radiosensitization in these knockdown cells. This finding indicates that Akt functions upstream of ALDH in radiation response. The comparison of low plating efficiencies under 3D-culture vs. high plating efficiencies under 2D-cultures, indicates that the minority of cells in a given tumor cell population in vitro represents CSCs.

In ALDH-positive cells, the expression of Nanog, Bmi1, P-Akt and Notch is markedly upregulated and ALDH-positive cells show a significantly enhanced DNA-DSB repair capacity as well as improved clonogenic cell survival. Downregulation of Nanog abrogated DNA-DSB repair efficacy and radiosensitized ALDH-positive cells. This finding indicates that the cellular radiation response of ALDH-positive cells is clearly dependent on the expression of Nanog. Furthermore, western blot data confirmed that Nanog regulates Notch expression as well as Akt activity. Inhibition of Akt and Notch prevented the modulatory effect of Nanog on the induction of ALDH activity and cellular radiation response. Thus, it can be concluded that high ALDH activity induces radioresistance of tumor cells via overexpression of Nanog and interacting pathways such as Akt and Notch summarized in summary figure.

5 Summary

Radiation therapy is applied alone or in combination with surgery and/or chemotherapy for therapy of most solid tumors. However, despite many advances in radiation oncology, radioresistance and cancer recurrence are still major problems. There are various mechanisms, which trigger radioresistance and tumor relapse and cancer stem cells (CSCs) have been identified as the major cause of radioresistance. Several mechanisms are described in CSCs to mediate radioresistance including stimulated DNA repair, hyperactivated survival pathways, like the PI3K/Akt as well as expression and stimulated activity of the CSC marker protein ALDH. As of yet, the precise mechanisms of how the CSC marker ALDH triggers therapy resistance are not fully understood. In the present study, the role of PI3K/Akt pathway and other CSC markers in the regulation of ALDH activity and radiation response of human cancer cell lines in vitro was investigated.

By the use of FACS-selected highly ALDH-positive subpopulations of breast cancer cell lines in vitro, it could be demonstrated that ALDH-positive cancer cells presented a significantly elevated radioresistance profile when compared to ALDH-negative subpopulations. Knockdown of Akt isoforms, Akt1, Akt2, and Akt3 led to downregulated ALDH activity in HBL-100 and HCT116 cancer cells. Yet, downregulation of Akt isoforms mediated radiosensitization of HBL-100 but not of MCF-7 breast cancer cells and inhibition of ALDH activity with DEAB treatment did not show any additional effect on post-irradiation cell survival after knockdown of Akt isoforms.

Assessing the protein expression profile of ALDH-positive cells revealed an upregulation of the stem cell markers Nanog, Bmi1 and Notch proteins as well stimulated P-Akt levels when compared to ALDH negative cells. In line with these data it could be demonstrated that ALDH-positive and radioresistant in contrast to ALDH-negative and radiosensitive cancer cells presented a stimulated DNA-DSB repair capacity. Moreover, knockdown of Nanog in ALDH-positive cancer cells resulted in an abrogation of the stimulated DNA-DSB repair capacity and consequently in a radiosensitization when compared to control cells. Additionally, knockdown of Nanog

led to downregulation of Notch expression and Akt activity. In line with this data, inhibition of Notch and Akt activity resulted in abrogation of stimulated post-irradiation cell survival as well as ALDH activity in Nanog overexpressing cancer cells. Further and most interestingly, it could be observed that nuclear translocation of Nanog is stimulated in a time dependent manner after radiation exposure of cancer cells. Accordingly, Nanog knockout DU145 cells present an impaired DNA-DSB repair and are more radiosensitive than Nanog expressing parental cells. These data confirmed the results obtained from Nanog knock down cells and thus supported the conclusion concerning the role of Nanog in post radiation response of cancer cells.

Altogether, the results presented in this study provide evidence that the high expression of ALDH in potential breast cancer stem cells is a consequence of upregulation of Nanog and Notch protein expression as well as stimulated Akt activity, which results in an improved DNA-DSB repair capacity. Compared to breast cancer cells with low ALDH activity these molecular alterations most likely result in the observed radioresistant phenotype of ALDH-positive breast cancer cells.

6 Zusammenfassung

Die Strahlentherapie wird allein oder in Kombination mit einer Operation und / oder Chemotherapie für die Behandlung der meisten soliden Tumoren angewendet. Trotz vieler Fortschritte der Radioonkologie bilden die Strahlenresistenz von Tumoren unter und das Wiederauftreten von Krebs nach erfolgter Therapie nach wie vor große Probleme. Es gibt verschiedene zelluläre und molekulare Mechanismen, die Strahlenresistenz sowie das Wiederauftreten eines Tumors auslösen können. In den letzten Jahren konnten Krebsstammzellen (CSCs) als Hauptursache für die Strahlenresistenz identifiziert werden. Für CSCs wurden verschiedene Mechanismen zur Vermittlung der Strahlenresistenz beschrieben, darunter eine stimulierte DNA-Reparatur, hyperaktivierte Überlebenswege wie PI3K / Akt sowie die Expression und stimulierte Aktivität des CSC-Markerproteins ALDH. Die genauen Mechanismen, wie der CSC-Marker ALDH Therapieresistenz auslöst, sind allerdings noch nicht vollständig geklärt. In der vorliegenden Studie wurde die Rolle des PI3K / Akt-Signalwegs und anderer CSC-Marker bei der Regulation der ALDH-Aktivität und der Strahlungsantwort von menschlichen Krebszelllinien in vitro untersucht.

Durch die Verwendung von FACS-selektierten hoch ALDH-positiven Subpopulationen von Brustkrebszelllinien in vitro konnte gezeigt werden, dass ALDH-positive im Vergleich zu ALDH-negativen Subpopulationen ein signifikant erhöhtes Strahlenresistenzprofil aufweisen. Knock-down der drei Akt-Isoformen Akt1, Akt2 und Akt3 führte zu einer Herunterregulation der ALDH-Aktivität sowohl in HBL-100- als auch in HCT116-Krebszellen. Eine Herunterregulierung von Akt-Isoformen vermittelte eine starke Radiosensibilisierung beiHBL-100- jedoch nicht bei MCF-7-Brustkrebszellen; eine Hemmung der ALDH-Aktivität durch Behandlung mit DEAB zeigte jedoch keinen zusätzlichen Effekt auf das Zellüberleben nach Bestrahlung im Kontext herunterregulierter Akt-Isoformen.

Die Analyse des Proteinexpressionsprofils von ALDH-positiven Zellen ergab im Vergleich zu ALDH-negativen Zellen eine Hochregulation der Stammzellmarker Nanog, Bmi1 und Notch sowie einen stimulierten P-Akt-Spiegel. In Übereinstimmung mit diesen Daten konnte gezeigt werden, dass ALDH-positive und strahlenresistente

ALDH-positive Krebszellen im Gegensatz zu ALDH-negativen und strahlenempfindlichen Zellen eine stimulierte DNA-DSB-Reparaturkapazität aufweisen. Darüber hinaus führte der Unterdrückung von Nanog in ALDH-positiven Krebszellen zu einer Aufhebung der stimulierten DNA-DSB-Reparaturkapazität und damit zu einer Radiosensitivierung. Zusätzlich resultierte die Herunterregulation der Nanog-Expression in einer verringerten Notch-Expression sowie reduzierter Akt-Aktivität. In Übereinstimmung mit diesen Daten kam es durch Hemmung der Notch- und Akt-Aktivität zur Aufhebung des signifikant verbesserten Zellüberlebens nach Bestrahlung sowie einer Unterdrückung der ALDH-Aktivität in Nanog-überexpri-mierenden Krebszellen. Weiterhin konnte interessanter Weise beobachtet werden, dass nach Strahlenexposition die nukleare Translokation von Nanog zeitabhängig stimuliert wird. Dementsprechend weisen Nanog-Knockout-DU145-Zellen eine beeinträchtigte DNA-DSB-Reparatur auf und sind signifikant strahlenempfindlicher als Nanog-exprimierende Parentalzellen. Diese Daten bestätigten die Ergebnisse an Nanog-Knock-down-Zellen und stützten somit die Schlussfolgerung bezüglich einer wichtigen Rolle von Nanog bei der zellulären Strahlenreaktion von Krebszellen.

Insgesamt zeigen die in dieser Studie vorgestellten Ergebnisse, dass die hohe Expression von ALDH in Brustkrebszellen eine Folge der Hochregulation der Nanog- und Notch-Proteinexpression sowie einer stimulierten Akt-Aktivität ist. Dieses Zusammenspiel führt zu einer verbesserten DNA-DSB-Reparaturkapazität. Im Vergleich zu Brustkrebszellen mit niedriger ALDH-Aktivität führen diese molekularen Veränderungen höchstwahrscheinlich zu dem beobachteten strahlenresistenten Phänotyp von ALDH-positiven Brustkrebszellen.

7 References

1. Du W, Elemento O. Cancer systems biology: embracing complexity to develop better anticancer therapeutic strategies. Oncogene 2015; 34:3215-3225.
2. Marusyk A, Almendro V, Polyak K. Intra-tumour heterogeneity: a looking glass for cancer? Nat Rev Cancer 2012; 12:323-334.
3. Quail DF, Joyce JA. Microenvironmental regulation of tumor progression and metastasis. Nat Med 2013; 19:1423-1437.
4. Vogelstein B, Kinzler KW. Cancer genes and the pathways they control. Nat Med 2004; 10:789-799.
5. Liotta LA, Kohn EC. The microenvironment of the tumour-host interface. Nature 2001; 411:375-379.
6. Harbeck N, Gnant M. Breast cancer. Lancet 2017; 389:1134-1150.
7. Akram M, Iqbal M, Daniyal M et al. Awareness and current knowledge of breast cancer. Biol Res 2017; 50:33.
8. Perou CM, Sorlie T, Eisen MB et al. Molecular portraits of human breast tumours. Nature 2000; 406:747-752.
9. Tonnessen BH, Pounds L. Radiation physics. J Vasc Surg 2011; 53:6S-8S.
10. Baskar R, Itahana K. Radiation therapy and cancer control in developing countries: Can we save more lives? Int J Med Sci 2017; 14:13-17.
11. Pazos M, Schonecker S, Reitz D et al. Recent Developments in Radiation Oncology: An Overview of Individualised Treatment Strategies in Breast Cancer. Breast Care (Basel) 2018; 13:285-291.
12. Mladenov E, Iliakis G. Induction and repair of DNA double strand breaks: the increasing spectrum of non-homologous end joining pathways. Mutat Res 2011; 711:61-72.
13. Abbotts R, Wilson DM, 3rd. Coordination of DNA single strand break repair. Free Radic Biol Med 2017; 107:228-244.
14. Li GM. Mechanisms and functions of DNA mismatch repair. Cell Res 2008; 18:85-98.
15. Davis AJ, Chen DJ. DNA double strand break repair via non-homologous end-joining. Transl Cancer Res 2013; 2:130-143.
16. Mari PO, Florea BI, Persengiev SP et al. Dynamic assembly of end-joining complexes requires interaction between Ku70/80 and XRCC4. Proc Natl Acad Sci U S A 2006; 103:18597-18602.
17. Rogakou EP, Pilch DR, Orr AH et al. DNA double-stranded breaks induce histone H2AX phosphorylation on serine 139. J Biol Chem 1998; 273:5858-5868.
18. Scully R, Xie A. Double strand break repair functions of histone H2AX. Mutat Res 2013; 750:5-14.
19. McGranahan N, Swanton C. Clonal Heterogeneity and Tumor Evolution: Past, Present, and the Future. Cell 2017; 168:613-628.
20. Lloyd MC, Cunningham JJ, Bui MM et al. Darwinian Dynamics of Intratumoral Heterogeneity: Not Solely Random Mutations but Also Variable Environmental Selection Forces. Cancer Res 2016; 76:3136-3144.
21. Kreso A, Dick JE. Evolution of the cancer stem cell model. Cell Stem Cell 2014; 14:275-291.

22. Peitzsch C, Tyutyunnykova A, Pantel K et al. Cancer stem cells: The root of tumor recurrence and metastases. Semin Cancer Biol 2017; 44:10-24.
23. Becker AJ, Mc CE, Till JE. Cytological demonstration of the clonal nature of spleen colonies derived from transplanted mouse marrow cells. Nature 1963; 197:452-454.
24. Till JE, Mc CE. A direct measurement of the radiation sensitivity of normal mouse bone marrow cells. Radiat Res 1961; 14:213-222.
25. McCulloch EA, Till JE. The radiation sensitivity of normal mouse bone marrow cells, determined by quantitative marrow transplantation into irradiated mice. Radiat Res 1960; 13:115-125.
26. Lapidot T, Sirard C, Vormoor J et al. A cell initiating human acute myeloid leukaemia after transplantation into SCID mice. Nature 1994; 367:645-648.
27. Gopalan V, Islam F, Lam AK. Surface Markers for the Identification of Cancer Stem Cells. Methods Mol Biol 2018; 1692:17-29.
28. Chanmee T, Ontong P, Kimata K et al. Key Roles of Hyaluronan and Its CD44 Receptor in the Stemness and Survival of Cancer Stem Cells. Front Oncol 2015; 5:180.
29. Toole BP. Hyaluronan in morphogenesis. Semin Cell Dev Biol 2001; 12:79-87.
30. Jung T, Castellana D, Klingbeil P et al. CD44v6 dependence of premetastatic niche preparation by exosomes. Neoplasia 2009; 11:1093-1105.
31. Desai B, Ma T, Zhu J et al. Characterization of the expression of variant and standard CD44 in prostate cancer cells: identification of the possible molecular mechanism of CD44/MMP9 complex formation on the cell surface. J Cell Biochem 2009; 108:272-284.
32. Kim Y, Lee YS, Choe J et al. CD44-epidermal growth factor receptor interaction mediates hyaluronic acid-promoted cell motility by activating protein kinase C signaling involving Akt, Rac1, Phox, reactive oxygen species, focal adhesion kinase, and MMP-2. J Biol Chem 2008; 283:22513-22528.
33. Bourguignon LY, Spevak CC, Wong G et al. Hyaluronan-CD44 interaction with protein kinase C(epsilon) promotes oncogenic signaling by the stem cell marker Nanog and the Production of microRNA-21, leading to down-regulation of the tumor suppressor protein PDCD4, anti-apoptosis, and chemotherapy resistance in breast tumor cells. J Biol Chem 2009; 284:26533-26546.
34. Bourguignon LY, Wong G, Earle C et al. Hyaluronan-CD44v3 interaction with Oct4-Sox2-Nanog promotes miR-302 expression leading to self-renewal, clonal formation, and cisplatin resistance in cancer stem cells from head and neck squamous cell carcinoma. J Biol Chem 2012; 287:32800-32824.
35. Bourguignon LY, Peyrollier K, Xia W et al. Hyaluronan-CD44 interaction activates stem cell marker Nanog, Stat-3-mediated MDR1 gene expression, and ankyrin-regulated multidrug efflux in breast and ovarian tumor cells. J Biol Chem 2008; 283:17635-17651.
36. Vasiliou V, Nebert DW. Analysis and update of the human aldehyde dehydrogenase (ALDH) gene family. Hum Genomics 2005; 2:138-143.
37. Ma I, Allan AL. The role of human aldehyde dehydrogenase in normal and cancer stem cells. Stem Cell Rev 2011; 7:292-306.
38. Gentry T, Foster S, Winstead L et al. Simultaneous isolation of human BM hematopoietic, endothelial and mesenchymal progenitor cells by flow sorting based on

aldehyde dehydrogenase activity: implications for cell therapy. Cytotherapy 2007; 9:259-274.

39. Capoccia BJ, Robson DL, Levac KD et al. Revascularization of ischemic limbs after transplantation of human bone marrow cells with high aldehyde dehydrogenase activity. Blood 2009; 113:5340-5351.
40. Vassalli G. Aldehyde Dehydrogenases: Not Just Markers, but Functional Regulators of Stem Cells. Stem Cells Int 2019; 2019:3904645.
41. Tanei T, Morimoto K, Shimazu K et al. Association of breast cancer stem cells identified by aldehyde dehydrogenase 1 expression with resistance to sequential Paclitaxel and epirubicin-based chemotherapy for breast cancers. Clin Cancer Res 2009; 15:4234-4241.
42. Singh S, Arcaroli J, Chen Y et al. ALDH1B1 Is Crucial for Colon Tumorigenesis by Modulating Wnt/beta-Catenin, Notch and PI3K/Akt Signaling Pathways. PLoS One 2015; 10:e0121648.
43. Moreb JS, Baker HV, Chang LJ et al. ALDH isozymes downregulation affects cell growth, cell motility and gene expression in lung cancer cells. Mol Cancer 2008; 7:87.
44. Liu J, Xiao Z, Wong SK et al. Lung cancer tumorigenicity and drug resistance are maintained through ALDH(hi)CD44(hi) tumor initiating cells. Oncotarget 2013; 4:1698-1711.
45. Charafe-Jauffret E, Ginestier C, Iovino F et al. Aldehyde dehydrogenase 1-positive cancer stem cells mediate metastasis and poor clinical outcome in inflammatory breast cancer. Clin Cancer Res 2010; 16:45-55.
46. Deng Y, Zhou J, Fang L et al. ALDH1 is an independent prognostic factor for patients with stages II-III rectal cancer after receiving radiochemotherapy. Br J Cancer 2014; 110:430-434.
47. Ginestier C, Hur MH, Charafe-Jauffret E et al. ALDH1 is a marker of normal and malignant human mammary stem cells and a predictor of poor clinical outcome. Cell Stem Cell 2007; 1:555-567.
48. Jones RJ, Barber JP, Vala MS et al. Assessment of aldehyde dehydrogenase in viable cells. Blood 1995; 85:2742-2746.
49. Zhao D, McCaffery P, Ivins KJ et al. Molecular identification of a major retinoic-acid-synthesizing enzyme, a retinaldehyde-specific dehydrogenase. Eur J Biochem 1996; 240:15-22.
50. Rodriguez-Torres M, Allan AL. Aldehyde dehydrogenase as a marker and functional mediator of metastasis in solid tumors. Clin Exp Metastasis 2016; 33:97-113.
51. Elizondo G, Corchero J, Sterneck E et al. Feedback inhibition of the retinaldehyde dehydrogenase gene ALDH1 by retinoic acid through retinoic acid receptor alpha and CCAAT/enhancer-binding protein beta. J Biol Chem 2000; 275:39747-39753.
52. Kohn FR, Landkamer GJ, Manthey CL et al. Effect of aldehyde dehydrogenase inhibitors on the ex vivo sensitivity of human multipotent and committed hematopoietic progenitor cells and malignant blood cells to oxazaphosphorines. Cancer Res 1987; 47:3180-3185.
53. Kohn FR, Sladek NE. Effects of aldehyde dehydrogenase inhibitors on the ex vivo sensitivity of murine late spleen colony-forming cells (day-12 CFU-S) and hematopoietic repopulating cells to mafosfamide (ASTA Z 7557). Biochem Pharmacol 1987; 36:2805-2811.

54. Brennan SK, Meade B, Wang Q et al. Mantle cell lymphoma activation enhances bortezomib sensitivity. Blood 2010; 116:4185-4191.
55. Landen CN, Jr., Goodman B, Katre AA et al. Targeting aldehyde dehydrogenase cancer stem cells in ovarian cancer. Mol Cancer Ther 2010; 9:3186-3199.
56. Morimoto K, Kim SJ, Tanei T et al. Stem cell marker aldehyde dehydrogenase 1-positive breast cancers are characterized by negative estrogen receptor, positive human epidermal growth factor receptor type 2, and high Ki67 expression. Cancer Sci 2009; 100:1062-1068.
57. Duru N, Fan M, Candas D et al. HER2-associated radioresistance of breast cancer stem cells isolated from HER2-negative breast cancer cells. Clin Cancer Res 2012; 18:6634-6647.
58. Wang Y, Li W, Patel SS et al. Blocking the formation of radiation-induced breast cancer stem cells. Oncotarget 2014; 5:3743-3755.
59. Yanagawa Y, Chen JC, Hsu LC et al. The transcriptional regulation of human aldehyde dehydrogenase I gene. The structural and functional analysis of the promoter. J Biol Chem 1995; 270:17521-17527.
60. Alam M, Ahmad R, Rajabi H et al. MUC1-C oncoprotein activates ERK-->C/EBPbeta signaling and induction of aldehyde dehydrogenase 1A1 in breast cancer cells. J Biol Chem 2013; 288:30892-30903.
61. Canino C, Luo Y, Marcato P et al. A STAT3-NFkB/DDIT3/CEBPbeta axis modulates ALDH1A3 expression in chemoresistant cell subpopulations. Oncotarget 2015; 6:12637-12653.
62. Cojoc M, Peitzsch C, Kurth I et al. Aldehyde Dehydrogenase Is Regulated by beta-Catenin/TCF and Promotes Radioresistance in Prostate Cancer Progenitor Cells. Cancer Res 2015; 75:1482-1494.
63. Hoshino Y, Nishida J, Katsuno Y et al. Smad4 Decreases the Population of Pancreatic Cancer-Initiating Cells through Transcriptional Repression of ALDH1A1. Am J Pathol 2015; 185:1457-1470.
64. Shi J, Vakoc CR. The mechanisms behind the therapeutic activity of BET bromodomain inhibition. Mol Cell 2014; 54:728-736.
65. Yokoyama Y, Zhu H, Lee JH et al. BET Inhibitors Suppress ALDH Activity by Targeting ALDH1A1 Super-Enhancer in Ovarian Cancer. Cancer Res 2016; 76:6320-6330.
66. Zhao D, Mo Y, Li MT et al. NOTCH-induced aldehyde dehydrogenase 1A1 deacetylation promotes breast cancer stem cells. J Clin Invest 2014; 124:5453-5465.
67. Hirata N, Yamada S, Shoda T et al. Sphingosine-1-phosphate promotes expansion of cancer stem cells via S1PR3 by a ligand-independent Notch activation. Nat Commun 2014; 5:4806.
68. Chambers I, Colby D, Robertson M et al. Functional expression cloning of Nanog, a pluripotency sustaining factor in embryonic stem cells. Cell 2003; 113:643-655.
69. Mitsui K, Tokuzawa Y, Itoh H et al. The homeoprotein Nanog is required for maintenance of pluripotency in mouse epiblast and ES cells. Cell 2003; 113:631-642.
70. Gawlik-Rzemieniewska N, Bednarek I. The role of NANOG transcriptional factor in the development of malignant phenotype of cancer cells. Cancer Biol Ther 2016; 17:1-10.

71. Wong OG, Cheung AN. Stem cell transcription factor NANOG in cancers--is eternal youth a curse? Expert Opin Ther Targets 2016; 20:407-417.
72. Ambady S, Malcuit C, Kashpur O et al. Expression of NANOG and NANOGP8 in a variety of undifferentiated and differentiated human cells. Int J Dev Biol 2010; 54:1743-1754.
73. Chang DF, Tsai SC, Wang XC et al. Molecular characterization of the human NANOG protein. Stem Cells 2009; 27:812-821.
74. Theunissen TW, Costa Y, Radzisheuskaya A et al. Reprogramming capacity of Nanog is functionally conserved in vertebrates and resides in a unique homeodomain. Development 2011; 138:4853-4865.
75. Lin T, Chao C, Saito S et al. p53 induces differentiation of mouse embryonic stem cells by suppressing Nanog expression. Nat Cell Biol 2005; 7:165-171.
76. Moon JH, Kwon S, Jun EK et al. Nanog-induced dedifferentiation of p53-deficient mouse astrocytes into brain cancer stem-like cells. Biochem Biophys Res Commun 2011; 412:175-181.
77. Po A, Ferretti E, Miele E et al. Hedgehog controls neural stem cells through p53-independent regulation of Nanog. EMBO J 2010; 29:2646-2658.
78. Bourguignon LY, Earle C, Wong G et al. Stem cell marker (Nanog) and Stat-3 signaling promote MicroRNA-21 expression and chemoresistance in hyaluronan/CD44-activated head and neck squamous cell carcinoma cells. Oncogene 2012; 31:149-160.
79. Suzuki A, Raya A, Kawakami Y et al. Nanog binds to Smad1 and blocks bone morphogenetic protein-induced differentiation of embryonic stem cells. Proc Natl Acad Sci U S A 2006; 103:10294-10299.
80. Zhang J, Espinoza LA, Kinders RJ et al. NANOG modulates stemness in human colorectal cancer. Oncogene 2013; 32:4397-4405.
81. Shan J, Shen J, Liu L et al. Nanog regulates self-renewal of cancer stem cells through the insulin-like growth factor pathway in human hepatocellular carcinoma. Hepatology 2012; 56:1004-1014.
82. Zbinden M, Duquet A, Lorente-Trigos A et al. NANOG regulates glioma stem cells and is essential in vivo acting in a cross-functional network with GLI1 and p53. EMBO J 2010; 29:2659-2674.
83. Chiou SH, Wang ML, Chou YT et al. Coexpression of Oct4 and Nanog enhances malignancy in lung adenocarcinoma by inducing cancer stem cell-like properties and epithelial-mesenchymal transdifferentiation. Cancer Res 2010; 70:10433-10444.
84. Han J, Zhang F, Yu M et al. RNA interference-mediated silencing of NANOG reduces cell proliferation and induces G0/G1 cell cycle arrest in breast cancer cells. Cancer Lett 2012; 321:80-88.
85. Siu MK, Wong ES, Kong DS et al. Stem cell transcription factor NANOG controls cell migration and invasion via dysregulation of E-cadherin and FoxJ1 and contributes to adverse clinical outcome in ovarian cancers. Oncogene 2013; 32:3500-3509.
86. Ho B, Olson G, Figel S et al. Nanog increases focal adhesion kinase (FAK) promoter activity and expression and directly binds to FAK protein to be phosphorylated. J Biol Chem 2012; 287:18656-18673.
87. Brunner TB, Kunz-Schughart LA, Grosse-Gehling P et al. Cancer stem cells as a predictive factor in radiotherapy. Semin Radiat Oncol 2012; 22:151-174.

88. Ishizawa K, Rasheed ZA, Karisch R et al. Tumor-initiating cells are rare in many human tumors. Cell Stem Cell 2010; 7:279-282.
89. Galli R, Binda E, Orfanelli U et al. Isolation and characterization of tumorigenic, stem-like neural precursors from human glioblastoma. Cancer Res 2004; 64:7011-7021.
90. S SF, Szczesna K, Iliou MS et al. In vitro models of cancer stem cells and clinical applications. BMC Cancer 2016; 16:738.
91. Nunes T, Hamdan D, Leboeuf C et al. Targeting Cancer Stem Cells to Overcome Chemoresistance. Int J Mol Sci 2018; 19.
92. Chang L, Graham PH, Hao J et al. Acquisition of epithelial-mesenchymal transition and cancer stem cell phenotypes is associated with activation of the PI3K/Akt/mTOR pathway in prostate cancer radioresistance. Cell Death Dis 2013; 4:e875.
93. Farnie G, Clarke RB, Spence K et al. Novel cell culture technique for primary ductal carcinoma in situ: role of Notch and epidermal growth factor receptor signaling pathways. J Natl Cancer Inst 2007; 99:616-627.
94. Mundi PS, Sachdev J, McCourt C et al. AKT in cancer: new molecular insights and advances in drug development. Br J Clin Pharmacol 2016; 82:943-956.
95. Faes S, Dormond O. PI3K and AKT: Unfaithful Partners in Cancer. Int J Mol Sci 2015; 16:21138-21152.
96. Toulany M, Rodemann HP. Phosphatidylinositol 3-kinase/Akt signaling as a key mediator of tumor cell responsiveness to radiation. Semin Cancer Biol 2015; 35:180-190.
97. Manning BD, Toker A. AKT/PKB Signaling: Navigating the Network. Cell 2017; 169:381-405.
98. Alessi DR, James SR, Downes CP et al. Characterization of a 3-phosphoinositide-dependent protein kinase which phosphorylates and activates protein kinase Balpha. Curr Biol 1997; 7:261-269.
99. Stokoe D, Stephens LR, Copeland T et al. Dual role of phosphatidylinositol-3,4,5-trisphosphate in the activation of protein kinase B. Science 1997; 277:567-570.
100. Calleja V, Laguerre M, Parker PJ et al. Role of a novel PH-kinase domain interface in PKB/Akt regulation: structural mechanism for allosteric inhibition. PLoS Biol 2009; 7:e17.
101. Sarbassov DD, Guertin DA, Ali SM et al. Phosphorylation and regulation of Akt/PKB by the rictor-mTOR complex. Science 2005; 307:1098-1101.
102. Turner KM, Sun Y, Ji P et al. Genomically amplified Akt3 activates DNA repair pathway and promotes glioma progression. Proc Natl Acad Sci U S A 2015; 112:3421-3426.
103. Toulany M, Kehlbach R, Florczak U et al. Targeting of AKT1 enhances radiation toxicity of human tumor cells by inhibiting DNA-PKcs-dependent DNA double-strand break repair. Mol Cancer Ther 2008; 7:1772-1781.
104. Toulany M, Lee KJ, Fattah KR et al. Akt promotes post-irradiation survival of human tumor cells through initiation, progression, and termination of DNA-PKcs-dependent DNA double-strand break repair. Mol Cancer Res 2012; 10:945-957.
105. Park J, Feng J, Li Y et al. DNA-dependent protein kinase-mediated phosphorylation of protein kinase B requires a specific recognition sequence in the C-terminal hydrophobic motif. J Biol Chem 2009; 284:6169-6174.

106. Toulany M, Kasten-Pisula U, Brammer I et al. Blockage of epidermal growth factor receptor-phosphatidylinositol 3-kinase-AKT signaling increases radiosensitivity of K-RAS mutated human tumor cells in vitro by affecting DNA repair. Clin Cancer Res 2006; 12:4119-4126.
107. Viniegra JG, Martinez N, Modirassari P et al. Full activation of PKB/Akt in response to insulin or ionizing radiation is mediated through ATM. J Biol Chem 2005; 280:4029-4036.
108. Mueck K, Rebholz S, Harati MD et al. Akt1 Stimulates Homologous Recombination Repair of DNA Double-Strand Breaks in a Rad51-Dependent Manner. Int J Mol Sci 2017; 18.
109. Jia Y, Song W, Zhang F et al. Akt1 inhibits homologous recombination in Brca1-deficient cells by blocking the Chk1-Rad51 pathway. Oncogene 2013; 32:1943-1949.
110. Xiang T, Jia Y, Sherris D et al. Targeting the Akt/mTOR pathway in Brca1-deficient cancers. Oncogene 2011; 30:2443-2450.
111. Aster JC, Pear WS, Blacklow SC. The Varied Roles of Notch in Cancer. Annu Rev Pathol 2017; 12:245-275.
112. Schroeter EH, Kisslinger JA, Kopan R. Notch-1 signalling requires ligand-induced proteolytic release of intracellular domain. Nature 1998; 393:382-386.
113. Struhl G, Greenwald I. Presenilin is required for activity and nuclear access of Notch in Drosophila. Nature 1999; 398:522-525.
114. Ronchini C, Capobianco AJ. Induction of cyclin D1 transcription and CDK2 activity by Notch(ic): implication for cell cycle disruption in transformation by Notch(ic). Mol Cell Biol 2001; 21:5925-5934.
115. Weng AP, Millholland JM, Yashiro-Ohtani Y et al. c-Myc is an important direct target of Notch1 in T-cell acute lymphoblastic leukemia/lymphoma. Genes Dev 2006; 20:2096-2109.
116. Chen Y, Fischer WH, Gill GN. Regulation of the ERBB-2 promoter by RBPJkappa and NOTCH. J Biol Chem 1997; 272:14110-14114.
117. Wu F, Stutzman A, Mo YY. Notch signaling and its role in breast cancer. Front Biosci 2007; 12:4370-4383.
118. Ling H, Sylvestre JR, Jolicoeur P. Notch1-induced mammary tumor development is cyclin D1-dependent and correlates with expansion of pre-malignant multipotent duct-limited progenitors. Oncogene 2010; 29:4543-4554.
119. Murata J, Ohtsuka T, Tokunaga A et al. Notch-Hes1 pathway contributes to the cochlear prosensory formation potentially through the transcriptional down-regulation of p27Kip1. J Neurosci Res 2009; 87:3521-3534.
120. Sharma VM, Calvo JA, Draheim KM et al. Notch1 contributes to mouse T-cell leukemia by directly inducing the expression of c-myc. Mol Cell Biol 2006; 26:8022-8031.
121. Palomero T, Dominguez M, Ferrando AA. The role of the PTEN/AKT Pathway in NOTCH1-induced leukemia. Cell Cycle 2008; 7:965-970.
122. Meurette O, Stylianou S, Rock R et al. Notch activation induces Akt signaling via an autocrine loop to prevent apoptosis in breast epithelial cells. Cancer Res 2009; 69:5015-5022.

123. Beverly LJ, Felsher DW, Capobianco AJ. Suppression of p53 by Notch in lymphomagenesis: implications for initiation and regression. Cancer Res 2005; 65:7159-7168.
124. Mailhos C, Modlich U, Lewis J et al. Delta4, an endothelial specific notch ligand expressed at sites of physiological and tumor angiogenesis. Differentiation 2001; 69:135-144.
125. Meng RD, Shelton CC, Li YM et al. gamma-Secretase inhibitors abrogate oxaliplatin-induced activation of the Notch-1 signaling pathway in colon cancer cells resulting in enhanced chemosensitivity. Cancer Res 2009; 69:573-582.
126. Wang Z, Li Y, Ahmad A et al. Targeting Notch signaling pathway to overcome drug resistance for cancer therapy. Biochim Biophys Acta 2010; 1806:258-267.
127. Wang J, Wakeman TP, Lathia JD et al. Notch promotes radioresistance of glioma stem cells. Stem Cells 2010; 28:17-28.
128. Lee CW, Raskett CM, Prudovsky I et al. Molecular dependence of estrogen receptor-negative breast cancer on a notch-survivin signaling axis. Cancer Res 2008; 68:5273-5281.
129. Osipo C, Patel P, Rizzo P et al. ErbB-2 inhibition activates Notch-1 and sensitizes breast cancer cells to a gamma-secretase inhibitor. Oncogene 2008; 27:5019-5032.
130. Han N, Hu G, Shi L et al. Notch1 ablation radiosensitizes glioblastoma cells. Oncotarget 2017; 8:88059-88068.
131. Ruan J, Lou S, Dai Q et al. Tumor suppressor miR-181c attenuates proliferation, invasion, and self-renewal abilities in glioblastoma. Neuroreport 2015; 26:66-73.
132. Zhan JF, Wu LP, Chen LH et al. Pharmacological inhibition of AKT sensitizes MCF-7 human breast cancer-initiating cells to radiation. Cell Oncol (Dordr) 2011; 34:451-456.
133. Mihatsch J, Toulany M, Bareiss PM et al. Selection of radioresistant tumor cells and presence of ALDH1 activity in vitro. Radiother Oncol 2011; 99:300-306.
134. Minjgee M, Toulany M, Kehlbach R et al. K-RAS(V12) induces autocrine production of EGFR ligands and mediates radioresistance through EGFR-dependent Akt signaling and activation of DNA-PKcs. Int J Radiat Oncol Biol Phys 2011; 81:1506-1514.
135. Dehghan Harati M, Rodemann HP, Toulany M. Nanog Signaling Mediates Radioresistance in ALDH-Positive Breast Cancer Cells. Int J Mol Sci 2019; 20.
136. Baumann M, Krause M, Hill R. Exploring the role of cancer stem cells in radioresistance. Nat Rev Cancer 2008; 8:545-554.
137. Desai A, Yan Y, Gerson SL. Concise Reviews: Cancer Stem Cell Targeted Therapies: Toward Clinical Success. Stem Cells Transl Med 2019; 8:75-81.
138. Ling GQ, Chen DB, Wang BQ et al. Expression of the pluripotency markers Oct3/4, Nanog and Sox2 in human breast cancer cell lines. Oncol Lett 2012; 4:1264-1268.
139. Olsson E, Honeth G, Bendahl PO et al. CD44 isoforms are heterogeneously expressed in breast cancer and correlate with tumor subtypes and cancer stem cell markers. BMC Cancer 2011; 11:418.
140. Ricardo S, Vieira AF, Gerhard R et al. Breast cancer stem cell markers CD44, CD24 and ALDH1: expression distribution within intrinsic molecular subtype. J Clin Pathol 2011; 64:937-946.
141. Gargini R, Cerliani JP, Escoll M et al. Cancer stem cell-like phenotype and survival are coordinately regulated by Akt/FoxO/Bim pathway. Stem Cells 2015; 33:646-660.

142. Jain MV, Jangamreddy JR, Grabarek J et al. Nuclear localized Akt enhances breast cancer stem-like cells through counter-regulation of p21(Waf1/Cip1) and p27(kip1). Cell Cycle 2015; 14:2109-2120.
143. Mu X, Isaac C, Schott T et al. Rapamycin Inhibits ALDH Activity, Resistance to Oxidative Stress, and Metastatic Potential in Murine Osteosarcoma Cells. Sarcoma 2013; 2013:480713.
144. Zhou H, Yu C, Kong L et al. B591, a novel specific pan-PI3K inhibitor, preferentially targets cancer stem cells. Oncogene 2019; 38:3371-3386.
145. Vasudevan KM, Barbie DA, Davies MA et al. AKT-independent signaling downstream of oncogenic PIK3CA mutations in human cancer. Cancer Cell 2009; 16:21-32.
146. Toulany M, Maier J, Iida M et al. Akt1 and Akt3 but not Akt2 through interaction with DNA-PKcs stimulate proliferation and post-irradiation cell survival of K-RAS-mutated cancer cells. Cell Death Discov 2017; 3:17072.
147. Sahlberg SH, Gustafsson AS, Pendekanti PN et al. The influence of AKT isoforms on radiation sensitivity and DNA repair in colon cancer cell lines. Tumour Biol 2014; 35:3525-3534.
148. Croker AK, Allan AL. Inhibition of aldehyde dehydrogenase (ALDH) activity reduces chemotherapy and radiation resistance of stem-like ALDHhiCD44(+) human breast cancer cells. Breast Cancer Res Treat 2012; 133:75-87.
149. Charafe-Jauffret E, Ginestier C, Iovino F et al. Breast cancer cell lines contain functional cancer stem cells with metastatic capacity and a distinct molecular signature. Cancer Res 2009; 69:1302-1313.
150. Marcato P, Dean CA, Pan D et al. Aldehyde dehydrogenase activity of breast cancer stem cells is primarily due to isoform ALDH1A3 and its expression is predictive of metastasis. Stem Cells 2011; 29:32-45.
151. Marcato P, Dean CA, Giacomantonio CA et al. Aldehyde dehydrogenase: its role as a cancer stem cell marker comes down to the specific isoform. Cell Cycle 2011; 10:1378-1384.
152. Zhou L, Sheng D, Wang D et al. Identification of cancer-type specific expression patterns for active aldehyde dehydrogenase (ALDH) isoforms in ALDEFLUOR assay. Cell Biol Toxicol 2019; 35:161-177.
153. Bielecka ZF, Maliszewska-Olejniczak K, Safir IJ et al. Three-dimensional cell culture model utilization in cancer stem cell research. Biol Rev Camb Philos Soc 2017; 92:1505-1520.
154. Kenny PA, Lee GY, Myers CA et al. The morphologies of breast cancer cell lines in three-dimensional assays correlate with their profiles of gene expression. Mol Oncol 2007; 1:84-96.
155. Rich JN. Cancer stem cells: understanding tumor hierarchy and heterogeneity. Medicine (Baltimore) 2016; 95:S2-7.
156. Bahmad HF, Cheaito K, Chalhoub RM et al. Sphere-Formation Assay: Three-Dimensional in vitro Culturing of Prostate Cancer Stem/Progenitor Sphere-Forming Cells. Front Oncol 2018; 8:347.
157. Bodgi L, Bahmad HF, Araji T et al. Assessing Radiosensitivity of Bladder Cancer in vitro: A 2D vs. 3D Approach. Front Oncol 2019; 9:153.
158. Lagadec C, Vlashi E, Della Donna L et al. Radiation-induced reprogramming of breast cancer cells. Stem Cells 2012; 30:833-844.

159. Reynolds DS, Tevis KM, Blessing WA et al. Breast Cancer Spheroids Reveal a Differential Cancer Stem Cell Response to Chemotherapeutic Treatment. Sci Rep 2017; 7:10382.
160. Ghisolfi L, Keates AC, Hu X et al. Ionizing radiation induces stemness in cancer cells. PLoS One 2012; 7:e43628.
161. Awad O, Yustein JT, Shah P et al. High ALDH activity identifies chemotherapy-resistant Ewing's sarcoma stem cells that retain sensitivity to EWS-FLI1 inhibition. PLoS One 2010; 5:e13943.
162. Balber AE. Concise review: aldehyde dehydrogenase bright stem and progenitor cell populations from normal tissues: characteristics, activities, and emerging uses in regenerative medicine. Stem Cells 2011; 29:570-575.
163. Wu D, Mou YP, Chen K et al. Aldehyde dehydrogenase 3A1 is robustly upregulated in gastric cancer stem-like cells and associated with tumorigenesis. Int J Oncol 2016; 49:611-622.
164. Yasuda K, Torigoe T, Morita R et al. Ovarian cancer stem cells are enriched in side population and aldehyde dehydrogenase bright overlapping population. PLoS One 2013; 8:e68187.
165. Yu CC, Lo WL, Chen YW et al. Bmi-1 Regulates Snail Expression and Promotes Metastasis Ability in Head and Neck Squamous Cancer-Derived ALDH1 Positive Cells. J Oncol 2011; 2011.
166. Santini R, Pietrobono S, Pandolfi S et al. SOX2 regulates self-renewal and tumorigenicity of human melanoma-initiating cells. Oncogene 2014; 33:4697-4708.
167. Kurth I, Hein L, Mabert K et al. Cancer stem cell related markers of radioresistance in head and neck squamous cell carcinoma. Oncotarget 2015; 6:34494-34509.
168. Mu X, Isaac C, Greco N et al. Notch Signaling is Associated with ALDH Activity and an Aggressive Metastatic Phenotype in Murine Osteosarcoma Cells. Front Oncol 2013; 3:143.
169. Pal D, Kolluru V, Chandrasekaran B et al. Targeting aberrant expression of Notch-1 in ALDH(+) cancer stem cells in breast cancer. Mol Carcinog 2017; 56:1127-1136.
170. Suman S, Das TP, Damodaran C. Silencing NOTCH signaling causes growth arrest in both breast cancer stem cells and breast cancer cells. Br J Cancer 2013; 109:2587-2596.
171. Jeter CR, Liu B, Liu X et al. NANOG promotes cancer stem cell characteristics and prostate cancer resistance to androgen deprivation. Oncogene 2011; 30:3833-3845.
172. Tanno B, Leonardi S, Babini G et al. Nanog-driven cell-reprogramming and self-renewal maintenance in Ptch1 (+/-) granule cell precursors after radiation injury. Sci Rep 2017; 7:14238.
173. Kim J, Liu Y, Qiu M et al. Pluripotency factor Nanog is tumorigenic by deregulating DNA damage response in somatic cells. Oncogene 2016; 35:1334-1340.
174. Do HJ, Lim HY, Kim JH et al. An intact homeobox domain is required for complete nuclear localization of human Nanog. Biochem Biophys Res Commun 2007; 353:770-775.
175. Li XQ, Yang XL, Zhang G et al. Nuclear beta-catenin accumulation is associated with increased expression of Nanog protein and predicts poor prognosis of non-small cell lung cancer. J Transl Med 2013; 11:114.

176. Ma L, Zhang G, Miao XB et al. Cancer stem-like cell properties are regulated by EGFR/AKT/beta-catenin signaling and preferentially inhibited by gefitinib in nasopharyngeal carcinoma. FEBS J 2013; 280:2027-2041.
177. Noh KH, Kim BW, Song KH et al. Nanog signaling in cancer promotes stem-like phenotype and immune evasion. J Clin Invest 2012; 122:4077-4093.
178. Wang R, Sun Q, Wang P et al. Notch and Wnt/beta-catenin signaling pathway play important roles in activating liver cancer stem cells. Oncotarget 2016; 7:5754-5768.
179. Luo J, Wang P, Wang R et al. The Notch pathway promotes the cancer stem cell characteristics of CD90+ cells in hepatocellular carcinoma. Oncotarget 2016; 7:9525-9537.
180. Hu Y, Guo R, Wei J et al. Effects of PI3K inhibitor NVP-BKM120 on overcoming drug resistance and eliminating cancer stem cells in human breast cancer cells. Cell Death Dis 2015; 6:e2020.

8 Publication

Dehghan Harati M, Rodemann HP, Toulany M – Nanog signaling induces radioresistance in ALDH positive breast cancer stem cells – *International Journal of Molecular Science*. 2019. Mar 6;20(5). pii: E1151.

I hereby declare that the doctoral dissertation submitted with the title: “Role of PI3K/Akt pathway in cancer stem cell mediated radioresistance” was written independently using only the stated sources and aids and that quotes and excerpts literal or otherwise, are marked correspondingly. I declare that all experiments in the submitted dissertation have been performed by myself and have already been published in part in “International Journal of Molecular Science”, and have been cited correspondingly. I declare on oath that these statements are true and that I have concealed nothing. I am aware that false declarations or affirmations in lieu of an oath can be punished with a jail sentence of up to three years or with a fine.

9 Acknowledgments

Time always passes quickly. Looking back to the last few years of PhD studies, reminding me how much I were lucky to work in the great radiobiology group. I am honored to have done my thesis under supervision of Professor H. Peter Rodemann, who put scientific input without any doubt into my PhD work and especially I am thankful to him for teaching me not only the way of thinking but also the humanity.

Finishing my thesis successfully would not be possible without help of all people in the laboratory: Thanks to Mahmoud Toulany for supporting scientifically my PhD work and also his help for publishing the paper. Thanks to Klaus Dittmann for the scientific suggestions and especially for keeping the atmosphere of work always positive. Thanks to all lab members; Simone Rebholz, Felix Attenberger, Aadhya Tiwary, Tahereh Mohammadian, Eva Bathelt and Claus Mayer who not only were perfect friends but also helped me in a team manner to progress further my research.

Thanks to Professor Nils Cordes for accepting me in his laboratory for learning and establishing 3D-culture method. Thanks to Professor Yasufumi Kaneda and Professor Keisuke Nimura for kindly providing Nanog1 knockout and parental DU145 cell lines.

At the end, I have to say my great thanks to the people who were not part of laboratory team but were the most valuable people in my life:

Thanks to my love, Philipp, who supported me in all steps of my life and being with me in all ups and downs of PhD work. Thanks to my family; my mum, dad, brother and sister who are far away from me but they keep their love and support no matter of distances. I am more than glad to have such a family.

In the last sentence, I would love to mention a poem (from Jale Isfahani):

“The life is our unique artists scene,

Everybody sings his own melody and leaves the scene,

But the scene is constantly remaining,

Greeting to that melody that people keep as a memory!”